

**Channel Assignment Strategies for
Throughput Enhancement in High Density
Wireless Local Area Networks**

Micheal Drieberg

B.Eng., M.Sc.

Submitted in fulfillment of the requirements for the degree of

Doctor of Philosophy



Centre for Telecommunications and Micro-Electronics

Faculty of Health, Engineering and Science

Victoria University

June 2010

To my dear wife, Ai Yoon

ABSTRACT

The emergence of high density wireless local area network (WLAN) deployments in recent years is a testament to both the insatiable demands for wireless broadband services and the ubiquity of WLAN technology. The increased density of WLAN deployments brings with it the potential of increased capacity, extended coverage and exciting new applications. On the other hand, however, the corresponding increase in contention and interference can significantly degrade throughputs unless new challenges in channel assignment are addressed effectively.

This thesis deals with the investigation and development of practical channel assignment schemes in high density WLANs that can provide enhanced throughputs. Firstly, the minimum neighbour (MINE) channel assignment scheme is proposed. It is shown that in order to maximize throughput, each access point (AP) only needs to choose the channel with the minimum number of active neighbour nodes. Superior throughputs in dynamic loads and robust performance across various realistic scenarios are obtained with the MINE scheme.

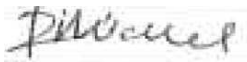
Secondly, the minimum neighbour with extended Kalman filter estimator (MINEK) scheme is developed. The MINEK scheme provides the estimation of the number of neighbour nodes, which is required for the practical application of the MINE scheme. For this purpose, an extended Kalman filter (EKF) estimator and the number of nodes by AP estimate are formulated. This scheme not only provides fast and accurate estimates but also successfully exploits channel switching information of neighbouring APs. The MINEK scheme achieves significantly improved throughputs over other channel assignment schemes.

Thirdly, client assisted channel assignment is explored. A study on the impact of interference on throughput with multiple APs is undertaken first using a novel approach that determines the possibility of parallel transmissions. In order to maximize its expected throughput, measurements from clients are used to assist the AP in determining the channel with the minimum number of conflict pairs. The client assisted minimum conflict pairs (MICPA) scheme can provide meaningful throughput improvements over other schemes that only utilize AP's measurements.

In summary, this thesis investigated practical channel assignment strategies for throughput enhancement in high density WLANs and verified their superior performance using simulations.

DECLARATION

“I, Micheal Drieberg, declare that the PhD thesis entitled “Channel Assignment Strategies for Throughput Enhancement in High Density Wireless Local Area Networks” is no more than 100,000 words in length including quotes and exclusive of tables, figures, appendices, bibliography, references and footnotes. This thesis contains no material that has been submitted previously, in whole or in part, for the award of any other academic degree or diploma. Except where otherwise indicated, this thesis is my own work”.



Signature

30th June 2010

Date

ACKNOWLEDGEMENTS

First of all, I would like to acknowledge the immense guidance, support and encouragement from my supervisor, Prof. Fu-Chun Zheng. He has always inspired me to aim higher and to keep on trying. Although separated by geographical distance, his commitment and dedication were highly evident throughout the whole research project. I am grateful for his invaluable advice and guidance which has enabled me to not only complete this dissertation but also become a better researcher.

My sincere thanks to Prof. Mike Faulkner for including me in the group's enriching research activities. I would also like to thank Assoc. Prof. Stephen Collins, Prof. Richard Thorn and Assoc. Prof. Aladin Zayegh for their kind support.

I gratefully acknowledge the financial support provided through the Faculty of Health, Engineering and Science Research Scholarship from Victoria University. I am also grateful to the management of Universiti Teknologi PETRONAS for their continual support.

I would like to especially acknowledge Rizwan Ahmad for the many helpful technical discussions. The assistance of Dr. Aruna Jayasuriya in OPNET is also much appreciated.

Special thanks to my colleagues who have shared this journey with me through its highs and lows. The encouragements, memories and friendships of Rizwan, Vandana, Kevin, Mustafa, Alamgir, Waqas, Shabbir, Robab and Reza will always be remembered.

Last but most importantly, I would like to give thanks to God for His love, hope and strength that have sustained me throughout this whole time.

TABLE OF CONTENTS

Abstract	iii
Declaration	v
Acknowledgements	vi
Table of Contents	vii
List of Figures	x
List of Tables	xiii
Abbreviations	xiv
List of Symbols	xvi
1 Introduction	1
1.1 Wireless Local Area Networks	1
1.2 Channel Assignment in WLANs.....	2
1.3 Contributions of the Thesis	4
1.4 Thesis Overview	8
2 Literature Review	10
2.1 IEEE 802.11 Standards	11
2.1.1 WLAN Architectures	13
2.1.2 MAC Protocol	15
2.1.3 Performance Analysis of DCF	19
2.2 High Density WLANs	30
2.3 Centralized Channel Assignment Schemes.....	34
2.3.1 Utilization MinMax Scheme	35
2.3.2 Degree of Saturation Scheme	40
2.3.3 Degree of Saturation with Cost Scheme	43
2.4 Distributed Channel Assignment Schemes	46
2.4.1 Weighted Coloring Scheme	47
2.4.2 Communication-Free Learning Scheme.....	51
2.4.3 Local Throughput Maximization Scheme.....	54

2.5	Summary	56
3	Minimum Neighbour Scheme	57
3.1	Minimum Neighbour Scheme	58
3.1.1	Minimum Neighbour Algorithm	58
3.1.2	Equal Candidate Channels	61
3.1.3	Asynchronous Operation	64
3.2	Performance Evaluation	66
3.2.1	Basic Performance	66
3.2.2	Number of Channels	72
3.2.3	Deployment Densities	76
3.2.4	Non-Uniform Topologies	78
3.2.5	Dynamic Topologies	82
3.2.6	Heterogeneous Networks	86
3.3	Summary	91
4	Minimum Neighbour with EKF Estimator Scheme	93
4.1	Estimation of the Total Number of Nodes	94
4.2	Estimation of the Number of Neighbour Nodes	102
4.3	Minimum Neighbour with EKF Estimator Scheme	105
4.4	Performance Evaluation	111
4.4.1	Upper Bound Performance	114
4.4.2	Normalized Density	116
4.4.3	Non-Saturated Load	116
4.4.4	Unequal Load	118
4.4.5	Fairness	120
4.4.6	Scalability	122
4.5	Summary	123
5	Client Assisted Minimum Conflict Pairs Scheme	125
5.1	Impact of Interference on Throughput with Multiple APs	126
5.2	Minimum Conflict Pairs Scheme	141
5.3	Performance Evaluation	146
5.3.1	Number of Conflict Pairs	146
5.3.2	Throughput	152
5.4	Summary	156

6	Conclusions and Future Work	158
6.1	Conclusions.....	158
6.2	Suggestions for Future Work.....	161
	References	164
A	OPNET Simulation Development	175

LIST OF FIGURES

2.1	IEEE 802.11b/g channels in 2.4GHz ISM frequency band.....	12
2.2	IEEE 802.11a channels in 5GHz U-NII frequency band.....	12
2.3	Basic service set architectures.....	14
2.4	Extended service set architecture.....	14
2.5	Basic access mechanism.....	17
2.6	Hidden node problem.....	17
2.7	RTS/CTS access mechanism.....	18
2.8	Markov chain model for DCF.....	20
2.9	Saturation throughput for IEEE 802.11b.....	28
2.10	Saturation throughput for IEEE 802.11a.....	29
2.11	APs deployed in New York City from WiGLE.....	32
2.12	WLAN network and corresponding graph coloured by DSATUR scheme.....	42
2.13	Interference graph with maximum clique of four.....	42
3.1	Throughput and composite functions for IEEE 802.11b and IEEE 802.11a.....	60
3.2	Initial and final channel assignment for MINE scheme.....	65
3.3	Aggregate throughput for MINE algorithm and LS algorithm.....	68
3.4	Aggregate throughput for MINE scheme ($\pi = 1.0$) and LS scheme ($\pi = 0.5$)...	70
3.5	Aggregate throughput with dynamic loads for IEEE 802.11b.....	71
3.6	Aggregate throughput for MINE scheme and LS scheme with $D = 4$ and $D = 12$ channels.....	73
3.7	Aggregate throughput for MINE scheme with various D channels.....	74
3.8	Aggregate throughput for MINE scheme and LS scheme with dynamic loads for $D = 4$ and $D = 12$ channels.....	75
3.9	Aggregate throughput for MINE scheme and LS scheme with various deployment densities.....	77
3.10	Uniform, non-uniform and real topologies.....	79
3.11	Aggregate throughput for MINE scheme and LS scheme with various non-uniformity for IEEE 802.11b.....	81

3.12	Aggregate throughput for MINE scheme and LS scheme with various non-uniformity for IEEE 802.11a.....	81
3.13	Aggregate throughput for MINE scheme and LS scheme in dynamic topology	84
3.14	Channel switches required for convergence with various dynamic topologies.....	84
3.15	Iterations required for convergence with various dynamic topologies.....	85
3.16	Aggregate throughput for various percentages of APs that implement MINE scheme.....	88
3.17	Throughput decomposition gains for various percentages of APs that implement MINE scheme.....	88
3.18	Throughput decomposition for various percentages of APs that implement MINE scheme when 10% of APs implement DSATUR scheme.....	90
3.19	Throughput decomposition gains for various percentages of APs that implement MINE scheme when 10% of APs implement DSATUR scheme....	90
4.1	Function $n = g(p)$ for IEEE 802.11b and IEEE 802.11a.....	97
4.2	Function $p = h(n)$ data set and curve fitting for IEEE 802.11b and IEEE 802.11a.....	100
4.3	A simple topology of four APs used to illustrate the MINEK scheme	108
4.4	An illustration of the MINEK scheme.....	109
4.5	A topology realization for moderate density scenario.....	113
4.6	Performance of MINEK scheme benchmarked against upper bounds.....	115
4.7	Throughput of MINEK scheme for IEEE 802.11a and IEEE 802.11b.....	115
4.8	Throughput of MINEK and other schemes with various offered loads for IEEE 802.11b with high density	117
4.9	Throughput of MINEK and other schemes with unequal loads for IEEE 802.11b with high density	119
4.10	Fairness of MINEK and other schemes with various offered loads for IEEE 802.11b with high density	121
4.11	Normalized throughput gain when a percentage of all APs employ the MINEK scheme	123
5.1	Classification of interference scenarios.....	128

5.2	Topologies with expected maximum throughput for each interference class	132
5.3	Throughput for Class-I interference topologies.....	134
5.4	Throughput for Class-II interference topologies	135
5.5	Throughput for Class-III interference topologies	136
5.6	Aggregate throughput for Class-I interference topologies for basic access and RTS/CTS mechanisms.....	137
5.7	Aggregate throughput for Class-II interference topologies with parallel and single transmissions.....	138
5.8	Aggregate throughput for Class-III interference topologies with parallel and single transmissions.....	140
5.9	Number of conflict pairs for each interference class.....	143
5.10	Relation between the number of conflict pairs and throughput for all interference classes	144
5.11	Different levels of client spread for a 20 AP topology.....	149
5.12	Number of conflict pairs for MICPA scheme and MINE scheme with high client spread	150
5.13	Number of conflict pairs for MICPA scheme and MINE scheme with different levels of client spread for IEEE 802.11a	151
5.14	Number of conflict pairs for MICPA scheme and MINE scheme with different deployment densities for IEEE 802.11a	152
5.15	Throughput of MICPA, MINE and random schemes with different levels of client spread for IEEE 802.11a	153
5.16	Throughput of MICPA, MINE and random schemes with different deployment densities for IEEE 802.11a	155
A.1	Network, node and process models in OPNET.....	176
A.2	WLAN MAC process model.....	176

LIST OF TABLES

2.1	IEEE 802.11b DSSS and IEEE 802.11a OFDM specifications and additional parameters.....	28
2.2	Maximum number of neighbour APs measured in six US cities	32
2.3	AP densities in several world cities.....	33
3.1	Performance comparison of default and enhanced MINE algorithms.....	69
3.2	Number of iterations and channel switches required for convergence for MINE scheme and LS scheme	70
3.3	Throughput gain with dynamic loads for IEEE 802.11b.....	71
3.4	IEEE 802.11a number of channels according to regions/countries.....	73
3.5	Throughput gains with dynamic loads for various deployment densities	77
4.1	Channel assignment information.....	104
4.2	MINEK scheme parameters.....	113
5.1	Characteristics of the levels of client spread	147
5.2	Number of conflict pairs for MICPA scheme and MINE scheme.....	150
5.3	Throughput of MICPA scheme and MINE scheme with different levels of client spread	153
5.4	Throughput of MICPA scheme and MINE scheme with different deployment densities	155

ABBREVIATIONS

ACK	Acknowledgement
AP	Access Point
BSS	Basic Service Set
BSSID	Basic Service Set Identifier
CFL	Communication-Free Learning
CSMA/CA	Carrier Sense Multiple Access with Collision Avoidance
CTS	Clear-To-Send
CUSUM	Cumulative Summary
DCF	Distributed Coordination Function
DIFS	DCF Interframe Space
DSATUR	Degree of Saturation
EKF	Extended Kalman Filter
ESS	Extended Service Set
FER	Frame Error Rate
GPS	Global Positioning System
GUI	Graphical User Interface
IBSS	Independent Basic Service Set
ISM	Industrial, Scientific and Medical
LAN	Local Area Network
MAC	Medium Access Control
MICPA	Minimum Conflict Pairs
MINE	Minimum Neighbour
MINEK	Minimum Neighbour with EKF Estimator
NAV	Network Allocation Vector
OFDM	Orthogonal Frequency Division Multiplexing
P2P	Peer-To-Peer
PCF	Point Coordination Function
PHY	Physical Layer
RMSE	Root Mean Squared Error

RSSI	Received Signal Strength Indicator
RTS	Request-To-Send
SIFS	Short Interframe Space
SNR	Signal to Noise Ratio
U-NII	Unlicensed National Information Infrastructure
VOIP	Voice Over Internet Protocol
WiGLE	Wireless Geographic Logging Engine
WLAN	Wireless Local Area Network

LIST OF SYMBOLS

a	alarm threshold
$b_{i,k}$	stationary distribution of the Markov chain
$b(t)$	backoff counter stochastic process
B	number of time slots in each time step
c_i	empty/busy indicator at time slot i
C	set of discrete non-overlapping channels
CW	contention window
CW_{\max}	maximum contention window
CW_{\min}	minimum contention window
d_{\max}	channel corresponding to the maximum expected throughput
D	number of non-overlapping channels
E	set of edges between vertices
ECC	set of equal candidate channels
$f_T(n)$	saturation throughput function
g	normalized innovation
$g(p)$	number of nodes as a function of conditional collision probability
G	interference graph
h	sensitivity of the measurement
$h(n)$	inverse function of $g(p)$
K	Kalman gain
m	maximum retransmission count
m'	maximum backoff stage
M_d	set of neighbouring APs on channel d
M_d^*	set of neighbouring APs on channel d in the previous iteration
n	number of contending nodes
nco	number of clients in the overlapping region O
$ncoi$	number of clients in the overlapping region O belonging to AP- i
nci	number of clients belonging to AP- i
n_k	total number of nodes at time k

\hat{n}_k	estimated total number of nodes at time k
$\hat{n}_{k,i}$	estimated number of nodes by AP- i at time k
N	number of associated nodes
N_d	total number of neighbour nodes on channel d
N_{HYS}	minimum difference in the number of neighbour nodes
p	conditional collision probability
p_k	discrete time measurement of the conditional collision probability
P	error variance of the new estimate
P_s	probability that a given transmission is successful
P_{tr}	probability that at least one node transmits
P_D	percentage of APs on DSATUR scheme
P_M	percentage of APs on MINE scheme
P_R	percentage of APs on random scheme
$P(a,b)$	source node a and destination node b pair
q	ratio of the number of successful transmissions by an AP over the total
Q	variance of the state noise
r	transmission range
R	estimated variance of the measurement
s	number of successful transmissions by an AP
$s(t)$	backoff stage stochastic process
S	total number of successful transmissions
S_{TH}	number of successful packet transmissions threshold
t_h	duration of header transmission
t_p	duration of payload transmission
t_δ	duration of propagation delay
t_σ	duration of an empty time slot
T_c	average time for a collision
T_d	throughput of an AP on channel d
T_s	average time for a successful transmission
$Trn(a,b)$	transmission from node a to node b
T_{WAIT}	minimum time between successive channel changes
u_k	net difference in the number of nodes at time k

\hat{u}_k	estimated net difference in the number of nodes at time k
v	drift parameter
V	set of vertices
w	state noise
W	minimum contention window
XP	number of conflict pairs
Y	number of neighbour APs
z	innovation
γ	measured ratio of the number of successful transmissions by an AP over the total
δ	distance between two APs
λ	mean number of AP on/off switches
π	channel switching probability
τ	transmission probability in each time slot

INTRODUCTION

1.1 Wireless Local Area Networks

Wireless local area networks (WLANs) have come a long way since being introduced in the consumer market around a decade ago [1]. Once thought to be just a replacement for wires in a local area network, there are now numerous WLAN applications ranging from the provision of internet access to the unified interconnection of electronic devices which span across consumer and business spheres [2-4]. In fact, new applications are still being discovered and developed today.

WLANs have changed the way many of us communicate, work, play and live [5]. Increasingly, WLANs are becoming an integral part of our lives. On any given day, WLAN technology would have helped us to be better connected, to manage our personal matters, to complete a task and enjoy our leisure activities. It is not surprising then, that almost all personal computing and communication devices such as laptops, personal digital assistants and even mobile phones now come pre-equipped with WLAN capabilities [6-7].

On another front, WLANs have been deployed almost everywhere imaginable including homes, offices, cafes, shopping malls, universities, airports and even cities [8-9]. Because of this, it has become increasingly rare to be out of coverage. More often

than not, several WLAN hotspots or access points (APs) can be detected at the same location. The ubiquitous WLAN APs deployed today are expected to number in the millions and are expected to grow strongly in the years to come [10-11].

The popularity of WLANs can be attributed to a combination of factors. The most important factors are, firstly, users' demand for faster broadband connections while being mobile with the convenience of anytime, anywhere, and, secondly, vendors' offer of high performance interoperable WLAN equipment at affordable prices [12]. These factors have strongly driven the proliferation of WLANs, which has resulted in their high density deployments in many parts of the world.

1.2 Channel Assignment in WLANs

The increased density of WLAN deployments can provide a myriad of users with improved capacity, enhanced coverage and seamless wireless broadband services. However, the corresponding increases in contention and interference, which can lead to significant degradation of throughputs, have posed new challenges in channel assignment. These challenges have to be mitigated effectively so that users can continue to enjoy creative and innovative services provided through WLANs. This will in turn ensure the continued growth and success of WLANs well into the future.

When nearby APs are assigned the same channel, co-channel interference and contention may cause a drastic reduction in throughput. With the limited number of channels to choose from, assigning them to APs in a way that maximizes throughput becomes truly challenging. This is further exacerbated by the fact that typical dense deployments of WLANs are set up in an uncoordinated manner and belong to different owners [13]. The ad hoc deployment of APs can result in closely located APs that

cannot be assigned the same channels. Furthermore, having multiple administrative domains severely limits the amount of cooperation, communication and control of what channel assignment strategies are used among different APs.

Up until now, for a WLAN deployment of considerable size, an administrator will first perform a radio frequency site survey. Using the information gained, the number of APs needed and their locations are determined in order to meet throughput and coverage requirements. This is followed by manual assignment of channels to each of the APs [14-15]. On the other hand, for small deployments like those found in homes, a channel may be selected randomly, although in most cases the APs are just left to operate on the factory default channel [16]. These methods are becoming inadequate as WLAN deployments become denser.

Channel assignment in WLANs has also been traditionally carried out in a fixed or static manner. Fixed channel assignment can be effective in coordinated deployment of APs belonging to a single administrator or sparsely located APs owned by different entities. However, in high density WLAN deployments, the performance of a fixed channel assignment quickly degrades while a dynamic channel assignment that can exploit the varying nature of traffic loads and other dynamics of the network is vastly superior [17].

Channel assignment in WLANs is distinctly different from traditional cellular communications systems [18-19]. WLANs are mostly unplanned, have irregular coverage and the same channel is used for both control and data information. In WLANs, a node will only transmit if it senses the channel to be idle. If there is transmission or interference, the nodes will wait until the channel becomes clear before transmitting. This makes WLANs highly robust against interference but at the price of a degradation in throughput. Due to these unique characteristics, channel assignment

schemes designed for cellular networks are at best inefficient when applied to WLANs [20-21].

Due to these reasons, channel assignment in WLANs has received considerable attention in recent times. Several channel assignment schemes have been proposed by researchers in the literature. We have divided these schemes into two categories, namely centralized and distributed schemes. Centralized schemes leverage on information of the whole network while distributed schemes have access to only local information. However, the uncoordinated nature in high density WLAN deployments prohibits the use of centralized schemes. Thus, only distributed schemes, which have to deal with imperfect information and lack of synchronization, can be applied.

Adopting a practical approach, we endeavour to develop channel assignment schemes that are effective, distributed, dynamic and have low complexity but are still able to provide acceptable performance. Finally, it can be concluded that channel assignment for throughput enhancement in high density WLANs is a very practical, important, interesting and challenging problem today that has significant impact not only for the present but also for the future.

1.3 Contributions of the Thesis

The main objective of this thesis is to investigate and develop practical channel assignment schemes in high density WLANs that can provide superior throughputs. In doing so, the relevant features of WLAN operation and characteristics of high density WLAN deployments are always kept in mind. As a result, several novel channel assignment schemes that possess the desirable attributes are proposed. The main contributions of this thesis can be summarized as follows:

- Identifies the features and performance analysis of IEEE 802.11 medium access mechanisms, and the characteristics of high density WLAN deployments that are pertinent to channel assignment.
- Performs a critical review of existing channel assignment schemes in WLANs and proposes a useful classification of these schemes.
- Proposes the minimum neighbour (MINE) channel assignment scheme, which maximizes throughputs by selecting the channel with the minimum number of active neighbour nodes.
- Performs extensive performance evaluation of the MINE scheme in a wide variety of realistic conditions by considering the numbers of channels, deployment densities, non-uniform topologies, dynamic topologies and heterogeneous networks.
- Proposes the minimum neighbour with extended Kalman filter estimator (MINEK) channel assignment scheme, which allows the practical estimation of the number of active neighbour nodes and exploits the channel switching information of neighbouring APs.
- Develops OPNET network simulations that accurately model the behaviour and performance of channel assignment schemes in realistic WLAN networks. Implements MINEK and several other channel assignment schemes in OPNET.
- Performs extensive performance evaluation of the MINEK scheme across several performance metrics and factors which include upper bound performance, normalized density, non-saturated loads, unequal loads, fairness and scalability.
- Performs a study on the impact of interference on throughput with multiple APs using a novel approach that determines the possibility of parallel transmissions. Presents a useful and practical classification of interference scenarios.

- Proposes the client assisted minimum conflict pairs (MICPA) channel assignment scheme, which uses clients' measurements to assist the AP in selecting the channel with the minimum number of conflict pairs in order to maximize its expected throughputs.
- Performs extensive performance evaluation of the MICPA scheme by considering different levels of client spread and deployment density. Investigates the conditions in which the client assisted MICPA scheme is best deployed.

These contributions have led to the following publications:

1. M. Driberg, F.-C. Zheng and R. Ahmad, "MINEK: A Practical Distributed Channel Assignment Scheme for Dense WLANs," accepted for publication in *IET Communications*.
2. M. Driberg, F.-C. Zheng and R. Ahmad, "MICPA: A Client Assisted Channel Assignment Scheme for Throughput Enhancement in WLANs," submitted to *IEEE Transactions on Wireless Communications*.
3. M. Driberg, F.-C. Zheng, R. Ahmad, and M. Fitch, "Impact of Interference on Throughput in Dense WLANs with Multiple APs," in *Proc. IEEE International Symposium on Personal, Indoor and Mobile Radio Communications (PIMRC)*, Tokyo, Japan, Sept. 2009, pp. 752-756.
4. M. Driberg, F.-C. Zheng, R. Ahmad, and M. Fitch, "Performance of Asynchronous Channel Assignment Scheme in Non-Uniform and Dynamic Topology WLANs," in *Proc. IEEE International Symposium on Personal, Indoor and Mobile Radio Communications (PIMRC)*, Tokyo, Japan, Sept. 2009, pp. 2085-2089.

5. M. Drieberg, F.-C. Zheng, and R. Ahmad, "Evaluation of Asynchronous Channel Assignment Scheme in Heterogeneous WLANs," in *Proc. ACoRN Workshop on Multihop Wireless Networking Workshop*, Sydney, Australia, July 2009.
6. M. Drieberg, F.-C. Zheng, R. Ahmad, S. Olafsson, and M. Fitch, "Effectiveness of Asynchronous Channel Assignment Scheme in Heterogeneous WLANs," in *Proc. IEEE International Symposium on Wireless and Pervasive Computing (ISWPC)*, Melbourne, Australia, Feb. 2009, pp. 1-5.
7. M. Drieberg, F.-C. Zheng, and R. Ahmad, "Performance Evaluation of Asynchronous Channel Assignment Scheme for Dense WLANs," in *Proc. ACoRN Workshop on Co-operative Wireless Communications*, Melbourne, Australia, July 2008.
8. M. Drieberg, F.-C. Zheng, R. Ahmad, and S. Olafsson, "An Asynchronous Distributed Dynamic Channel Assignment Scheme for Dense WLANs," in *Proc. IEEE International Conference on Communications (ICC)*, Beijing, China, May 2008, pp. 2507-2511.
9. M. Drieberg, F.-C. Zheng, R. Ahmad, and S. Olafsson, "An Asynchronous Channel Assignment Scheme: Performance Evaluation," in *Proc. IEEE Vehicular Conference (VTC) Spring*, Singapore, May 2008, pp. 2147-2151.
10. M. Drieberg, F.-C. Zheng, R. Ahmad, and S. Olafsson, "An Improved Distributed Dynamic Channel Assignment Scheme for Dense WLANs," in *Proc. International Conference on Information, Communications and Signal Processing (ICICS)*, Singapore, Dec. 2007, pp. 1-5.

1.4 Thesis Overview

The remainder of the thesis is organized as follows. In Chapter 2, a review of the relevant literature is presented. Firstly, an introduction to the IEEE 802.11 standards with an emphasis on its medium access mechanisms is given. Next, the pertinent characteristics and new challenges in channel assignment faced by high density WLAN deployments are highlighted. Finally, a critical review of existing channel assignment schemes is presented.

In Chapter 3, the minimum neighbour (MINE) channel assignment scheme is proposed. Initially, a detailed description of the MINE scheme is given. This includes the formulation of the minimum neighbour algorithm, the selection of equivalent candidate channels and the asynchronous operation of the scheme. This is followed by extensive performance evaluation of the MINE scheme. In this, its basic performance and its performance in a wide variety of realistic scenarios are shown.

The minimum neighbour with extended Kalman filter estimator (MINEK) channel assignment scheme is proposed in Chapter 4. The MINEK scheme provides fast and accurate estimates of the number of neighbour nodes, which is critical to the application of the MINE scheme to practice. Firstly, the extended Kalman filter (EKF) estimator used to estimate the total number of nodes is described. Next, the number of nodes by AP estimate, which allows the estimation of the number of neighbour nodes, is derived. This is followed by the description of the complete MINEK scheme. The simulation development in OPNET is presented next. Finally, extensive performance evaluation of the MINEK scheme through packet level simulations is presented.

In Chapter 5, client assisted channel assignment is investigated. A study on the impact of interference on throughput with multiple APs is presented. This is followed by the

identification of the number of conflict pairs, which is a metric shown to correlate well with the expected throughput. The proposed client assisted minimum conflict pairs (MICPA) scheme, which uses clients' measurements to assist the AP in selecting the channel with the minimum number of conflict pairs, is fully described next. Lastly, extensive performance evaluation of the MICPA scheme and comparisons with other schemes are shown. Chapter 6 concludes the thesis and provides suggestions for future work.

LITERATURE REVIEW

In the previous chapter, an introduction to channel assignment in WLANs and the objectives and contributions of the research were presented. In this chapter, a critical review of the relevant literature is undertaken. This provides the necessary background information and lays a solid foundation for the thesis and material in subsequent chapters.

Any study of WLANs is incomplete without an understanding of the IEEE 802.11 standards. With regards to this, the pertinent features of IEEE 802.11 are summarized and presented. Due to its operation in unlicensed bands, the main component of IEEE 802.11 lies in its medium access. Because of this reason, medium access mechanisms and their performance analysis are explored in detail. The latter provides an invaluable analytical framework for predicting the performance of WLANs.

Millions of WLANs have been deployed and are in operation today. The majority of these are small scale deployments consisting of several APs. Since they can be deployed by anyone, these WLANs are mostly unplanned, uncoordinated and unmanaged. Coupled with the increasing popularity of WLAN technology, the advent of high density WLANs became inevitable. The characteristics of these high density WLANs are investigated. These findings provide the motivation and an appreciation for the

challenges faced with regards to channel assignment in WLANs.

A critical review of existing channel assignment schemes in the literature is presented. Due to their important distinct differences, we propose a useful classification that groups them into two categories. Centralized schemes are schemes that utilize information of the whole network. On the contrary, distributed schemes make use of only local information. Due to the inherent lack of coordination and communication, distributed schemes are particularly well suited for the majority of WLANs.

This chapter is organized as follows. In Section 2.1, the IEEE 802.11 standard features, medium access mechanisms and their performance analysis are presented. Next, high density WLAN deployments are investigated in Section 2.2. In Section 2.3 and Section 2.4, centralized and distributed channel assignment schemes are respectively reviewed. Finally, the chapter is summarized in Section 2.5.

2.1 IEEE 802.11 Standards

The growth and success of WLANs have been nothing less than spectacular. Today, they are a key component of the pervasive communication environment that we live in. One of the reasons for the phenomenal success of WLANs lies in the interoperability of devices across vendors, through the adoption of IEEE 802.11 standards by industry consortium Wi-Fi Alliance.

The IEEE 802.11 group of standards is the de-facto standard for WLANs [22-23]. It specifies three high speed physical layer (PHY) technologies, namely the IEEE 802.11a, IEEE 802.11b and IEEE 802.11g [24-26]. IEEE 802.11b uses Direct Sequence Spread Spectrum (DSSS) while IEEE 802.11a/g employ Orthogonal Frequency Division

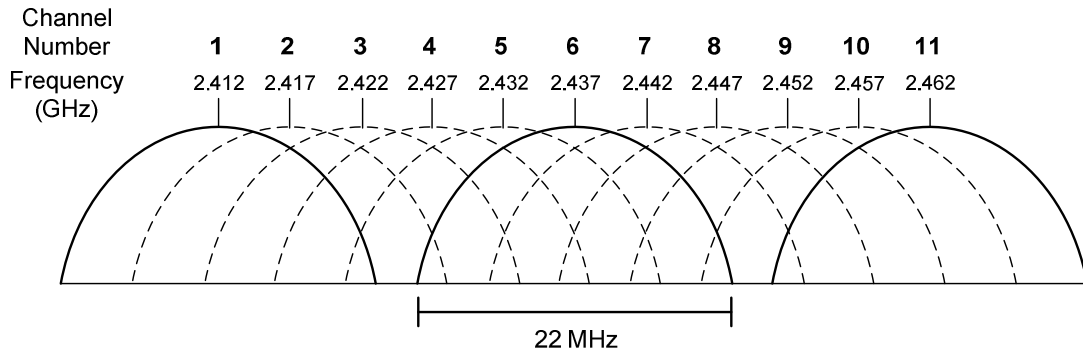


Figure 2.1: IEEE 802.11b/g channels in 2.4GHz ISM frequency band.

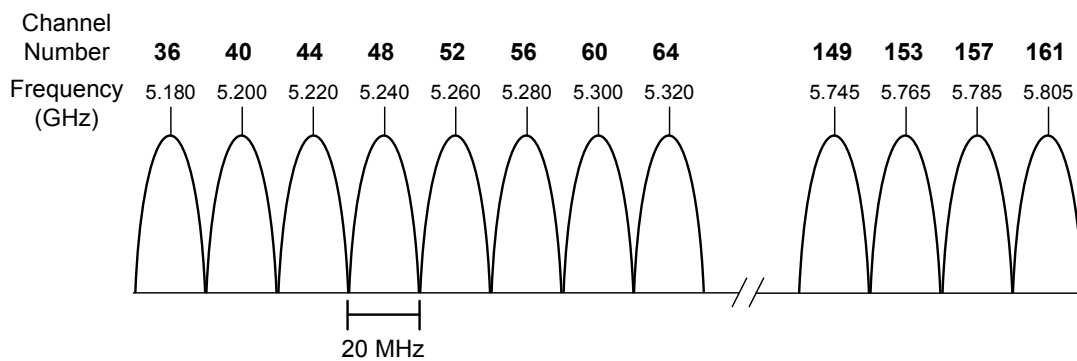


Figure 2.2: IEEE 802.11a channels in 5GHz U-NII frequency band.

Multiplexing (OFDM). IEEE 802.11b offers data rates of 1, 2, 5.5 and 11 Mbps while IEEE 802.11a/g support data rates from 6 up to 54 Mbps.

Both IEEE 802.11b/g utilize the unlicensed 2.4 GHz industrial, scientific and medical (ISM) band. On the other hand, IEEE 802.11a operates on the 5 GHz unlicensed national information infrastructure (U-NII) band. As shown in Fig. 2.1, there are 11 channels in the ISM band, which are spaced 5 MHz apart. However, the IEEE 802.11b/g signals occupy a bandwidth of 22 MHz. In order to avoid interference from adjacent channels, a minimum separation of five channels is required. Therefore, only 3 non-overlapping channels are available, namely Channel 1, Channel 6 and Channel 11. In the U-NII band, the number of channels available is higher. As is shown in Fig. 2.2,

with an IEEE 802.11a signal bandwidth of 20 MHz, 12 non-overlapping channels can be used.

2.1.1 WLAN Architectures

The IEEE 802.11 WLAN architecture consists of components that interact to provide the prescribed services [27-28]. The basic building block of this architecture is the basic service set (BSS). A BSS is a set of nodes (or stations) that communicate among themselves. The most basic WLAN is the independent BSS (IBSS), which consists of nodes without any connection to an external network. In an IBSS, all nodes communicate directly with one another. These types of networks are typically created on an ad hoc basis, have a short lifespan and serve a specific purpose, such as exchanging contacts or sharing presentation files.

As one may expect, the utility of an IBSS is quite limited. In order to communicate with nodes that are farther away or in another network, an infrastructure BSS has to be used. The central component of an infrastructure BSS is the AP, which normally provides the connection to a wired local area network (LAN) and eventually to the internet. In infrastructure BSS, all nodes communicate through the AP, even if the node wants to communicate to another node in the same BSS. Before a node can transmit data through the AP, it has to first be associated to the AP by exchanging important information such as radio synchronization and supported data rates. The infrastructure BSS is simply referred to as a BSS. Fig. 2.3 illustrates the independent and infrastructure BSSs. Not surprisingly, the majority of WLANs which are deployed in homes, offices and small businesses are infrastructure BSSs.

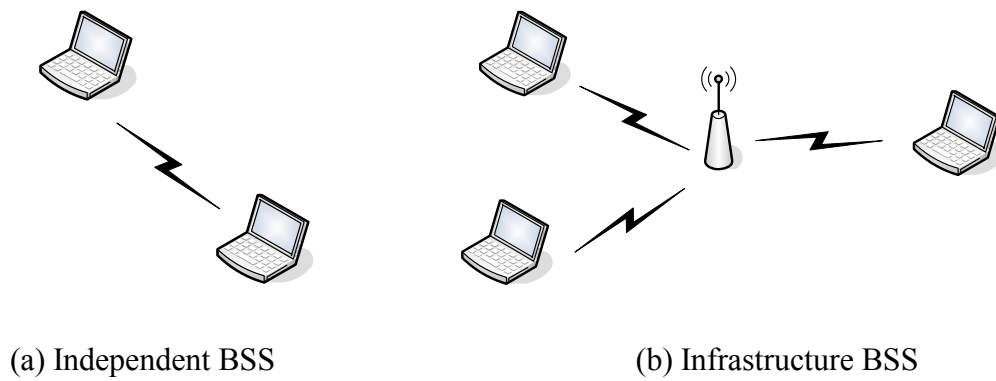


Figure 2.3: Basic service set architectures.

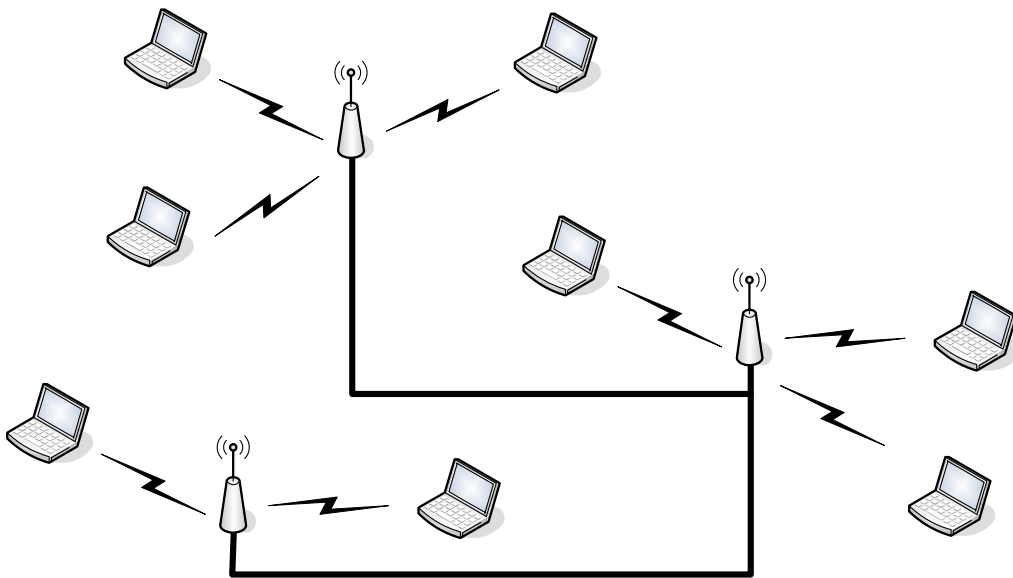


Figure 2.4: Extended service set architecture.

Finally, it may be desirable to interconnect several infrastructure BSSs to form an extended service set (ESS) for extended coverage, internetworking between BSSs and node mobility. In ESS, APs communicate and cooperate to forward traffic and facilitate movement of nodes between BSSs. This communication normally takes place through a wired LAN. Fig. 2.4 shows an example of ESS architecture. ESSs are commonly deployed in places such as university campuses and large corporations.

2.1.2 MAC Protocol

The IEEE 802.11 specifies a common medium access control (MAC) which provides reliable data delivery and coordinates the access among nodes to the shared wireless channel. The fundamental access method of the MAC is called distributed coordination function (DCF). The DCF is a random access scheme, based on carrier sense multiple access with collision avoidance (CSMA/CA). Using this protocol, a node will only transmit if it senses the channel to be idle. In order to avoid collisions, a binary exponential backoff procedure is adopted.

The standard also defines an optional access method called the point coordination function (PCF). PCF allows the transmission of time sensitive data in a contention-free period, which alternates with a contention period complying with DCF. With PCF, a point coordinator, which is implemented in the AP, coordinates the transmissions of nodes by polling them one at a time. The operation of PCF with multiple APs within interference range may require additional coordination, which is not specified in the standard. Due to this and other ambiguities, the vast majority of vendors have not implemented PCF in their APs [29-31]. Furthermore, PCF is also not specified in the interoperability requirements of Wi-Fi Alliance. Therefore PCF will not be discussed further.

In DCF, a node that wants to transmit has to first sense the channel to determine if it is busy or idle. This is the carrier sensing feature of the protocol. Two mechanisms for carrier sensing are used, namely physical sensing and virtual sensing. In physical sensing, a node listens to the channel to determine if there are any ongoing transmissions. With virtual sensing, reservation information in the form of network allocation vectors (NAVs) is read from packet headers. Keeping track of NAVs allows

nodes to know of impending packet transmissions from other nodes. If either sensing mechanisms indicates a busy channel, the channel is determined as busy. Otherwise, the channel is determined as idle.

If the channel has been idle for a period of more than DCF interframe space (DIFS), the node may transmit immediately. However, if the channel is sensed to be busy, it has to wait until the channel becomes idle for a DIFS. At this point, the node generates a random backoff interval. The backoff counter is decreased as long as the channel is idle and is frozen when the channel is busy. Once the counter reaches zero, the node is allowed to transmit. The random backoff interval prevents the simultaneous transmissions of several nodes right after the channel becomes idle, which results in a collision. This is the collision avoidance feature of the protocol.

The DCF utilizes a slotted binary exponential backoff scheme. This means that nodes can only transmit at the beginning of each time slot. The backoff interval is chosen uniformly in the range $[0, CW-1]$ where CW is the contention window. The value of CW depends on the number of previously failed transmissions. Initially, CW is set to CW_{\min} , the minimum contention window. After each failed transmission, CW is doubled, up to the maximum value of CW_{\max} , the maximum contention window. After a successful transmission, CW is reset back to CW_{\min} .

There are two mechanisms for packet transmissions in DCF. The default scheme is a two-way handshaking technique (DATA-ACK), known as the basic access mechanism. As shown in Fig. 2.5, a source node sends a DATA frame and waits for an acknowledgement (ACK). After a successful reception, the destination node waits for a duration of short interframe space (SIFS) and replies with a positive acknowledgement. Note that SIFS is shorter than DIFS, which enables higher priority for control frames such as ACK frames. In the wireless medium, an explicit acknowledgement is required

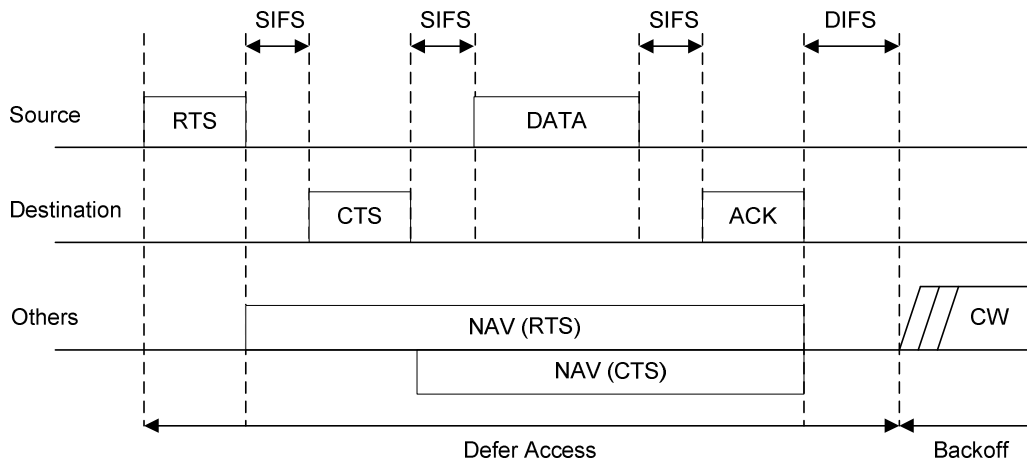


Figure 2.7: RTS/CTS access mechanism.

hear the source node interfere with the latter's transmission due to their close proximity to the destination node. The hidden node problem is easily illustrated by an example. Consider the WLAN network in Fig. 2.6 that consists of an AP, Node A and Node B. Now, the AP is in the transmission range of both nodes. However, Node A is out of the transmission range of Node B and vice versa. Here lies the problem, when Node A transmits to the AP, Node B which cannot hear the ongoing transmission may start its own transmission and cause a collision. Thus, Node B is a hidden node to Node A and vice versa.

Fig. 2.7 shows the packet exchanges involved in the RTS/CTS mechanism. A source node sends a RTS frame to inform the destination and other nodes of its intention to transmit a DATA frame. If the RTS is received successfully, the destination node replies with CTS. Note that CTS would have notified any hidden nodes of the impending DATA transmission. After receiving CTS, the source node proceeds by sending DATA. Finally, the destination node replies with an ACK. Since collisions may only occur for RTS, which is generally shorter than DATA, the RTS/CTS mechanism can shorten the

duration of collisions. The problem of hidden nodes is also minimized because other nodes defer their transmissions based on the NAVs contained in RTS and CTS.

Whether the basic access mechanism or the RTS/CTS mechanism is employed can be configured by specifying an appropriate value for the RTS threshold. The RTS threshold specifies the packet size and packets larger than this are transmitted using RTS/CTS mechanism. For example, if the RTS threshold is set to 0 bytes, all packets will be transmitted using the RTS/CTS mechanism. If one desires to only employ the basic access mechanism, the RTS threshold should be set to 2347 bytes, which is the maximum allowable packet size. A setting between these two values means that packets smaller than or equal to the threshold are sent using the basic access mechanism while larger packets are sent using the RTS/CTS mechanism. The default RTS threshold setting on most APs is around 500 bytes.

2.1.3 Performance Analysis of DCF

In his seminal paper, Bianchi proposed a two-dimensional Markov chain model for analyzing the saturation throughput of IEEE 802.11 DCF [35]. The proposed analytical model is simple yet highly accurate. The saturation throughput is defined as the throughput limit reached as the offered load is increased. It is also the maximum throughput that can be obtained in stable conditions. In the analysis, the following assumptions are made: the channel is ideal (no errors), all nodes can hear each other (no hidden nodes) and all nodes always have packets to send (saturated). Later, Wu et al. modified Bianchi's model (that assumed infinite retry) to take into account finite retry limit, as specified in the standard [36].

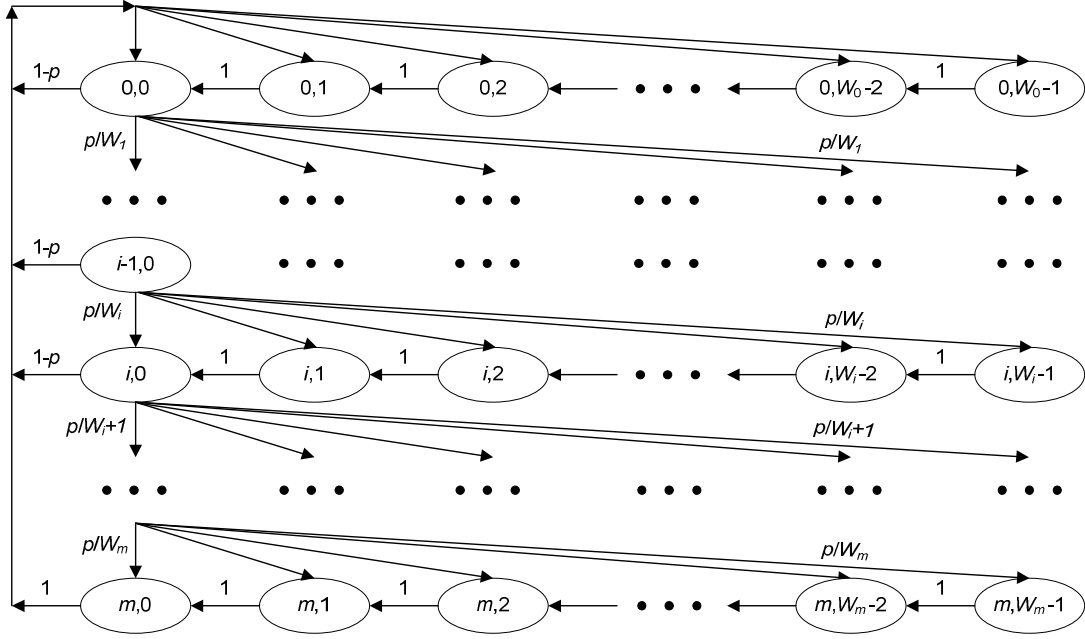


Figure 2.8: Markov chain model for DCF.

Consider a fixed number of n contending nodes. Let $b(t)$ and $s(t)$ be the stochastic processes representing the backoff counter and backoff stage of a given node at time t respectively. The key approximation in this model is the assumption that the collision probability of a packet transmitted by each node is constant and independent of previous retransmissions. The conditional collision probability, p , refers to the probability of a collision conditioned upon a packet being transmitted. With this assumption, the bi-dimensional process $\{s(t), b(t)\}$ can be modeled as a two-dimensional Markov chain, as shown in Fig. 2.8. Note that (2.1.1) – (2.1.19) can be found in [35-36].

The following notations are used in the analysis: $W = CW_{\min}$ and

$$\begin{cases} W_i = 2^i W & i \leq m' \\ W_i = 2^{m'} W & i > m' \end{cases} \quad 0 \leq i \leq m \quad (2.1.1)$$

where i is the backoff stage, m and m' are the maximum retransmission count and maximum backoff stage respectively. The maximum retransmission count is the number of retries for a packet before it is discarded. The maximum backoff stage, $m' = \log_2(CW_{\max}/CW_{\min})$. The values of CW_{\min} and CW_{\max} are standardized and PHY dependent.

A node that has new packets to send begins at the top of the Markov chain. It firstly chooses a random value from the initial contention window range of $[0, W_0-1]$ for the backoff counter and occupy the corresponding state on the zeroth backoff stage. After the medium is sensed idle for the required DIFS, the backoff counter is decremented every time an idle slot time elapses. This is represented by the right-to-left state transition on the same backoff stage. When the backoff counter reaches zero, the node will transmit the packet. If the transmission is successful, a transition to the top of the Markov chain follows and the process repeats from the beginning for the next packet.

However, if the transmission is unsuccessful due to collision, the backoff stage will be incremented and a new backoff counter value will be chosen randomly from the now doubled-contention window range $[0, W_1-1]$. This is represented by an up-to-down state transition to the corresponding first backoff stage state. For every subsequent unsuccessful transmission, an up-to-down transition to the corresponding incremented backoff stage state will take place. Finally, at the maximum backoff stage state, which corresponds to the maximum retransmission count, the packet will be discarded if the transmission is still unsuccessful. Therefore, from this state, the only transition is back to the top of the Markov chain on the zeroth backoff stage state where the process is repeated for a new packet.

Therefore, in the Markov chain, the nonzero one-step transition probabilities are

$$\begin{cases} P\{i, k | i, k+1\} = 1 & k \in [0, W_i - 2], i \in [0, m] \\ P\{0, k | i, 0\} = (1-p)/W_0 & k \in [0, W_0 - 1], i \in [0, m-1] \\ P\{i, k | i-1, 0\} = p/W_i & k \in [0, W_i - 1], i \in [1, m] \\ P\{0, k | m, 0\} = 1/W_0 & k \in [0, W_0 - 1] \end{cases} \quad (2.1.2)$$

The first equation in (2.1.2) accounts for the decrements of the backoff counter at the beginning of each empty time slot. The second equation shows that after a successful transmission, a new packet starts from the zeroth backoff stage. After an unsuccessful transmission, the backoff stage increases, as shown in the third equation. Finally, the fourth equation reflects the fact that at the maximum retry limit, regardless of whether the transmission is successful or not, a new packet is started from the zeroth backoff stage.

It is important to keep in mind the intermediate goal of the following analysis, which is to express the probability, τ , that a node transmits in a randomly chosen time slot as a function of p . Note that the time slot here is defined as the variable time between two consecutive decrements of the backoff counter. Let $b_{i,k} = \lim_{t \rightarrow \infty} P\{s(t) = i, b(t) = k\}$, $i \in (0, m)$, $k \in (0, W_i - 1)$ be the stationary distribution of the Markov chain. Firstly, the steady-state probability of each state, $b_{i,k}$ is expressed as a function of $b_{0,0}$. Note that

$$b_{i-1} \cdot p = b_{i,0} \quad 0 < i \leq m, \quad (2.1.3)$$

which gives

$$b_{i,0} = p^i b_{0,0} \quad 0 \leq i \leq m. \quad (2.1.4)$$

Due to the regular structure of the chain, where $b_{i,k}$ can be recursively determined from the steady-state probabilities of W_i-k+1 preceding states on the same i^{th} backoff stage, for each $k \in (0, W_i - 1)$, we have

$$b_{i,k} = \frac{W_i - k}{W_i} \left\{ \begin{array}{ll} (1-p) \sum_{j=0}^{m-1} b_{j,0} + b_{m,0} & i = 0 \\ p \cdot b_{i-1,0} & 0 < i \leq m \end{array} \right\}. \quad (2.1.5)$$

Using (2.1.4) and the fact that $b_{0,0} = (1-p) \sum_{j=0}^{m-1} b_{j,0} + b_{m,0}$, (2.1.5) can be rewritten as

$$b_{i,k} = \frac{W_i - k}{W_i} b_{i,0} \quad 0 \leq i \leq m. \quad (2.1.6)$$

So, by (2.1.4) and (2.1.6), the steady-state probability of every state, $b_{i,k}$ is now expressed as functions of $b_{0,0}$ and p .

At this stage, there are two distinct cases in the model:

Case i) $m \leq m'$ (packet will be discarded after $m+1$ trials and every stage involves an increasing contention window) and

Case ii) $m > m'$ (CW_{\max} is reached after $m'+1$ trials and remains the same for next $m-m'$ stages).

Applying the normalization condition, $b_{0,0}$ can be determined as follows:

Case i) $m \leq m'$

$$\begin{aligned} 1 &= \sum_{i=0}^m \sum_{k=0}^{W_i-1} b_{i,k} = \sum_{i=0}^m b_{i,0} \sum_{k=0}^{W_i-1} \frac{W_i - k}{W_i} = \sum_{i=0}^m b_{i,0} \frac{W_i + 1}{2} \\ &= \sum_{i=0}^m b_{0,0} \cdot p^i \frac{2^i W + 1}{2} \\ &= \frac{b_{0,0}}{2} \left[W \frac{(1 - (2p)^{m+1})}{(1 - 2p)} + \frac{(1 - p^{m+1})}{(1 - p)} \right] \end{aligned} \quad (2.1.7)$$

which, after some manipulation, gives,

$$b_{0,0} = \frac{2(1-2p)(1-p)}{W(1-p)(1-(2p)^{m+1}) + (1-2p)(1-p^{m+1})}. \quad (2.1.8)$$

Case ii) $m > m'$

$$\begin{aligned} 1 &= \sum_{i=0}^m \sum_{k=0}^{W_i-1} b_{i,k} = \sum_{i=0}^m b_{i,0} \sum_{k=0}^{W_i-1} \frac{W_i - k}{W_i} = \sum_{i=0}^m b_{i,0} \frac{W_i + 1}{2} \\ &= \sum_{i=0}^{m'} b_{0,0} \cdot p^i \frac{2^i W + 1}{2} + \sum_{i=m'+1}^m b_{0,0} \cdot p^i \frac{2^{m'} W + 1}{2} \\ &= \frac{b_{0,0}}{2} \left[\sum_{i=0}^{m'} ((2p)^i W + p^i) + \sum_{i=m'+1}^m (p^i 2^{m'} W + p^i) \right] \\ &= \frac{b_{0,0}}{2} \left[W \left[\sum_{i=0}^{m'} (2p)^i + \sum_{i=m'+1}^m (p^i 2^{m'}) \right] + \sum_{i=0}^m p^i \right] \\ &= \frac{b_{0,0}}{2} \left[W \left[\frac{(1-(2p)^{m'+1})}{(1-2p)} + \frac{2^{m'} p^{m'+1} (1-p^{m-m'})}{(1-p)} \right] + \frac{(1-p^{m+1})}{(1-p)} \right] \end{aligned} \quad (2.1.9)$$

which gives

$$b_{0,0} = \frac{2(1-2p)(1-p)}{W \left[(1-p)(1-(2p)^{m'+1}) + 2^{m'} p^{m'+1} (1-p^{m-m'}) (1-2p) \right] + (1-2p)(1-p^{m+1})}. \quad (2.1.10)$$

Now, the probability τ that a node transmits in a randomly chosen time slot can be determined. Since transmissions occur when the backoff timer reaches zero, regardless of the backoff stage,

$$\tau = \sum_{i=0}^m b_{i,0} = \frac{1-p^{m+1}}{1-p} b_{0,0} \quad (2.1.11)$$

which is obtained using (2.1.4) and summation of the geometric series. Therefore, the expression for τ is as follows:

Case i) $m \leq m'$

$$\tau = \frac{2(1-2p)(1-p^{m+1})}{W(1-p)(1-(2p)^{m+1}) + (1-2p)(1-p^{m+1})}. \quad (2.1.12)$$

Case ii) $m > m'$

$$\tau = \frac{2(1-2p)(1-p^{m+1})}{W[(1-p)(1-(2p)^{m+1}) + 2^{m'} p^{m'+1}(1-p^{m-m'})(1-2p)] + (1-2p)(1-p^{m+1})}. \quad (2.1.13)$$

Although τ has been expressed in terms of p , the value of p is still unknown. It is important to note that the probability p that a transmitted packet collides is equal to the probability that at least one of the remaining $n-1$ nodes transmits. Furthermore, in steady state, every node transmits with probability τ . This gives

$$p = 1 - (1 - \tau)^{n-1}. \quad (2.1.14)$$

Therefore (2.1.12) to (2.1.14) represent a nonlinear system in the two unknowns τ and p , which can be solved numerically. At this stage, the derivations of τ and p are complete.

The analysis proceeds by determining the probability and average duration of each event that can happen in a time slot, with the eventual aim of obtaining the saturation throughput. Let P_{tr} be the probability that there is at least one transmission in the considered time slot. With n contending nodes that each transmits with probability τ ,

$$P_{tr} = 1 - (1 - \tau)^n. \quad (2.1.15)$$

Let P_s be the probability that a transmission is successful, given that there is at least one transmission. Note that a transmission is successful if there is exactly one transmission.

Therefore,

$$P_s = \frac{n\tau(1-\tau)^{n-1}}{P_r} = \frac{n\tau(1-\tau)^{n-1}}{1-(1-\tau)^n}. \quad (2.1.16)$$

Now, the normalized saturation throughput $f_T(n)$, which is defined as the fraction of time that the channel is used to successfully transmit payload bits, can be expressed as

$$\begin{aligned} f_T(n) &= \frac{E[\text{time to transmit payload information in a time slot}]}{E[\text{length of a time slot}]} \\ &= \frac{P_r P_s E[t_p]}{(1-P_r)t_\sigma + P_r P_s T_s + P_r(1-P_s)T_c} \end{aligned} \quad (2.1.17)$$

where $E[t_p]$ is the average time taken to transmit payload, t_σ is the duration of an empty time slot and T_s and T_c are the average time for a successful transmission and a collision, respectively. Note that the average length of a time slot is obtained by observing that an empty time slot, a successful transmission and a collision occur with probabilities $(1-P_r)$, $P_r P_s$ and $P_r(1-P_s)$, respectively.

Next, the expressions for T_s and T_c are determined. Let t_h be the time taken to transmit the packet header and t_δ be the propagation delay. As expected, T_s and T_c differ for basic access and RTS/CTS mechanisms. For basic access,

$$\begin{cases} T_s^{bas} = t_h + E[t_p] + t_\delta + SIFS + ACK + t_\delta + DIFS \\ T_c^{bas} = t_h + E[t_p^*] + t_\delta + DIFS \end{cases} \quad (2.1.18)$$

where $E[t_p^*]$ is the average time taken to transmit the longest payload. For RTS/CTS,

$$\begin{cases} T_s^{rts} = RTS + t_\delta + SIFS + CTS + t_\delta + SIFS + t_h + E[t_p] + t_\delta + SIFS \\ \quad + ACK + t_\delta + DIFS \\ T_c^{rts} = RTS + t_\delta + DIFS \end{cases} \quad (2.1.19)$$

Finally, given the standard specifications and values of related parameters, the saturation throughput of IEEE 802.11 DCF can be determined for any number of contending nodes using (2.1.17).

Let us apply the performance analysis to practical examples based on IEEE 802.11b and IEEE 802.11a (IEEE 802.11g is omitted due to its performance being very similar to IEEE 802.11a because both use OFDM PHY). The standard specifications for IEEE 802.11b and IEEE 802.11a and additional parameters are shown in Table 2.1. The analytical saturation throughput is generated for both basic access and RTS/CTS mechanisms and several combinations of data and control rates that are of most interest. Note that for each combination, the control rate used cannot be higher than the data rate. The notation *access mechanism (data rate, control rate)* is used to provide a unique reference for each combination of data and control rates. For example, basic access (11,1) refers to basic access mechanism with data rate of 11 Mbps and control rate of 1 Mbps. Fig. 2.9 and Fig 2.10 show the analytical saturation throughput obtained for IEEE 802.11b and IEEE 802.11a, respectively.

TABLE 2.1

IEEE 802.11b DSSS and IEEE 802.11a OFDM specifications and additional parameters

	IEEE 802.11b DSSS	IEEE 802.11a OFDM
Packet Payload	1024 bytes	1024 bytes
MAC Header	224 bits	224 bits
PHY Header	192 μ s	20 μ s
DATA	(224 bits + packet payload) / data rate + PHY Header	$4 \lceil (246 \text{ bits} + \text{packet payload}) / (4 \times \text{data rate}) \rceil + \text{PHY Header}$
ACK	112 bits/control rate + PHY Header	$4 \lceil 134 \text{ bits} / (4 \times \text{control rate}) \rceil + \text{PHY Header}$
Slot Time, t_σ	20 μ s	9 μ s
SIFS	10 μ s	16 μ s
DIFS	50 μ s	34 μ s
Data Rate	11 Mbps	54 Mbps
Control Rate	1 Mbps	24 Mbps
CW_{\min}	32	16
CW_{\max}	1024	1024
Max. Backoff Stage, m'	5	6
Max. Retransmission, m	6	6
Propagation Delay, t_δ	1 μ s	1 μ s

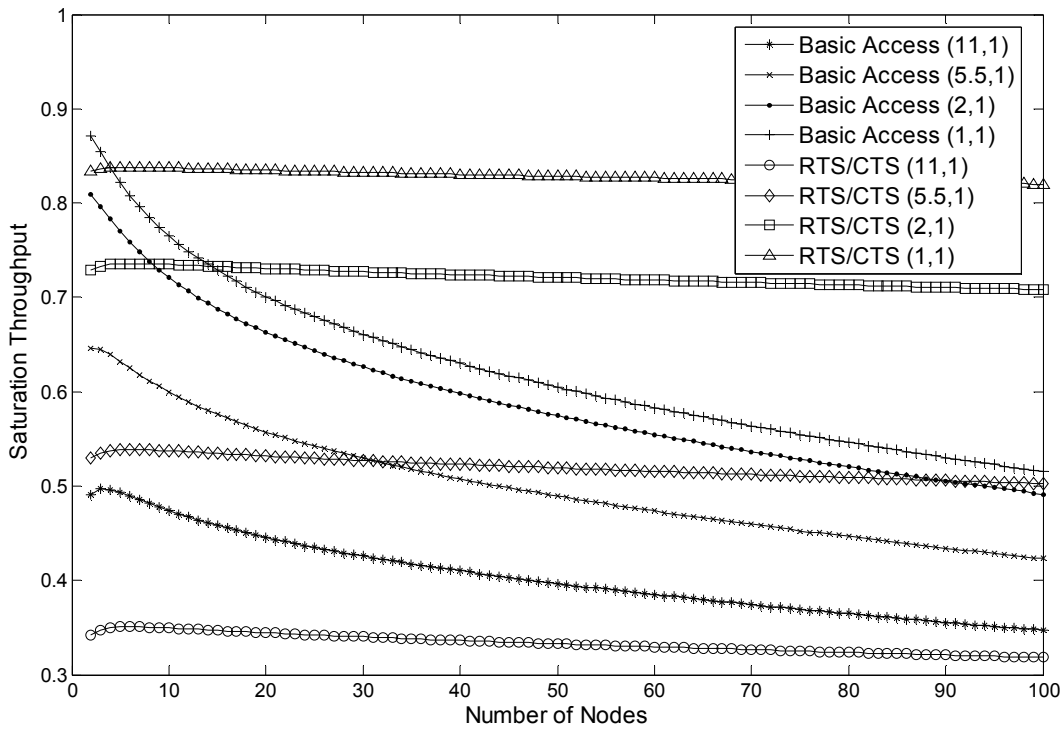


Figure 2.9: Saturation throughput for IEEE 802.11b.

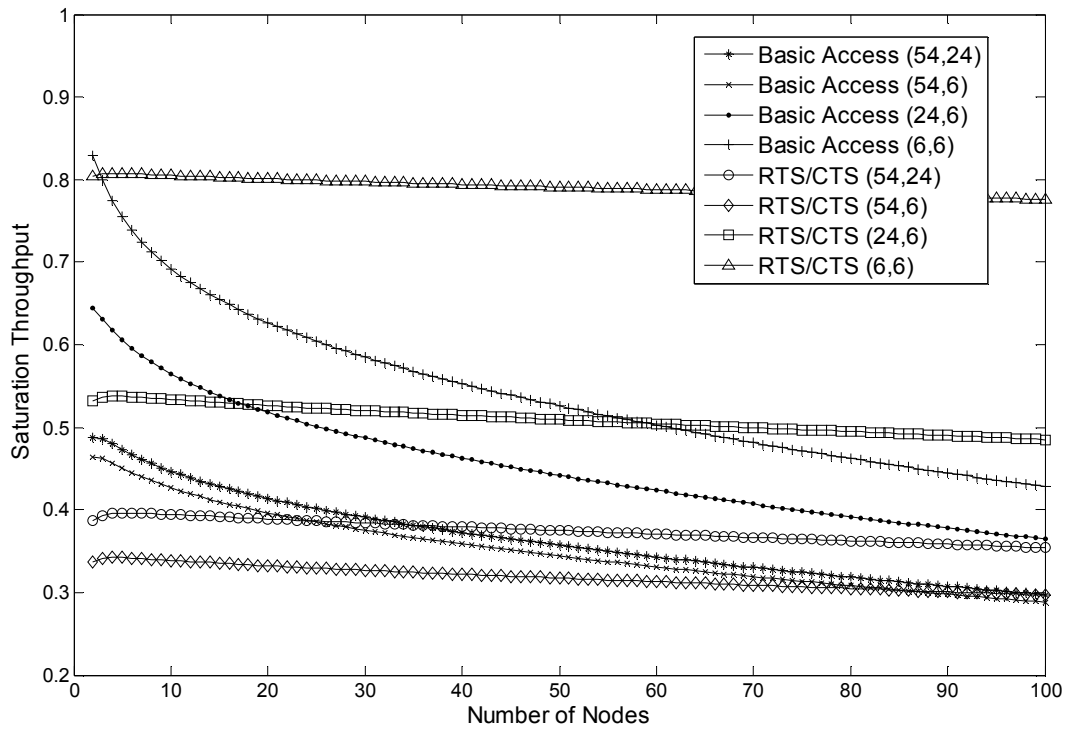


Figure 2.10: Saturation throughput for IEEE 802.11a.

At first, it might appear that RTS/CTS (1,1) and RTS/CTS (6,6) rate combinations give the best throughput for IEEE 802.11b and IEEE 802.11a, respectively. However, the throughput shown in both figures is normalized to the data rate. Therefore, in terms of absolute throughput, basic access (11,1) and basic access (54,24) give the best performance for IEEE 802.11b and IEEE 802.11a respectively.

It is interesting to observe that when the data rate is equal to the control rate (as in (1,1) and (6,6) for IEEE 802.11b and IEEE 802.11a respectively), RTS/CTS outperforms basic access. This is due to the shorter collision duration because of the shorter length of RTS as mentioned previously. However, when using high data rates (as in (11,1) and (54,24)), the assumption of a shorter transmission duration for RTS is no longer valid due to the lower control rates. Therefore, for the normally employed high data rate combinations, basic access mechanism always gives better throughput

performance. This can be observed from both figures and has also been independently concluded in [37-39].

2.2 High Density WLANs

Over the past few years, we have personally witnessed the exponential growth of WLAN technology. On one hand, almost all personal computing and communications devices now come pre-equipped with WLAN capabilities. On the other hand, WLAN APs are increasingly deployed in homes, offices, shopping malls and small businesses. These complimentary developments ensure that users are always within coverage, have high speed access and stay connected.

A recent survey conducted by Wi-Fi Alliance at the end of 2009 showed that WLAN capability has become a highly sought after feature in consumer electronics [40]. In the same report, data from market research firm In-Stat indicated that 475 million Wi-Fi chipsets were shipped in 2009 and predicted that shipments will grow at an annual rate of more than 25 percent for the next four years. These findings show that the proliferation of WLAN technology will continue well into the foreseeable future.

In the past, WLANs were mainly deployed by network professionals in large corporations. These medium to large scale deployments were carefully planned and tested to satisfy coverage and performance requirements [41-42]. Recently, with the increased affordability of WLAN equipment, any user can now deploy WLAN APs. By contrast, these smaller scale deployments are characterized by ad hoc planning and a lack of active management. These somewhat chaotic deployments make up the majority of WLANs found today and have become the norm rather than the exception [13]. The uncoordinated deployment of WLANs by users within close proximity has resulted in

high density WLANs. These dense deployments have become a common feature of all metropolises around the globe.

Since these networks are independently deployed by a multitude of users, the characteristics and attributes of these networks are generally unknown, but nonetheless important. This information can provide invaluable insights into and guidelines for the design of WLANs that are more efficient, scalable and robust. Thankfully, there exists a legion of enthusiasts who collect information on these WLAN deployments. These measurements are performed by scanning for beacons that APs periodically broadcast to advertise their presence. The most common technique employed is known as wardriving, where one drives a car and uses a laptop equipped with freely available software such as Netstumbler to detect WLAN APs [43-44].

The information collected can be shared at websites such as the wireless geographic logging engine (WiGLE) [45]. WiGLE maps the detected APs using global positioning system (GPS) information and has around 20 million unique APs in its database as of early 2010. A quick search in WiGLE provides proof that high density deployments of APs already exist in many cities around the world. For example, Fig. 2.11 shows the APs deployed around New York City obtained from WiGLE.

Several works have compiled and analyzed such information for the purpose of investigating the characteristics of these WLAN deployments. Parameters of interest include the channels employed, proportion of APs by vendors, security settings and most importantly to our study, density of APs. In [13], data from the Intel Place Lab project consisting of around 26 thousand APs from six US cities have been examined. By assuming a conservative transmission range of 50m, the distribution and maximum number of neighbour APs as shown in Table 2.2 have been obtained by the authors. Neighbour APs are defined as APs that are located within the reference AP's



Figure 2.11: APs deployed in New York City from WiGLE.

TABLE 2.2

Maximum number of neighbour APs measured in six US cities.

City	No. of APs	Max. No. of Neighbour APs
Chicago	2370	20
Washington D.C	2177	39
Boston	2551	42
Portland	8683	85
San Diego	7934	54
San Francisco	3037	76

transmission range. It was found that in most cities, several hundreds of APs suffer interference from at least three other neighbour APs. In fact, this is true for more than half of all APs in Portland. In both San Francisco and Portland, a particular AP has around 80 neighbour APs.

TABLE 2.3

AP densities in several world cities.

City	Area (km ²)	No. of APs	Density (AP/ km ²)
San Francisco	213	69502	326
Seattle	165	64923	395
Boston	225	164072	729
Manhattan	105	194651	1854
Paris	7934	30904	3189

In another study, a database consisting of over 5 million APs collected through systematic scanning by Skyhook Wireless in 75 US cities was used [46]. A similar research has been undertaken in Paris which involved data collection of over 30 thousand APs [47]. Both studies reached a similar conclusion, that these WLAN deployments consistently have very high density. The AP densities in these cities are shown in Table 2.3. Our conservative calculations show that a density of 382 AP/km² equates to an average of having three other neighbour APs. As can be seen, most cities shown have a density that is significantly higher than this value. Furthermore, due to large areas of parks and water bodies, actual AP densities may even be higher.

While the increased density of deployment can be highly beneficial in terms of capacity and coverage, a corresponding increase in contention and interference can lead to a significant degradation of throughputs if left unchecked. This recent development has given rise to new challenges in channel assignment, an issue that was not previously thought to be critical.

Furthermore, channel assignment in WLANs comes with its own unique set of difficulties. Firstly, with only 3 and 12 non-overlapping channels in IEEE 802.11b and IEEE 802.11a, the number of channels available is highly insufficient. This is especially true since most APs have a significantly higher number of interfering neighbour APs.

Secondly, dense WLAN networks belong to different owners and hence are managed by different entities. This severely limits the amount of cooperation that can exist among different networks. Lastly, the load on each network is subject to changes with time. Channel assignments have to be updated accordingly in adapting to these dynamics.

Therefore, an effective, distributed and dynamic channel assignment scheme is needed in order to maximize the throughputs achievable in these networks. As deployments of WLANs continue to accelerate, channel assignment has to be addressed urgently so that the services provided through WLANs can be perpetually enjoyed by users.

2.3 Centralized Channel Assignment Schemes

Channel assignment in WLANs has been actively researched. These can be broadly divided into two categories, namely centralized and distributed schemes. In centralized schemes, information of the whole network is usually assumed. On the other hand, distributed schemes normally have access to only local information. Generally, centralized schemes provide superior performance due to the availability of complete information. However, they are only applicable to scenarios such as a campus wide or enterprise networks where all APs are controlled by the same entity. For the majority of WLAN deployments found today, APs belong to different owners and have different administrative domains. The inherent lack of coordination and communications in these networks practically mean that only distributed schemes can be applied.

Centralized channel assignment schemes leverage on the communication and cooperation among all APs in the network. Information transfers between APs and the central controller are facilitated through its high speed wired connections. The central controller may request for measurements and other information from APs. APs then

carry out measurements and report back with the required information. With this information, the central controller generates a new channel assignment and directs the relevant APs to change their channels. This process is repeated at appropriate intervals or when a network change is detected. The high processing power of central controllers allows the execution of complex algorithms that involve large amounts of data in a timely manner. This enables the centralized channel assignment schemes to not only dynamically track but also exploit the varying nature of network attributes such as traffic load.

Although our main interest is in distributed schemes due to their significantly wider applicability, the survey of centralized schemes is important for several reasons. Firstly, it provides a solid foundation and rich background for the study of channel assignment schemes. Secondly, it enables an appreciation of the main issues and limitations faced in distributed schemes, where only local information is available. Last but not least, centralized schemes can be useful as performance benchmarks when evaluating the performance of distributed schemes.

2.3.1 Utilization MinMax Scheme

By using the traffic load information on each AP, Leung and Kim [18] formulated the channel assignment problem with the objective function of minimizing the effective channel utilization at the AP with the highest utilization. The effective channel utilization of AP- i , u_i is defined as the fraction of time the channel is sensed busy or is used for transmission by AP- i :

$$u_i = \rho_i + \sum_{d \in C} X_{i,d} \left[\sum_{j \in \text{IntL}(i,1)} \rho_j X_{j,d} + \sum_{(m,n) \in \text{IntL}(i,2)} \rho_m \rho_n X_{m,k} X_{n,k} \right] \quad (2.3.1)$$

where ρ_i is the offered traffic load of AP- i , $X_{i,d} = 1$ if AP- i is on channel d and $X_{i,d} = 0$ otherwise, $C = \{1,2,\dots,D\}$ is the discrete non-overlapping channel set (e.g. $D = 3$ for IEEE 802.11b/g and $D = 12$ for IEEE 802.11a), $IntL(i,1)$, the level-1 interferers is the set of interfering APs where transmission by any AP can cause enough interference for AP- i to detect channel busy, and $IntL(i,2)$, the level-2 interferers is the set of pairs of interfering APs where simultaneous transmission by any of these pairs of APs can cause a channel busy detection by AP- i . Higher level interferers are not considered due to their very low probability of occurrence.

The problem of minimizing the maximum utilization was shown to be NP-complete, which is when a solution is simple to verify but finding the solution entails an exhaustive search through all possible combinations. In view of this, a heuristic based on subset search, the utilization minmax (Uminmax) algorithm, was proposed in [18]:

Algorithm 1: Uminmax

- 1) A random channel assignment is generated. Set $U_{\max} = \max (u_i)$, the maximum utilization.
- 2) Identify AP- i with the maximum utilization, which is known as the bottleneck AP. In case of a tie, one such AP is chosen randomly.
- 3) Identify the current channel d assigned to AP- i . For each channel d_{test} apart from channel d and each co-channel AP- j in $IntL(i,1)$, temporarily assign AP- j with channel d_{test} . Calculate the corresponding maximum utilization, $U_{\max}(j,d_{\text{test}})$ where AP- j is assigned channel d_{test} . Let U'_{\max} be the minimum among all $U_{\max}(j,d_{\text{test}})$.

- 4) Compare U'_{\max} with U_{\max} :
 - i) if $U'_{\max} < U_{\max}$, replace U_{\max} with U'_{\max} as the new best assignment. Continue with step 2.
 - ii) if $U'_{\max} = U_{\max}$, with a predefined probability, replace U_{\max} with U'_{\max} as the new best assignment. Continue with step 2.
 - iii) if $U'_{\max} > U_{\max}$, a local optimum has been reached. Continue with step 5.
- 5) Repeat steps 1-4 with a number of random initial assignments. The final solution is chosen as the channel assignment that gives the lowest U_{\max} .
- 6) Test if constraint $u_i < 1$ holds for all APs. If yes, then the solution is feasible. If not, it is considered that no feasible solution can be found for the network that is under consideration.

In order to evaluate its performance, the Uminmax scheme has been applied to two cellular hexagonal networks with known optimal assignments for verification [18]. For the smaller network of 7 cells with 21 APs, Uminmax generated the optimal channel assignment. However, for the second case of a large network of 37 cells with 111 APs, only a suboptimal solution is obtained. Nevertheless the suboptimal solution was shown to be very good, with a probability higher than 99% of generating a solution within the top 0.001th percentile. Furthermore, in the worse case, only 2 sectors were found to share the same channel.

In a later work by Zhao and Leung [48], the shortcomings of the original Uminmax algorithm were highlighted. Firstly, the original Uminmax algorithm does not consider changing the channel of the bottleneck AP itself, which may be more effective than changing the channels of just its interferers. Secondly, when there are multiple bottleneck APs, the original Uminmax algorithm either selects one of them randomly or

terminates the algorithm with a predefined probability. This may be premature because possible improvements may still exist around other bottleneck APs. In order to prevent this, all bottleneck APs are examined and the best improvement is selected from among them. The enhanced Uminmax algorithm (steps 2 – 4 are modified) is as follows [48]:

Algorithm 2: Enhanced Uminmax

- 1) A random channel assignment is generated. Set $U_{\max} = \max (u_i)$, the maximum utilization.
- 2) Identify all bottleneck APs.
- 3) For each bottleneck AP- i , identify its current channel d . For each channel d_{test} apart from channel d and for AP- i and each co-channel AP- j in $\text{IntL}(i,1)$, temporarily assign only AP- i or AP- j with channel d_{test} . Calculate the corresponding maximum utilization, $U_{\max}(i,d_{\text{test}})$ or $U_{\max}(j,d_{\text{test}})$ where AP- i or AP- j is assigned channel d_{test} . Let U'_{\max} be the minimum among all $U_{\max}(i,d_{\text{test}})$ and $U_{\max}(j,d_{\text{test}})$.
- 4) Compare U'_{\max} with U_{\max} :
 - i) if $U'_{\max} < U_{\max}$, replace U_{\max} with U'_{\max} as the new best assignment. Continue with step 2.
 - ii) otherwise, a local optimum has been reached. Continue with step 5.
- 5) Repeat steps 1-4 with a number of random initial assignments. The final solution is chosen as the channel assignment that gives the lowest U_{\max} .
- 6) Test if constraint $u_i < 1$ holds for all APs. If yes, then the solution is feasible. If not, it is considered that no feasible solution can be found for the network that is under consideration.

Furthermore, the traffic loads in wireless networks are known to vary in time. The performance of any static scheme, such as the original Uminmax scheme, is limited at best. In view of this, an adaptive capability has also been incorporated into the Uminmax scheme. In the adaptive Uminmax scheme, time is divided into equal interval called adaptive period (1-10 minutes). All APs will run a prediction algorithm based on the current load to predict the load in the next adaptive period. The predicted load will then be fed to the central controller that runs the enhanced Uminmax algorithm which in turn will provide an updated channel assignment.

However, this scheme only takes into account the downlink traffic from APs to nodes. The increasing popularity of applications such as voice over internet protocol (VOIP) and peer-to-peer (P2P), whose traffic is known to be symmetric, suggests that uplink traffic can no longer be ignored. For example, measurement studies obtained from actual WLAN networks have shown that uplink traffic can be significant, varying from 18% to 89% of downlink traffic [49].

On the other hand, the Uminmax scheme has an apparent weakness in that it does not explore nor accept any channel changes that do not lower the utilization of the bottleneck AP, even if they can lower the utilization of other APs. For example, consider a network where there is a highly congested section. Naturally, the bottleneck AP will be located in this section. The other sections of this network are less congested. Now, the Uminmax scheme will only search around the bottleneck AP for channel changes that can reduce its utilization. When it can no longer do so, the algorithm terminates. Now, it is highly probable that some channel changes in the less congested areas can result in lower utilization for the APs there, without compromising the utilization of the bottleneck AP.

Furthermore, the performance evaluation of Uminmax was mostly carried out in cellular hexagonal networks and assuming that all APs have the same utilization. This is understandable as the optimal channel assignment for these networks is well known and comparisons can be easily made to the performance of Uminmax. However, as mentioned before, WLAN deployments are unplanned and irregular. Therefore, it is certainly interesting to evaluate the performance of the Uminmax scheme in these representative networks. For this reason and also due to being one of the highly cited works, performance comparisons to the Uminmax scheme are provided in Section 4.4.

2.3.2 Degree of Saturation Scheme

The channel assignment problem is formulated as the classical graph colouring problem in [50-52]. The interference in the WLAN network is modeled as an interference graph, $G = (V, E)$ where V is the set of vertices and E is the set of edges between vertices. In this graph, the APs are the vertices and an edge connects each pair of APs whose BSSs interfere with each other when assigned the same channel. Colours represent the channels assigned. The vertex colouring problem assigns colours to all vertices such that no pair of vertices connected by an edge have the same colour. The corresponding channel assignment formulation thus becomes assigning channels to all APs so that no pair of interfering APs uses the same channel, $f_c: V(G) \rightarrow C$, where $C = \{1, 2, \dots, D\}$ is the discrete non-overlapping channel set.

The graph colouring problem, even in its simplest form is well known to be NP-hard. Therefore, a heuristic algorithm called degree of saturation (DSATUR) has been proposed. The DSATUR algorithm was chosen because of its simplicity and ability to produce good colourings for most graphs. The degree of saturation of a vertex is defined

as the number of distinct colours used by its neighbours while the ordinary degree refers to the number of neighbours. The DSATUR algorithm is described as follows [51]:

Algorithm 3: Degree of Saturation

- 1) At initialization, all vertices have their degree of saturation set to zero.
- 2) Select the vertex with highest degree of saturation.
- 3) If there is more than one vertex with the highest degree of saturation, the vertex with the highest ordinary degree is selected.
- 4) In the event of a tie, the vertex is selected randomly.
- 5) The selected vertex will be coloured with smallest number of colours required for an admissible colouring. A colouring is admissible if every vertex has a different colour from all of its neighbours.
- 6) This process is repeated until all vertices are coloured.

The operation of the DSATUR scheme can be illustrated through a simple example. Consider the WLAN network of four APs shown in Fig. 2.12. Firstly, the corresponding interference graph is constructed based on the interference among the APs. Since initially none of the vertices have been coloured, the degree of saturation of all vertices is equal to zero. So the vertex with the highest ordinary degree is selected, which is V_2 . Vertex V_2 is coloured with colour 1. Since V_2 is coloured, vertices V_1 , V_3 , and V_4 all have degree of saturation of one. So the vertex with the highest ordinary degree is chosen. Both V_3 and V_4 have an ordinary degree of two, so one of them is selected randomly, suppose V_3 . Vertex V_3 is coloured with colour 2. Now V_1 and V_4 have degree of saturation of one and two respectively. So V_4 is selected and coloured with colour 3, the

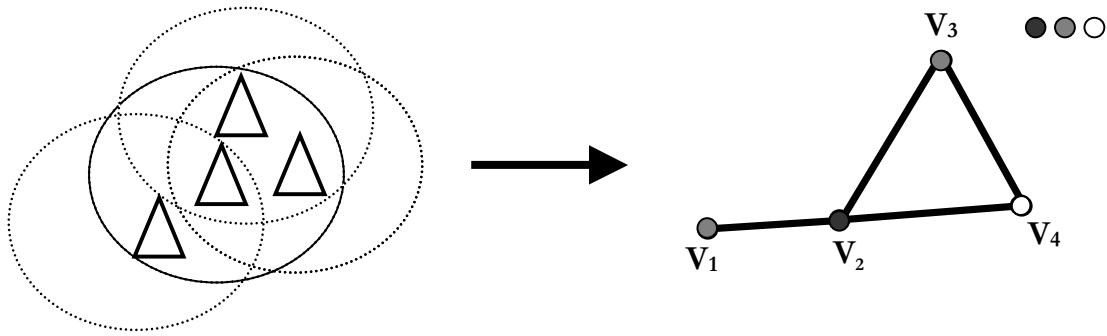


Figure 2.12: WLAN network and corresponding graph coloured by DSATUR scheme.

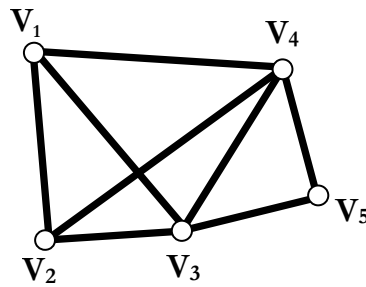


Figure 2.13: Interference graph with maximum clique of four.

only colour that provides an admissible colouring. Finally, V_1 is coloured with colour 2. The final colouring is shown in Fig. 2.12.

The main weakness of this scheme is its inability to provide a feasible colouring for graphs with a high density of vertices and edges, which correspond to dense WLAN deployments. For example, consider the interference graph in Fig. 2.13. The graph has a maximum clique of four, formed by V_1 , V_2 , V_3 and V_4 . With only three channels in IEEE 802.11b/g, it is not possible to find an admissible colouring for this graph. Therefore it can be concluded that the DSATUR scheme is not able to produce an assignment for graphs that have a maximum clique that is higher than the number of channels.

In addition, the DSATUR scheme fails to take into account the difference in the contention and load contributed by different APs. For example, measurement studies of

real WLAN networks have shown that loads across APs can vary vastly [53]. However, each AP is treated equally in the DSATUR scheme although some APs may be highly congested while other APs are idle. When the DSATUR scheme is unable to produce a feasible assignment, having a heavily loaded AP share the same channel with an idle AP may still be preferable due to its marginal effect.

2.3.3 Degree of Saturation with Cost Scheme

The main problem with the DSATUR scheme was its inability to provide any feasible channel assignment for graphs that have high density of vertices. In order to overcome this limitation, several works in the literature have removed the constraint that vertices connected by an edge have to be assigned different channels (admissible colouring). Instead, channels are assigned in such a way that a certain proposed cost is either minimized or maximized.

Using this idea, Villegas, Vidal and Paradells have proposed a channel assignment scheme, which adapted the DSATUR algorithm to incorporate a cost that seeks to maximize the estimated capacity (which we named as DSATUR with Cost scheme (DSATURwC)) [54-56]. The saturation degree of a vertex maintains its definition from the original DSATUR scheme, which is the number of distinct colours used by its neighbours. However, the definition for the ordinary degree of a vertex, which is the number of neighbour APs, has been modified. The new ordinary degree is the total interference caused to all its neighbours.

For computing the interference, a square matrix A is used. The elements of the matrix, $a[i][j] \forall i, j \in V$ represent the average signal level received by AP- j from the BSS of AP- i . Subsequently, $a[i][j] = 0$ if $(i, j) \notin E$ or $i = j$ because APs that are out of range

cannot interfere with each other and an AP does not interfere with itself. The total interference caused by AP- i can be found by summing elements from the i th row of A .

An accurate prediction of the capacity of WLAN nodes is very complex and is still an open research problem. In view of this, the authors have adopted an approach based on the fact that in the long term, every competing node has the same probability of accessing the channel. Although this may result in errors for individual flows, it was shown that global capacity predictions are adequately accurate. Given a set of N nodes, the predicted capacity for each node, Γ_i is given by

$$\Gamma_i = s_H(i, N_i') \cdot f_T(|N_i'|) \quad (2.3.2)$$

where $f_T(n)$ is the saturation throughput function, N_i' is a subset of nodes from N that competes with node i for the channel and s_H is the effective share of the channel attributed to node i , given by

$$s_H(i, N_i') = \begin{cases} 1/|N_i'|; & (1 - \sum_{j \in N_i': j \neq i} u_j) \leq 1/|N_i'| \\ 1 - \sum_{j \in N_i': j \neq i} u_j; & \text{otherwise} \end{cases} \quad (2.3.3)$$

where u_j is the utilization of node j . If the average utilization of contending nodes is greater than $1/|N_i'|$, long term fairness ensures that each node receives only $1/|N_i'|$ share of the channel. Otherwise, any excess capacity not utilized by contending nodes will be captured by node i .

Now, since u_j represents the utilization of node j , $u_j = \Gamma_j / f_T(|N_j'|)$. Therefore, in order to determine Γ_i in (2.3.2), the values of Γ_j for all j in N_i' are required. This implies that Γ_i needs to be known in advance to obtain Γ_i . To overcome this inconsistency and to minimize the error introduced, a simple heuristic has been proposed. According to this heuristic, Γ_i is computed first for nodes that have a higher number of contending nodes

(degree) and so on.

The number of competing nodes in N_i can be well approximated by two methods: the maximum interference clique (CL method) and the nodes within range (CR method). In the CL method, the resolution of the clique problem, which is NP-hard is required. Although the CL method is more accurate, its computation complexity can become prohibitive when the number of APs becomes large, typically when it is more than 20. In these cases, the CR method is generally preferred.

The colour assigned to a particular vertex is given by the function $f_c(v)$ and $f_c(v) = 0$ for vertices that have yet to be assigned a colour. The DSATUR with Cost scheme is given as follows [56]:

Algorithm 4: DSATUR with Cost

```
1: while All_Vertex_Coloured = false do
2:    $v \leftarrow \text{Max\_Saturation\_Degree}(G, f_c(v))$ 
3:   if Max_Saturation_Tie = true then
4:      $v \leftarrow \text{Max\_New\_Ordinary\_Degree}(A)$ 
5:   end if
6:    $f_c(v) \leftarrow \text{Max\_Predicted\_Capacity}(v, G)$ 
7: end
```

Firstly, the vertex with the highest saturation degree is selected (note that the symbol “ \leftarrow ” in the algorithm means “is assigned with”). If there is a tie, then the vertex with the highest new ordinary degree is selected. After a vertex has been selected, it is assigned a channel, $f_c(v)$ that maximizes the predicted capacity of the coloured vertices, given by

$$f_c(v) = \arg \max_{d \in C} \sum_{i \in V: f_c(i) \neq 0} \Gamma_i \quad (2.3.4)$$

where C is the non-overlapping channel set (this scheme actually allows assignment of overlapping channels but for simplicity and comparison purposes, we restrict the assignment to only non-overlapping channels). Here, Γ_i is obtained from a simplified version of the capacity estimator in (2.3.2), which only considers the APs and their interference with each other (clients are not taken into account). The algorithm is repeated until every vertex has been coloured (every AP has been assigned a channel).

The quality of the channel assignment was found to be considerably impacted by the choice of the first channel assigned. Because of this, the algorithm is repeated D times, each time starting with a different channel. Finally, the best channel assignment from among these is chosen.

2.4 Distributed Channel Assignment Schemes

Recently, distributed channel assignment schemes have garnered much interest due to their wide applicability in WLAN deployments. The uncoordinated nature in the majority of these networks basically precludes the use of centralized schemes. Without a common communications platform, the time and overheads required in disseminating network information through a network of arbitrary size are prohibitive at best. Therefore, distributed schemes that can operate on only localized information are well suited for these deployments where communication and cooperation are highly difficult or even impossible.

Distributed schemes obtain local information through measurements performed by the AP and its clients. These measurements can provide useful information concerning the

presence and activities of neighbouring APs and their clients. Harnessing this information, each AP generates a new channel assignment and changes its own channel if required. This process is repeated at appropriate intervals or when a local change is detected. Because of this, distributed schemes are able to dynamically track the varying nature of the network to a certain extent. With less information to process, distributed schemes can be designed to have lower complexity. Another motivation for this is that APs typically have less processing power when compared to central controllers.

Due to the reasons outlined above, the primary interest of this work is in distributed channel assignment schemes. In this section, relevant and important distributed schemes in the literature will be reviewed. This exercise is carried out with several objectives in mind. Firstly, a survey of distributed schemes provides the necessary knowledge of the state of the art work in this area. Secondly, it enables an understanding of the limitations of having only local information and the lack of control over other APs. Finally, existing distributed schemes are useful for comparing the performance of our proposed schemes.

2.4.1 Weighted Coloring Scheme

Mishra et al. modeled the channel assignment as a weighted variant of the graph colouring problem in [57]. The weights assigned to each pair of APs reflect the relative importance of assigning different channels for them. The weights are set according to interference information reported from the client nodes associated with each AP since the clients have an extended view of the network.

Similar to the graph formulation earlier, a graph $G = (V, E)$ corresponding to the network is defined. The set of vertices, $V = \{ap_1, ap_2, \dots, ap_n\}$ represents n APs that form the network. The weighted graph colouring problem can be stated as follows: A

channel assignment, $f_c(ap_i)$, $ap_i \in V$ is a function $f_c: V(G) \rightarrow C$ that assigns channels from C , the set of non-overlapping channels, to every AP such that an objective function is optimized.

A weight function defined on G , $W_T(ap_i, ap_j)$ denotes the normalized weight on the edge (ap_i, ap_j) . The weight is proportional to the number of clients associated with the two corresponding APs that are affected if they are assigned the same channel. An interference factor (I-factor), denoted by $I(ap_i, ap_j)$ is assigned to each edge to represent the interference between the channels assigned to both APs. For non-overlapping channels, the I-factor is defined as follows: $I(ap_i, ap_j) = 1$ if ap_i and ap_j are on the same channel and $I(ap_i, ap_j) = 0$ otherwise. Subsequently, the product $W_T(ap_i, ap_j) \times I(ap_i, ap_j)$ is defined as the I-value. The I-value represents the total effect of interference on all clients that are located within the overlapping region between the two APs.

Therefore, given G and W_T , the weighted coloring (Hminmax) scheme finds the channel assignment that minimizes the maximum I-value of each AP:

$$f_c(ap_i) = \arg \min_{d \in C} \max_{\forall (ap_i, ap_j) \in E} I(ap_i, ap_j) \times W_T(ap_i, ap_j). \quad (2.4.1)$$

In other words, for each AP, Hminmax assigns channel d that minimizes the maximum impact of interference among all overlap regions between ap_i and all other APs. The Hminmax scheme is executed at each AP in a distributed manner and is given as follows [57].

Algorithm 5: Hminmax Scheme

- 1: $f_c(ap_i) \leftarrow 1$
 - 2: $h_{\max}(d) \leftarrow \max_{\forall (ap_i, ap_j) \in E \wedge f_c(ap_j)=d} I(ap_i, ap_j) \times W_T(ap_i, ap_j)$
 - 3: $d_{\min} \leftarrow \arg \min_{d \in C} h_{\max}(d)$
 - 4: $f_c(ap_i) \leftarrow d_{\min}$
-

Initially, all APs are assigned the same channel (a random channel assignment can also be used). Next, each AP ap_i determines the maximum I-value, $h_{\max}(d)$ on any edge that connects a neighbour AP that is using channel d . The channel d_{\min} is the channel that gives the minimum maximum I-value across all channels. Finally, ap_i is assigned the channel d_{\min} that minimizes interference on its maximum edge.

In order to construct the local graph, which consists of the AP and its neighbouring APs, the following method has been proposed. During periods of low activity, an AP ap_i can randomly request its client to perform a passive scan of each channel. During this scan, packets are captured from neighbouring APs and their clients. Thus, an edge is created between ap_i and for every ap_j that is contained in the scans performed. The weights of an edge can then be determined as follows. Let $Nscan_{ap_i}$ be the number of scans performed by clients of ap_i and let $Nscan_{ap_i}(ap_j)$ be the number of scans performed by clients of ap_i that reported interference with ap_j . Hence, the weight on the edge (ap_i, ap_j) is given by

$$W_T(ap_i, ap_j) = \frac{Nscan_{ap_i}(ap_j)}{Nscan_{ap_i}}. \quad (2.4.2)$$

Simulations and field trial results have shown the superior performance of the Hminmax scheme.

However, the method of determining the weights assigned to edges may present some inaccuracies. Firstly, in periods of congestions, all clients may be backlogged with packets to send and are therefore not available to perform scans. Secondly, for similar reasons, clients with a lower load may end up performing more scans than clients with higher loads. Subsequently, the weights assigned will mostly be reflective of the interference encountered by clients that have low traffic only. This is opposed to what is desired, where higher representation in the weights should be given to clients with higher loads. Finally, APs' measurements are not taken into account. Note that the AP is either the destination or the source of all transmissions. Therefore, if an AP suffers high interference, its opportunity to access the medium will be severely limited while packets received from clients will suffer a high probability of collisions.

Furthermore, the most important performance metric, which is the throughput of the Hminmax scheme, is not shown. The only performance metrics used are the maximum I-value of all edges, the summation of I-value of all edges and the number of edges with nonzero I-values. The authors have argued that a higher I-value on an edge corresponds to lower throughput and performed a simple two APs simulation to support their claim. However, the generalization of this assertion to the complex interactions of a network of APs is highly uncertain. Due to this reason, whether the performance metrics shown can be taken as a good representation of throughput remains doubtful. In fact, our work on the impact of interference on throughput in Section 5.1 has shown that there are many instances where higher throughputs are obtained for cases corresponding to higher I-value. In view of this and also because it is one of the more popular works, the

Hminmax scheme has been implemented and its performance evaluation and comparison shown in Section 4.4.

2.4.2 Communication-Free Learning Scheme

Leith et al. proposed a communication-free learning (CFL) channel assignment scheme in [58-60]. The CFL scheme does not require any form of communications between APs or any estimation of the network interference graph. The scheme is based on a simple learning rule that adaptively selects the best channel in terms of minimum interference. Interference measurements are carried out at appropriate intervals by the AP. The exact interference measure used may include received signal strength indicator (RSSI), signal to noise ratio (SNR) or frame error rate (FER). The basic idea of the CFL scheme is to assign higher probability for selecting channels that have a history of less interference. When an AP switches into a channel, it will remain in that channel until the interference exceeds a certain threshold. Once the interference threshold is exceeded, the probabilistic channel switching is performed again.

In the CFL scheme, each AP maintains a vector ψ with D (number of channels) elements that represent the probabilities of selecting each channel. The CFL algorithm can be described as follows [58]:

Algorithm 6: Communication-Free Learning

- 1) At initialization, set $\psi = [1/D \ 1/D \ 1/D \ \dots \ 1/D]^T$.
- 2) Perform random selection of a channel with the probability ψ_i for channel i . For the selected channel i , measure the interference and determine the following: A success if the measurement is within acceptable levels and failure otherwise.

- 3) If success, assign $\psi_i = 1$ and $\psi_j = 0$ for all $j \neq i$.
- 4) If failure, $\psi_i = (1 - l_p) \psi_i$ and $\psi_j = (1 - l_p) \psi_j + l_p / (D - 1)$ for all $j \neq i$. The learning parameter, $0 < l_p < 1$ and is a design parameter.
- 5) Repeat step 2 after an interval.

The probability of selecting every channel is set to $1/D$ at initialization. A channel is then selected randomly based on the current channel probabilities. An interference measurement is taken on this channel. The result of this measurement is compared against a predetermined threshold for which any level below this is considered a success. If the outcome is a success, the probability of selecting that channel is set to one while the probability of selecting all other channels is set to zero. This creates a degree of stickiness in that as long as the interference in the current channel is below the threshold, an AP will continue to operate on this channel. If the result of the measurement is above the threshold, it is considered a failure. If the outcome is a failure, the probability of selecting that channel is multiplicatively decreased and the reduced probability is evenly distributed to all other channels. Therefore, an AP will stay on the current channel as long as the interference level is acceptable. Otherwise, a channel is chosen randomly based on the current channel probabilities, which reflect past experience.

It has been shown that the CFL scheme is guaranteed to converge provided that the number of channels is large enough for an admissible colouring. The convergence rate has also been investigated in terms of several factors. The impact of learning is compared to that of no learning, which is when there is no updating of channel probabilities. The learning steps (steps 3 – 4) were found to provide up to four orders of magnitude improvement in the convergence rate when compared to no learning. The

value of learning parameter, l_p also has an effect on the convergence rate. This parameter determines the factor by which an AP will discount the previous success on a channel (and marks up other channels) on experiencing a failure on the current channel. The value of l_p in the range of 0.1 to 0.3 was found to correspond to the highest convergence rate. Similarly, having more channels than is required for a feasible channel assignment also increased the rate of convergence. An increase of 25% to 50% in the number of channels is sufficient to effect a reduction of up to two orders of magnitude in the convergence time. Simulation and experimental implementation of the CFL scheme has shown increased throughput and fast convergence time of around 20 iterations.

However, the CFL scheme's performance has only been compared to the case when all APs are assigned to the same channel. A more meaningful comparison could have been made against the random channel assignment. Furthermore, the deployment scenarios considered are sparse enough for an admissible colouring. By contrast, most of the deployment densities found in practice have significantly higher densities, for which better channel assignment schemes are critically needed. Lastly, the performance of the CFL scheme is highly sensitive to the setting of the interference threshold, for which the determination of its value is a non-trivial task. A low threshold may cause the CFL scheme to loop indefinitely while a high threshold may cause premature convergence when improvements can still be found.

2.4.3 Local Throughput Maximization Scheme

Luo and Shankaranarayanan proposed a scheme based on a neural network model in [61]. Similarly to a cellular neuron that changes its state based on information of neighbouring neurons, each AP calculates the best channel to switch to in the next period based on the traffic load of neighbouring APs. It then switches into the best channel with a fixed probability. Its objective is to improve the aggregate throughput of the network by maximizing the local throughput at each AP. The LS scheme (which we named after its authors) offers both simplicity and potentially a significant performance gain.

In the LS scheme, it is assumed that every AP periodically broadcasts the number of clients that is associated with it, which gives an indication of its load. For this reason, each AP maintains a table that keeps track of the number of clients of neighbouring APs and the channel that they currently occupy. It is also assumed that all APs can perform the algorithm synchronously. The LS algorithm can be described as follows [61]:

Algorithm 7: Luo Shankaranarayanan

- 1) For every AP, determine its throughput when using channel $d \in C$, given by

$$T_d(i) = \frac{N(i)}{\sum_{j \in M_d} N(j)} f_T\left(\sum_{j \in M_d} N(j)\right) \quad (2.4.3)$$

where $N(i)$ is the number of nodes associated with AP- i , M_d is the set of all neighbouring APs (including AP- i) that is using the same channel d and $f_T(n)$ is the throughput function of a channel that is shared by n competing nodes.

- 2) Find the channel $d_{\max}(i)$ for which the corresponding throughput $T_d(i)$ is maximized,

$$d_{\max}(i) = \arg \max_{d \in C} T_d(i). \quad (2.4.4)$$

- 3) Switch into channel d_{\max} with the switching probability, π .
- 4) Repeat step 1 after an interval.

An AP determines the throughput it will obtain when occupying channel d using (2.4.3) and the load information of neighbouring APs. This calculation is repeated for every channel. Next, it compares the calculated throughput for each channel and chooses the best channel, the channel that provides it with the highest throughput. Finally, it switches into the best channel with a fixed switching probability. This process is repeated at appropriate intervals.

It has been shown that the performance of the scheme is adversely affected if the switching probability $\pi=1$ because all APs will simply oscillate back and forth between two channel settings. The optimal value of the switching probability was found to be $\pi=0.5$, that gave the best aggregate throughput in the shortest convergence time. Simulation results have shown that the LS scheme can offer up to 70% improvement in aggregate throughput in less than 20 iterations.

Unfortunately, there are three key limitations in the LS scheme. Firstly it implicitly assumes perfect knowledge of the throughput function, which may not be feasible. This is because the exact throughput function depends on many factors including the exact distribution of the packet payload used by each individual node. Secondly, it assumes that all APs can perform the algorithm and switch into the new best channel synchronously. The dissemination of synchronization information to all APs in a timely and efficient manner is very challenging, especially in a distributed scenario. Thirdly, it assumes that each AP will broadcast the number of nodes associated with it. This new capability involves changes to existing MAC protocols that are likely to be backwards incompatible. Clearly, these assumptions are hard if not impossible to satisfy in practice.

2.5 Summary

In this chapter, the IEEE 802.11 standard features have been introduced. In particular, the medium access mechanisms have been described and their performance analysis explored in detail. Next, the characteristics of actual WLANs have been investigated. The findings showed that high density WLANs have become the norm in most cities. Increased contention and interference in these networks can significantly degrade achievable throughputs if left unmitigated. In order to maximize throughputs, effective channel assignment strategies are critically needed.

A survey of centralized and distributed schemes has been undertaken. Through this exercise, the background and an appreciation for the issues involved in channel assignment for WLANs have been gained. However, the inherent lack of coordination and communications in the majority of these networks practically means that only distributed schemes can be applied. Nevertheless, the availability of only local information and lack of control over other APs present serious challenges. In view of these limitations and taking a practical perspective, low complexity schemes that are able to provide acceptable and robust performance are highly preferred.

MINIMUM NEIGHBOUR SCHEME

In the previous chapter, existing channel assignment schemes in the literature were reviewed. The strengths and weaknesses of these schemes were highlighted and discussed. These schemes were found to vary in their complexity, performance and robustness. Although each scheme has its respective advantages, their relative merits can be difficult to determine due to the different frameworks employed, assumptions made and level of details considered. Nevertheless, from a practical and implementation point of view, low complexity schemes that are able to provide acceptable performance are deemed most attractive.

One such scheme is the LS scheme [61], described in Section 2.4.3. Retaining the desirable attributes while overcoming the limitations of this scheme, the minimum neighbour (MINE) channel assignment scheme [62-63] is proposed in this chapter. For the MINE scheme, it is shown that in order to maximize throughput, each AP only needs to choose the channel with the minimum number of active neighbour nodes. Active neighbour nodes are nodes associated with neighbouring APs (i.e. other APs that is within transmission range of the reference AP) that have packets to send. Simulation results show that the proposed MINE scheme not only converges significantly faster and requires less channel switches, but also achieves better throughput in dynamic load

scenarios. Furthermore, its performance is shown to be highly robust across various realistic scenarios found in practice.

This chapter is organized as follows. In Section 3.1, the proposed MINE scheme is presented and described. This is followed by extensive performance evaluation of the MINE scheme by considering a wide variety of realistic scenarios in Section 3.2. Finally, the chapter is summarized in Section 3.3.

3.1 Minimum Neighbour Scheme

In this section, we propose the MINE scheme that overcomes the limitations of the LS scheme. It is shown that in order to maximize throughput, each AP only needs to choose the channel with the minimum number of neighbour nodes. The MINE scheme has the following key features: it does not require knowledge of the throughput function, it is asynchronous and it has a much lower complexity.

3.1.1 Minimum Neighbour Algorithm

It is useful to recall that in the LS scheme, firstly, every AP will determine its throughput at each channel. Secondly, each AP will choose the channel with the maximum throughput. The detailed description of the LS scheme and related equations can be found in Section 2.4.3. However, the LS scheme assumes perfect knowledge of the throughput function, which may not be feasible in practice.

In fact, the LS scheme's algorithm can be simplified, so that it does not require any knowledge of the throughput function and also reduces the implementation complexity. Firstly, the sum of all the associated nodes of its neighbouring APs, which is also

defined as the neighbour nodes (i.e. the nodes associated with all APs in set M_d less AP- i), $N_d(i)$ can be given as

$$N_d(i) = \left(\sum_{j \in M_d} N(j) \right) - N(i) \quad (3.1.1)$$

where $N(i)$ is the number of nodes associated with AP- i and M_d is the set of all neighbouring APs (including AP- i) that is using the same channel d . Associated nodes are defined as nodes that are associated with a particular AP, while neighbour nodes refer to nodes that are associated with a neighbouring AP. Therefore, if $f_T(n)/n$ is a monotonically decreasing function, the maximization in (2.4.4) can now be rewritten as

$$\begin{aligned} d_{\max}(i) &= \arg \max_{d \in C} T_d(i) \\ &= \arg \max_{d \in C} \frac{N(i)}{N(i) + N_d(i)} f_T(N(i) + N_d(i)) \\ &= \arg \min_{d \in C} N_d(i) \end{aligned} \quad (3.1.2)$$

where $T_d(i)$ is the throughput of AP- i when using channel d and $f_T(n)$ is the throughput function of a channel that is shared by n competing nodes.

In the second line of (3.1.2), T_d can now be clearly seen as the share of throughput attributed to the AP that has N nodes when sharing with N_d neighbour nodes in the same channel. The simplification in (3.1.2) is due to the fact that $N > 0$ is a constant and independent of d (i.e. the number of nodes associated with any AP does not change with the channel used), that $N_d \geq 0$ and that $f_T(n)/n$ is normally a monotonically decreasing function. This means that in order to maximize throughput, APs only need to choose the channel with the minimum number of neighbour nodes. This is intuitive since it concurs with the expectation that one should use the channel that has the least number of nodes already using it.

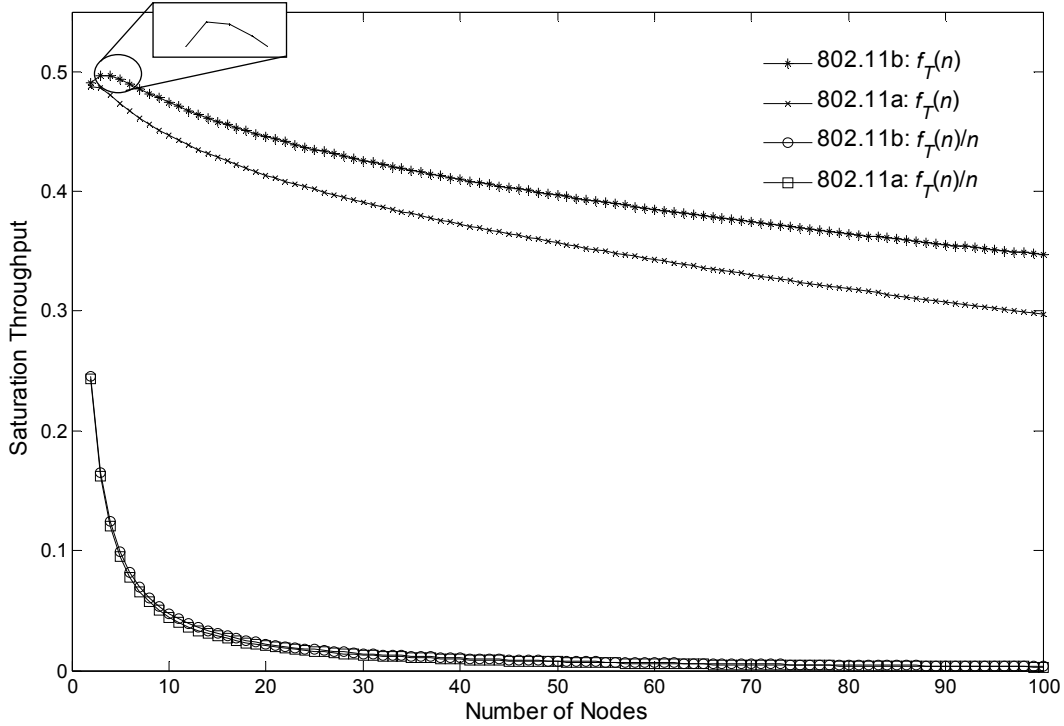


Figure 3.1: Throughput and composite functions for IEEE 802.11b and IEEE 802.11a.

Furthermore, the simplification also removes the dependence on the knowledge of the throughput function, which has a very important implication. In practice, the throughput function $f_T(n)$ may not be known or even impossible to estimate because the exact function depends on many factors including the exact distribution of the packet payload and data rates used by each individual node. Therefore, a simplified algorithm that is not dependent on the knowledge of the throughput function is very practical and can be easily implemented. Finally, it has a lower complexity with a reduction of two multiplicative operations per AP per updating period.

In order to show that the composite function $f_T(n)/n$ is indeed a monotonically decreasing function, we consider a practical example obtained for IEEE 802.11a/b based on the basic access mode of the MAC. The throughput functions $f_T(n)$ are derived from the analytical model described in Section 2.1.3. The typical set of parameters in

Table 2.1 is used and the corresponding throughput and composite functions generated are plotted in Fig. 3.1. The throughput shown is normalized to the channel data rate.

In Fig. 3.1, note that the throughput function for IEEE 802.11a is strictly monotonically decreasing. However, the corresponding throughput function for IEEE 802.11b is not strictly monotonically decreasing. We note that the function increases when the number of nodes is very small, when there are only 2 to 3 competing nodes. When there are very few nodes, the channel may not be used optimally due to wastage in empty slots during the backoff operation. This behaviour is caused by the value of CW_{\min} which is the initial size of the contention window. Not surprisingly, practical systems are designed such that the maximum throughput occurs when the number of nodes is small. Nevertheless, it is important to note that (3.1.2) is still valid because the composite functions for both IEEE 802.11a/b are strictly monotonically decreasing, even in this increasing part of the throughput function.

3.1.2 Equal Candidate Channels

In this section, further enhancement to the MINE algorithm is presented. One particular situation which needs to be addressed further is when the channel with the minimum number of neighbour nodes in (3.1.2) is not unique. This occurs when multiple channels have the same minimum number of neighbour nodes. These channels are defined as equal candidate channels in the set ECC ,

$$ECC_i = \{\arg \min_{d \in C} N_d(i)\}. \quad (3.1.3)$$

Now, if $|ECC| = 1$, then d_{\max} is unique, which is equivalent to (3.1.2). In cases where $|ECC| > 1$, rules for selecting d_{\max} need to be established. A simple option would be to select the lowest numbered channel as d_{\max} ,

$$d_{\max}(i) = \min(ECC_i). \quad (3.1.4)$$

However, this leads to longer convergence time and the skewing of higher probabilities to lower numbered channels. In order to mitigate these problems, we propose the following rules to further enhance the algorithm.

The first rule is stay on the current channel if it is one of the equal candidate channels:

If $d^*(i) \in ECC_i$, then

$$d_{\max}(i) = d^*(i) \quad (3.1.5)$$

where d^* is the channel that the AP is currently occupying, which is also the channel that gave the maximum throughput for the previous iteration of the algorithm. The second rule states that otherwise, select channel d_{\max} from ECC on a random basis.

The proposed enhancement can significantly reduce the number of iterations and channel switches required for convergence, especially with a higher number of channels. It also makes each equal candidate channel equally probable when averaged over all APs. More importantly, it guarantees that the scheme will converge to the upper bound performance in a single iteration when the number of available channels is greater than the number of neighbour APs ($D > Y$, where Y is the number of neighbour APs).

Proposition 3.1.1. *The MINE scheme converges to the upper bound performance in a single iteration if the number of channels is greater than the number of neighbour APs, $D > Y$.*

Proof. Let AP- i be an arbitrary AP in the network. Assume that the number of channels is greater than the number of neighbour APs, that is $D > Y$, where D and Y are integers. During the first iteration, AP- i runs the MINE scheme once and determines the channel with the minimum number of neighbour nodes. We now consider two cases:

Case i) AP- i is currently operating on channel d^* that has no neighbour nodes. Since channel d^* has no neighbour nodes, by (3.1.3) it must be one of the equal candidate channels, $d^* \in ECC$. Since $d^* \in ECC$, by the first rule, $d_{\max}(i) = d^*(i)$. Therefore, AP- i remains on channel d^* .

Case ii) AP- i is currently operating on channel d^* that has some neighbour nodes. Since $D > Y$, there exists a channel d with no neighbour nodes, that is $\exists d \in C : N_d(i) = 0$. Since $N_d(i) = 0$, channel d must also belong to the ECC set. Without loss of generality, let channel d be the randomly selected channel from the set ECC according to the second rule. Therefore, AP- i switches to channel d that has no neighbour nodes.

Note that in both cases, AP- i never switches into a channel that has neighbour nodes. Since AP- i was arbitrary and both cases are exhaustive, it follows that at the end of the first iteration, every AP would have stayed or switched into a channel that has no neighbour nodes. On subsequent iterations, only Case i) applies and every AP remains

on the channel with no neighbour nodes. Since all APs operate on channels that have no neighbour nodes, this corresponds to the upper bound performance, which is when all APs are free from any interference. Therefore, if the number of channels is greater than the number of neighbour APs, the MINE scheme will converge to the upper bound performance in a single iteration.

3.1.3 Asynchronous Operation

A channel assignment scheme with synchronous operation, such as the LS scheme, can be defined as a scheme where the algorithm and the channel switching are carried out simultaneously by all APs involved. Specifically, there is a predefined period where the information about each of the neighbouring APs' load and current channel is obtained. At the end of every period, all APs will simultaneously carry out the algorithm and channel switching. This process is then repeated for every period.

The assumption of having all APs performing the algorithm and switching simultaneously is too strong especially in a distributed scenario. One of the major obstacles will be the inability to disseminate synchronizing information to a network of arbitrary and unknown size in a timely manner. Apart from this, the amount of overhead will be prohibitive especially in larger networks. We also noticed that in the LS scheme, setting the switching probability to $\pi = 0.5$ instead of having all APs always switch into the best channel increases the convergence time for the algorithm. This was only made necessary due to the simultaneous or synchronous switching of all APs.

In view of this, the MINE scheme proposed employs asynchronous operation which allows each AP to carry out the algorithm and channel switching asynchronously. In the predefined period, each AP chooses a random time at which it will carry out the

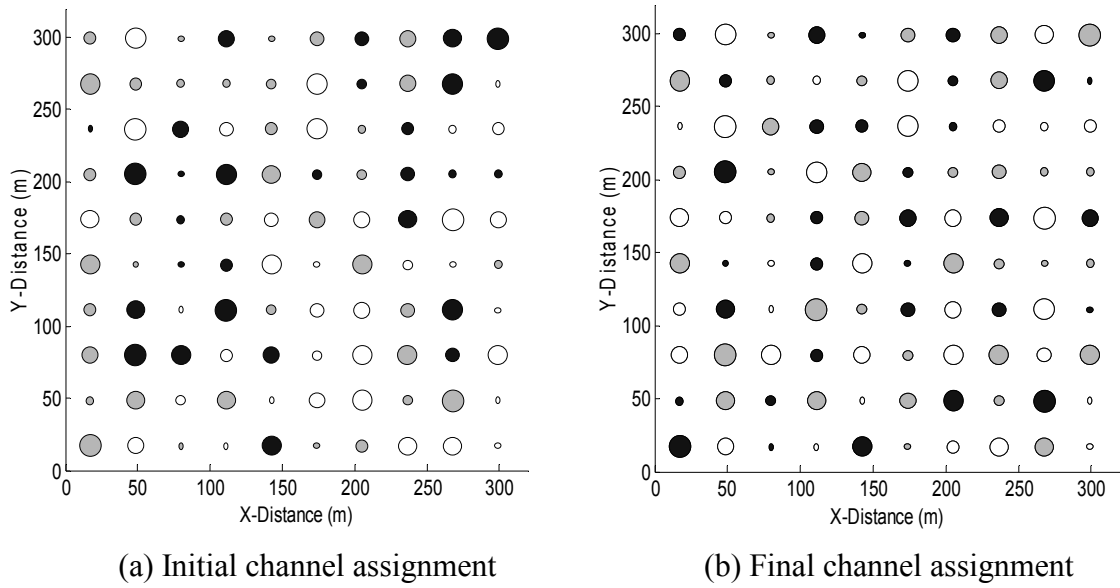


Figure 3.2: Initial and final channel assignment for MINE scheme.

algorithm and channel switching. The algorithm is carried out with the APs' current information about its neighbouring APs' load and their current channels. During every period, each AP would have a chance to carry out the algorithm and channel switching. Immediately after performing the algorithm and channel switching if necessary, the AP will broadcast the latest number of associated nodes and the new channel it is using. In this way, all neighbouring APs will always have the most updated information to use with the algorithm. Therefore, synchronization is not required and each AP can always switch into the best channel by setting $\pi = 1.0$, without inducing the oscillating effect and reach convergence significantly faster than the LS scheme.

Fig. 3.2 (a) shows one realization of a network of APs with the initial channel and number of associated nodes of each AP selected randomly. The size of each circle is proportional to the number of associated nodes of each AP. The different shades represent the different channels used by each of the AP ($D = 3$). Fig. 3.2 (b) shows the channel assignment after the MINE scheme has converged. It can be clearly seen that

neighbouring APs with a high number of associated nodes will be assigned different channels whenever possible to maximize the throughput.

3.2 Performance Evaluation

In this section, extensive performance evaluation of the proposed MINE scheme will be presented. Firstly, basic performance of the MINE scheme in simple scenarios is presented in order to understand its fundamental behaviour and typical performance gains. Secondly, the performance of the MINE scheme across a wide variety of scenarios that arises in practice is investigated to determine its robustness. This is achieved by considering the number of channels, deployment densities, non-uniform topologies, dynamic topologies and heterogeneous networks [64-66].

3.2.1 Basic Performance

Extensive high-level simulations were carried out in MATLAB to evaluate the performance of the proposed MINE scheme. MATLAB simulator allows shorter simulation time by utilizing the previously derived theoretical results for MAC layer performance. On the other hand, packet-level simulations in OPNET, which simulates the exact MAC mechanisms and transmissions in the channel, are required when considering detailed aspects of the system, as will be shown in Chapter 4. Furthermore, the focus of the performance comparison here will be against the LS scheme for which the MINE scheme improves upon. Nevertheless, comparisons to several other channel assignment schemes, which were introduced in Chapter 2, will be undertaken in the next chapter where more in-depth system characteristics are taken into account.

A network consisting of 100 APs is used and the number of nodes associated with

each AP is randomly selected from 1 to $AP_{\max} = 10$. For simplicity, APs are located in a grid/uniform topology. Each node has an average of $Y = 8$ interfering neighbour APs within its transmission range of 50m while the number of channels for IEEE 802.11b and IEEE 802.11a are $D = 3$ and $D = 12$ respectively (results similar to IEEE 802.11b are expected from IEEE 802.11g due to the same number of channels, $D = 3$). The throughput of each AP is determined using (2.4.3), which is then summed up to provide a good approximation for the aggregate throughput [56]. IEEE 802.11a/b specifications and additional parameters from Table 2.1 are used. All results shown are obtained using the average of 1000 independent realizations with randomly generated initial channels and number of associated nodes.

a) **Minimum Neighbour Algorithm**

Fig. 3.3 shows the aggregate throughput against the number of iterations for both the simplified MINE algorithm described in Section 3.1.1 and the LS algorithm. Note that in this particular case, the MINE algorithm also employs synchronous operation in order to determine if there is any performance difference to the LS algorithm. From the figure, it is clear that the MINE algorithm gives the same performance as the LS algorithm without requiring any knowledge of the throughput function and with reduced computational complexity. The number of channel switches and iterations required for convergence is also exactly the same for both algorithms. The results are consistent for both IEEE 802.11b and IEEE 802.11a throughput functions. This shows that the MINE algorithm is still valid for non-strictly monotonically decreasing functions found in practical systems.

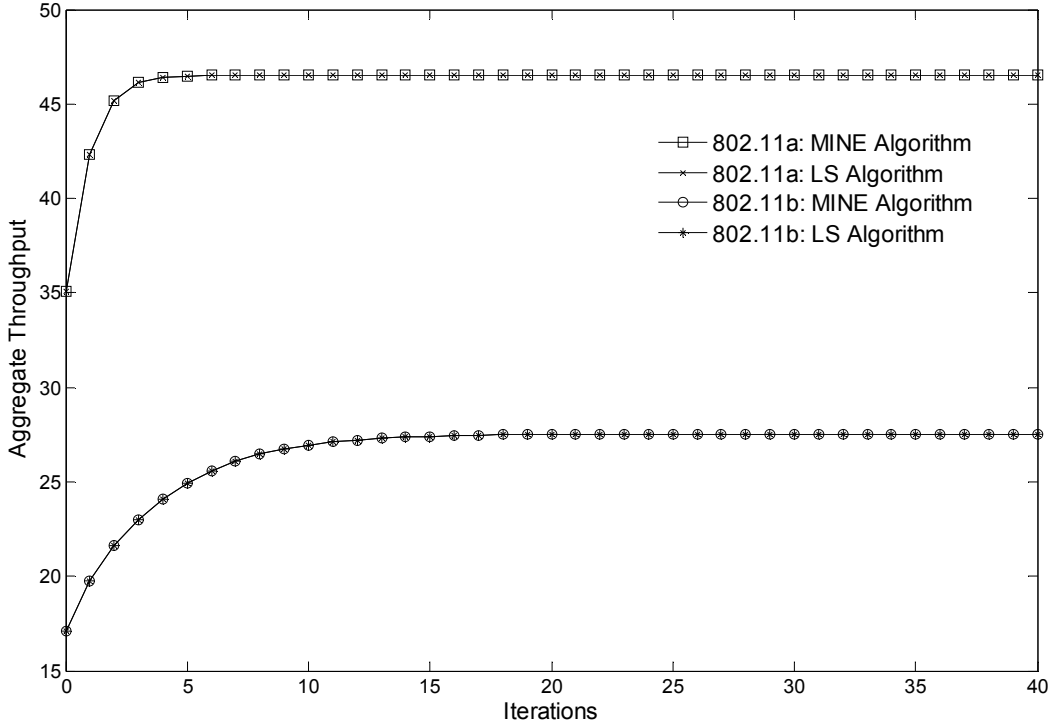


Figure 3.3: Aggregate throughput for MINE algorithm and LS algorithm.

b) Equal Candidate Channels

Table 3.1 shows the performance of the enhanced MINE algorithm for selecting d_{\max} from the set of equal candidate channels described in Section 3.1.2. Recall that for the default algorithm, d_{\max} is simply chosen as the lowest numbered channel. The enhanced algorithm significantly reduces both convergence time and channel switches, with reductions of up to 52% and 71% respectively. We note that the reduction for IEEE 802.11a is significantly higher because having $D = 12$ channels increases the probability of having equal candidate channels, which the enhancement capitalizes. The results also show that the enhanced MINE algorithm only requires a single iteration to converge for the case of IEEE 802.11a ($D = 12, Y = 8$). This confirms Proposition 3.1.1, which states that the enhanced algorithm guarantees single iteration convergence when the number of channels is more than the number of interfering APs ($D > Y$).

TABLE 3.1

Performance comparison of default and enhanced MINE algorithms

		Default Algorithm	Enhanced Algorithm	% Change
802.11b	Iterations	3.669	3.458	-5.75
	Channel Switches	71.362	65.928	-7.61
802.11a	Iterations	2.117	1.000	-52.76
	Channel Switches	81.586	23.101	-71.69

c) Asynchronous Operation

The aggregate throughput against the number of iterations for both the MINE scheme with $\pi = 1.0$ (asynchronous operation) and LS scheme with the optimal $\pi = 0.5$ (synchronous operation) are shown in Fig. 3.4. The MINE scheme clearly outperforms the LS scheme with a significant reduction in convergence time for both IEEE 802.11b and IEEE 802.11a. In fact, Table 3.2 shows that reductions of up to 77% and 54% for the number of iterations and channel switches required for convergence respectively can be achieved with the MINE scheme. However, note that the faster convergence time does not translate into higher throughput performance. This is due to the static loads used in the simulations thus far.

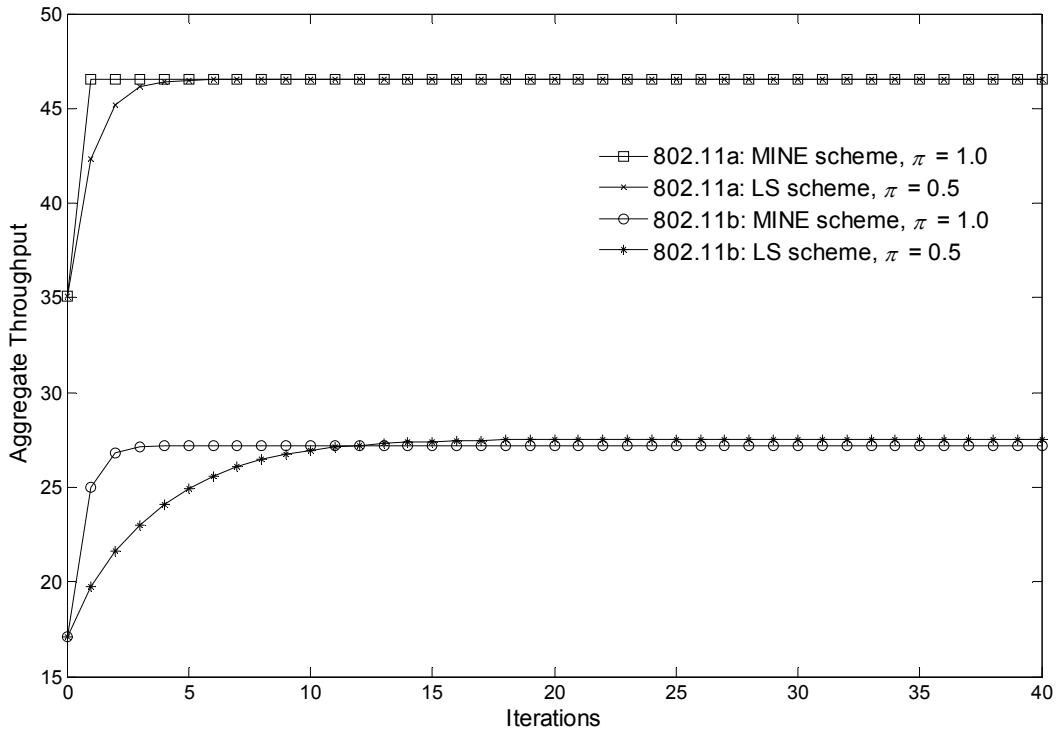


Figure 3.4: Aggregate throughput for MINE scheme ($\pi = 1.0$) and LS scheme ($\pi = 0.5$).

TABLE 3.2

Number of iterations and channel switches required for convergence
for MINE scheme and LS scheme

		LS Scheme	MINE Scheme	% Change
802.11b	Iterations	15.638	3.458	-77.89
	Channel Switches	145.145	65.928	-54.58
802.11a	Iterations	3.759	1.000	-73.40
	Channel Switches	33.105	23.101	-30.22

In order to evaluate the throughput gains achievable by the MINE scheme, the number of associated nodes of each AP is dynamically changed at each iteration according to a Gaussian distribution with mean = 0 and standard derivation, σ being a percentage of AP_{\max} . A higher standard deviation reflects a network load that is more dynamic.

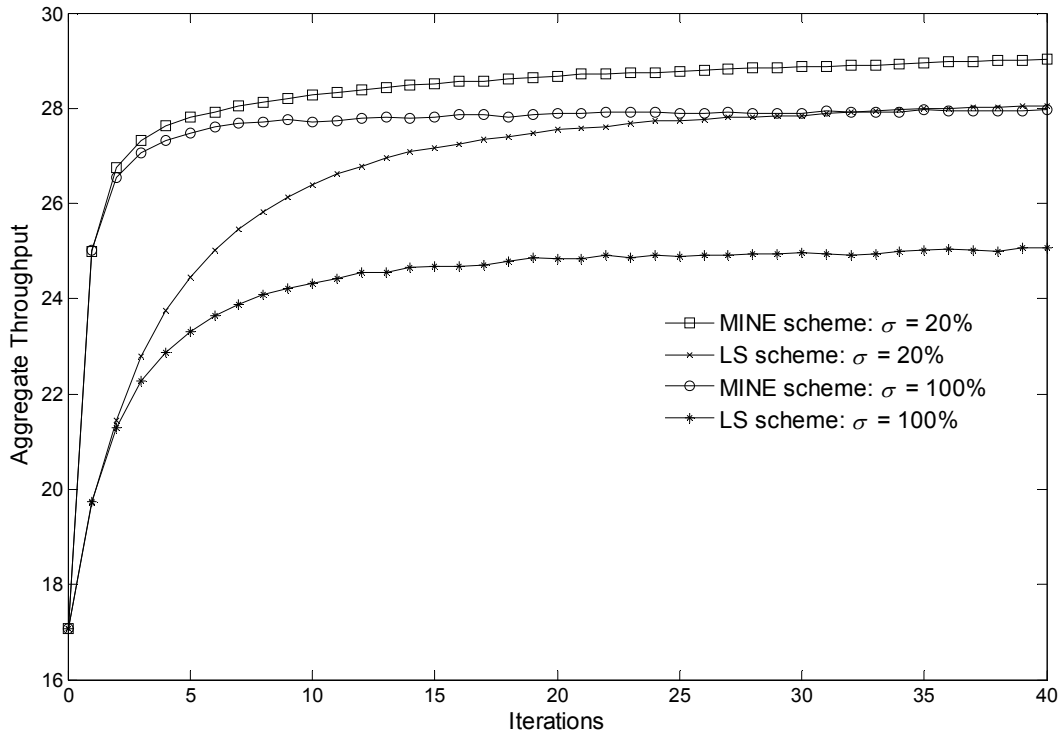


Figure 3.5: Aggregate throughput with dynamic loads for IEEE 802.11b.

TABLE 3.3

Throughput gain with dynamic loads for IEEE 802.11b

	LS Scheme	MINE Scheme	% Change
Throughput $\sigma = 20\%$	28.039	29.018	3.49
Throughput $\sigma = 100\%$	25.081	27.964	11.49

Furthermore, the number of nodes associated with each AP is lower and upper bounded by 1 and AP_{\max} respectively. The results are only shown for IEEE 802.11b which is representative of denser scenarios (with $D = 3$ and $Y = 8$). As expected, Fig. 3.5 shows that the MINE scheme outperforms the LS scheme in terms of aggregate throughput. As shown in Table 3.3, the throughput gain increases in more dynamic load scenarios and is as much as 11% when the standard deviation is 100% of AP_{\max} . This gain is due to the MINE scheme's faster convergence time which allows it to track the load changes more

closely when compared to the LS scheme. An impressive gain can also be achieved for IEEE 802.11a with comparable densities (see Section 3.2.3). These results show that the MINE scheme not only converges significantly faster and requires less channel switches, but also achieves better throughput in dynamic load scenarios.

3.2.2 Number of Channels

In order to investigate the effect of different number of channels, we will focus on IEEE 802.11a, that has $D = 12$ channels. Another reason for selecting IEEE 802.11a is that the number of channels available for operation varies according to the local regulatory requirements of a particular region. Although the majority of regions including the United States (US) allow operation on 12 channels, certain countries such as China and Japan can only operate on 4 channels. A list of the number of channels available according to regions/countries is shown in Table 3.4 [67]. Hence, it is important to determine if the proposed MINE scheme can provide acceptable performance when a different number of channels is available. In view of this, simulations using IEEE 802.11a specifications with D varied from 4 up to 12 channels have been performed.

Fig. 3.6 shows the aggregate throughput for both the MINE scheme and LS scheme with $D = 4$ and $D = 12$ channels. It is clear in both cases of operating channels, the significant reduction in convergence time for the MINE scheme is very evident. In fact, the reduction in convergence time is almost constant with an average of 75% reduction when D is increased from 4 to 12. This shows that the MINE scheme is able to maintain a significant reduction in convergence time across the different number of available channels. On the other hand, the reduction in channel switches required for convergence varies from a reduction of 51% when $D = 4$ to a still respectable 30% when $D = 12$.

TABLE 3.4

IEEE 802.11a number of channels according to regions/countries

Regions/Countries	Number of Channels, D
Americas (FCC)	12
China	4
ETSI	19
Israel	8
Japan (TELEC)	4
Korea	19
North America	12
Singapore	12
Taiwan	11

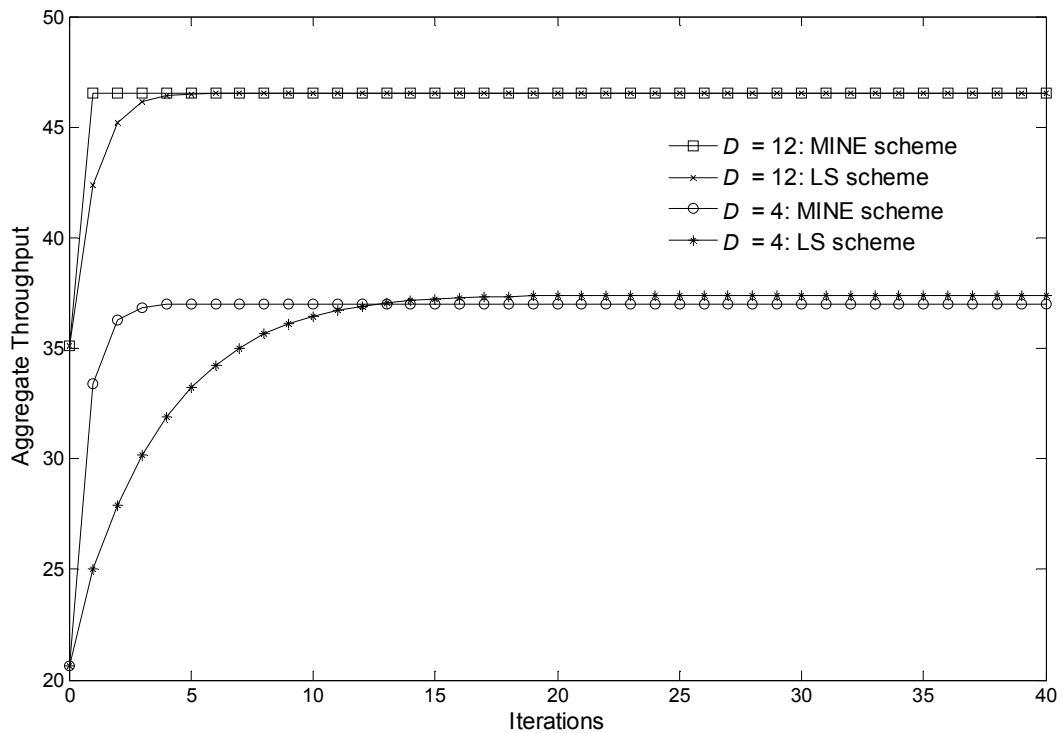


Figure 3.6: Aggregate throughput for MINE scheme and LS scheme with $D = 4$ and $D = 12$ channels.

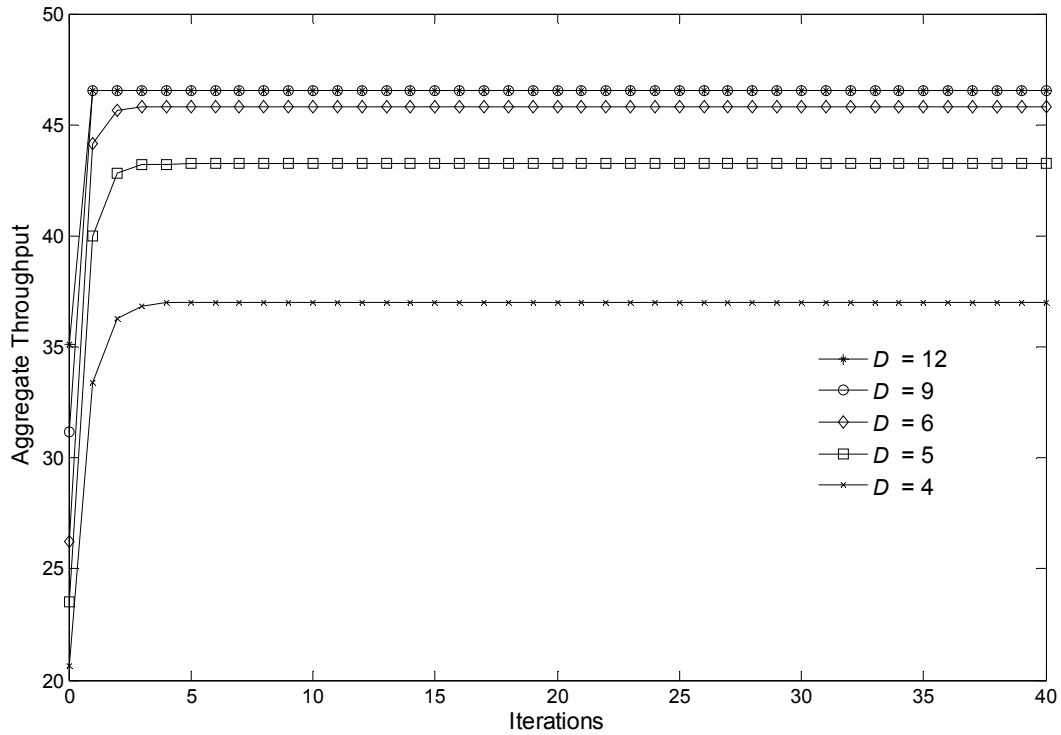


Figure 3.7: Aggregate throughput for MINE scheme with various D channels.

In Fig. 3.7, the performance of the MINE scheme when D is varied from 4 to 12 channels is shown. It is interesting to see the law of diminishing returns comes into effect as D is increased. The highest increment in throughput is obtained when D is increased from 4 to 5 and for each subsequent addition of a channel, the amount of increment decreases. The MINE scheme can achieve the upper bound performance (represented by the ideal interference free case, which is when all APs occupy channels without any interference from any other APs) for $D \geq 8$ channels. We also note that the MINE scheme converges to the upper bound performance in a single iteration when $D > 8$ channels. Recall that the enhancement for selecting d_{\max} from the equal candidate channels in the MINE scheme guarantees single iteration convergence when $D > Y$ (note that in the simulations, $Y = 8$ interfering APs).

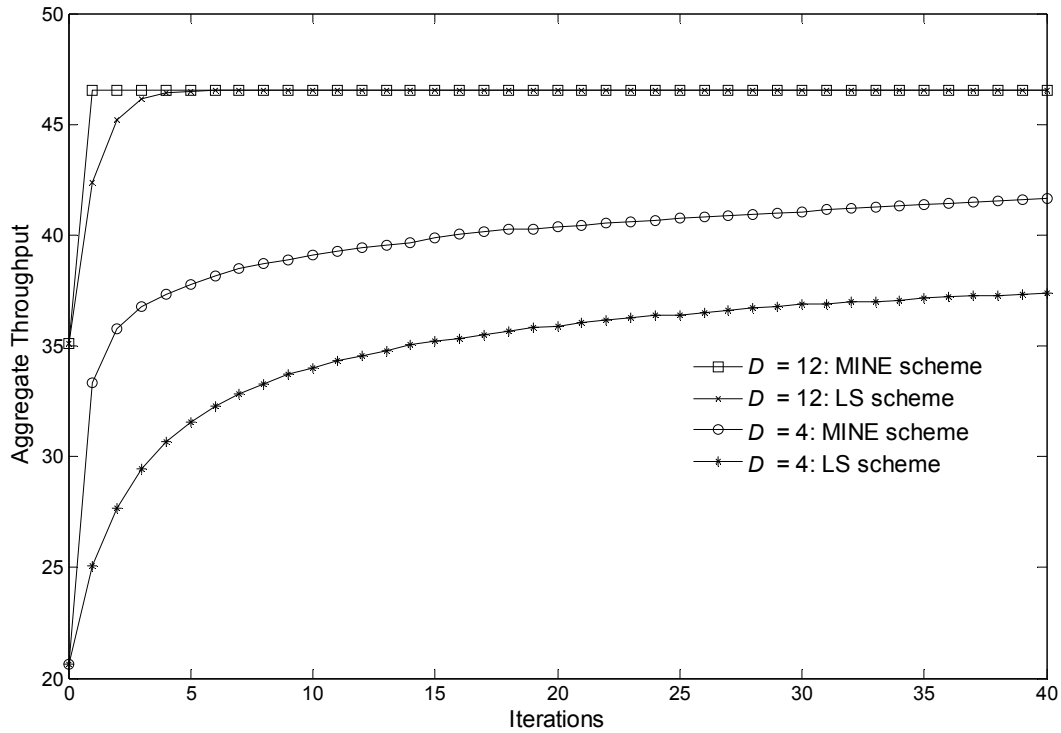


Figure 3.8: Aggregate throughput for MINE scheme and LS scheme with dynamic loads for $D = 4$ and $D = 12$ channels.

In order to evaluate the throughput gains achievable by the MINE scheme across different numbers of channels, dynamic load scenario is used. Recall that in dynamic load scenario, the number of associated nodes of each AP is dynamically changed according to a Gaussian distribution with mean = 0 and standard derivation, σ being a percentage of AP_{\max} . In this particular case, σ is set to 100% of AP_{\max} . Fig. 3.8 shows the aggregate throughput for both the MINE scheme and the LS scheme with $D = 4$ and $D = 12$ channels and dynamic loads. It can be noted that the MINE scheme outperforms the LS scheme for $D = 4$ but both schemes give similar throughput performance when $D = 12$. The reason for the better performance in the former is due to shorter convergence time which allows the MINE scheme to track the changes in the network more closely. However, when the number of channel increases and becomes comparable

to the number of interfering APs, as in the case of $D = 12$, the performance of both schemes becomes similar. This is because most, if not all APs have channels that are already different from their neighbouring APs and are not affected by the changing loads on them. Thus, we would expect better performance gains in denser deployment scenarios, which will be discussed in the next subsection.

3.2.3 Deployment Densities

WLAN deployments today vary from sparse to extremely dense. It was reported in [13] that in one city in the US, more than 8500 APs were deployed and in another city, one AP was found to have 85 interfering neighbour APs. Thus, it is imperative to determine the effectiveness of the proposed MINE scheme across different deployment densities.

Subsequently, using IEEE 802.11a with $D = 4$ channels, three test cases with increasing deployment densities have been chosen: $Y = 8$, $Y = 20$ and $Y = 24$ interfering neighbour APs. In the simulations of all test cases, due to a higher number of interfering neighbour APs ($Y = 24$), a sufficiently large grid of 17×17 consisting of 289 APs is used instead. Fig. 3.9 shows the aggregate throughput for both the MINE scheme and LS scheme with different deployment densities. It can be seen that the MINE scheme is able to maintain a significant reduction in convergence time over the LS scheme for all three test cases. The reduction in convergence time is almost constant with an average of 81% reduction. On the other hand, the reduction in channel switches required for convergence varies from a reduction of 52% when $Y = 8$ to 80% when $Y = 24$. When the deployment density increases (from $Y = 8$ to $Y = 24$), the throughput achieved reduces significantly. This is expected because as more neighbour APs get deployed, the amount of interference experienced will correspondingly increase.

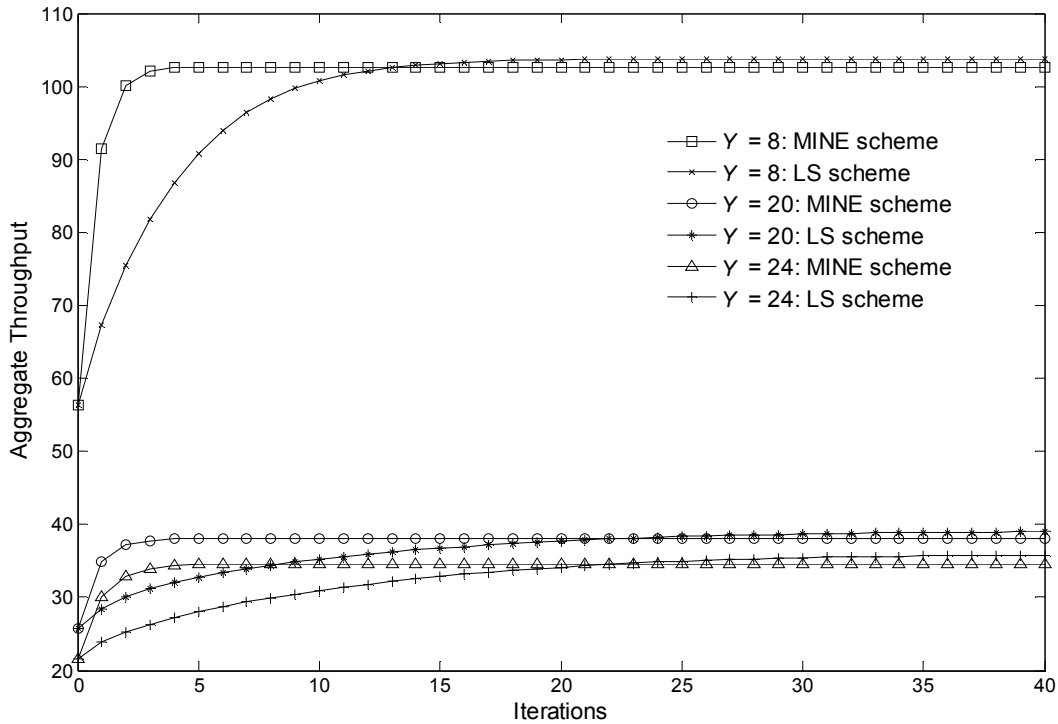


Figure 3.9: Aggregate throughput for MINE scheme and LS scheme with various deployment densities.

TABLE 3.5

Throughput gains with dynamic loads for various deployment densities

Density	LS Scheme	MINE Scheme	% Change
$Y = 8$	102.219	114.807	12.31
$Y = 20$	31.644	38.702	22.30
$Y = 24$	28.091	36.504	29.95

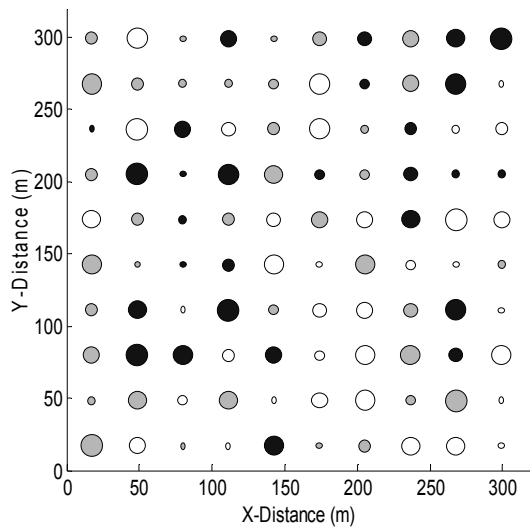
Now, the throughput performance of the MINE scheme is evaluated by employing dynamic loads across different deployment densities. Table 3.5 shows the throughput gains obtained in the test cases described above. Throughputs in excess of 100 are recorded due to the larger number of APs used (289 APs). As expected, we see the highest throughput gain for $Y = 24$ (highest density) while the $Y = 8$ (lowest density) showed the lowest throughput gain. This is because, in very dense deployment

scenarios, fast and accurate changes in channel switching are required when loads are changing in order to give improved throughput to all the APs and the network as a whole. The MINE scheme was able to provide that due to its significantly shorter convergence time. These results show that the MINE scheme is able to maintain a significant reduction in time and number of channel switches required for convergence and throughput gain in dynamic loads across different deployment densities.

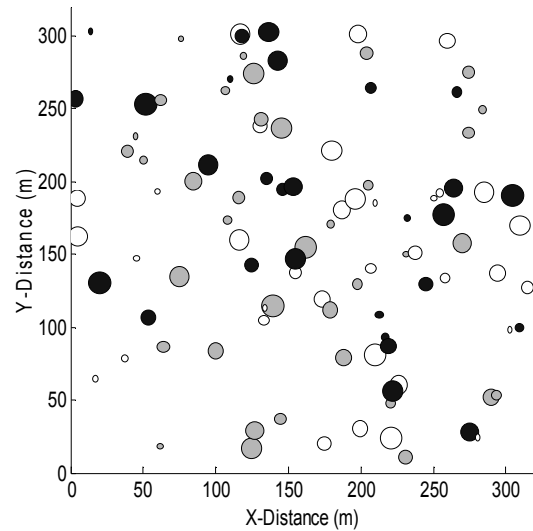
3.2.4 Non-Uniform Topologies

Traditional cellular networks typically deploy their base stations in a regular fashion in order to maximize capacity and coverage while minimizing harmful interference. This is possible due to the sole ownership of licensed frequency bands by the network operator. By contrast, WLANs' license-exempt operation and affordability means that almost anybody can deploy them. The inherent lack of coordination between different owners of WLAN APs results in highly non-uniform deployment topologies. In fact, based on actual WLANs deployment in several US cities, it was found that a typical AP has between 2 to 20 interfering neighbour APs [13]. This implies that certain APs in the network inevitably suffer more interference than others as a result of the non-uniformity.

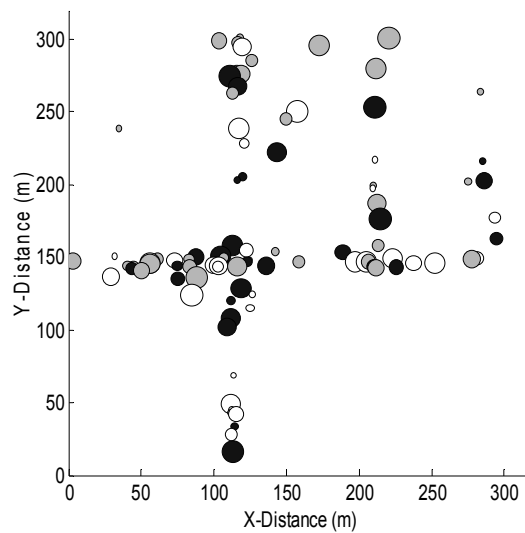
Fig. 3.10 shows a realization of the uniform, non-uniform and real topologies. For the uniform topology, APs are located in a grid whereas in the non-uniform topology, APs are randomly located. The real topology is taken from an actual WLAN deployment in Seattle, Washington based on the database provided by Intel Place Lab project. It is clear that APs in the non-uniform and real topologies suffer from differing levels of interference as opposed to the uniform topology. Upon closer inspection, we note that



(a) Uniform topology



(b) Non-uniform topology



(c) Real topology

Figure 3.10: Uniform, non-uniform and real topologies.

the real topology exhibits the highest non-uniformity in terms of the range of neighbour APs that a typical AP has.

To understand the effects of non-uniformity, we consider a constant sized topology with a specified number of APs (such as those in Fig. 3.10). It is useful to state here that in general, increased interference due to more neighbour APs results in reduced

throughput. So, in order to reduce the maximum number of neighbouring APs, the best topology will be one where the distance between APs is constant, which is the uniform topology. However, when the locations of APs are randomized, clusters of APs begin to form while some of the APs become increasingly isolated. With only a limited number of channels, large clusters are unable to cope with the increased interference while the isolated APs underutilize the channels available. An extreme form of this can be seen as the non-uniformity increases, as in the case of the real topology, where the majority of APs are found in a few very large clusters with the rest being outlying APs.

Fig. 3.11 and Fig. 3.12 show the aggregate throughput for both the MINE scheme and LS scheme in uniform and non-uniform topologies for IEEE 802.11b and IEEE 802.11a respectively. Firstly, it can be noted that the throughputs of the MINE scheme and LS scheme are similar in all levels of non-uniformity. Nevertheless, the MINE scheme still outperforms the LS scheme in terms of the number of iterations and channel switches required for convergence, with 80% to 90% reductions in the case of the real topology.

Secondly, we note that there is an evident degradation in the throughput of both schemes due to the non-uniformity of the non-uniform and real topologies for both IEEE 802.11b and IEEE 802.11a. For IEEE 802.11b, the degradation is at 7% and 47% for the non-uniform and real topologies respectively whereas for IEEE 802.11a, a degradation of 14% has been observed for only the case of the real topology. As mentioned before, the degradation is due to the increased interference in the large clusters of APs due to the increased non-uniformity. This also explains the relatively smaller degradation for IEEE 802.11a because with $D = 12$ channels, IEEE 802.11a can withstand higher interference when compared with IEEE 802.11b's $D = 3$ channels.

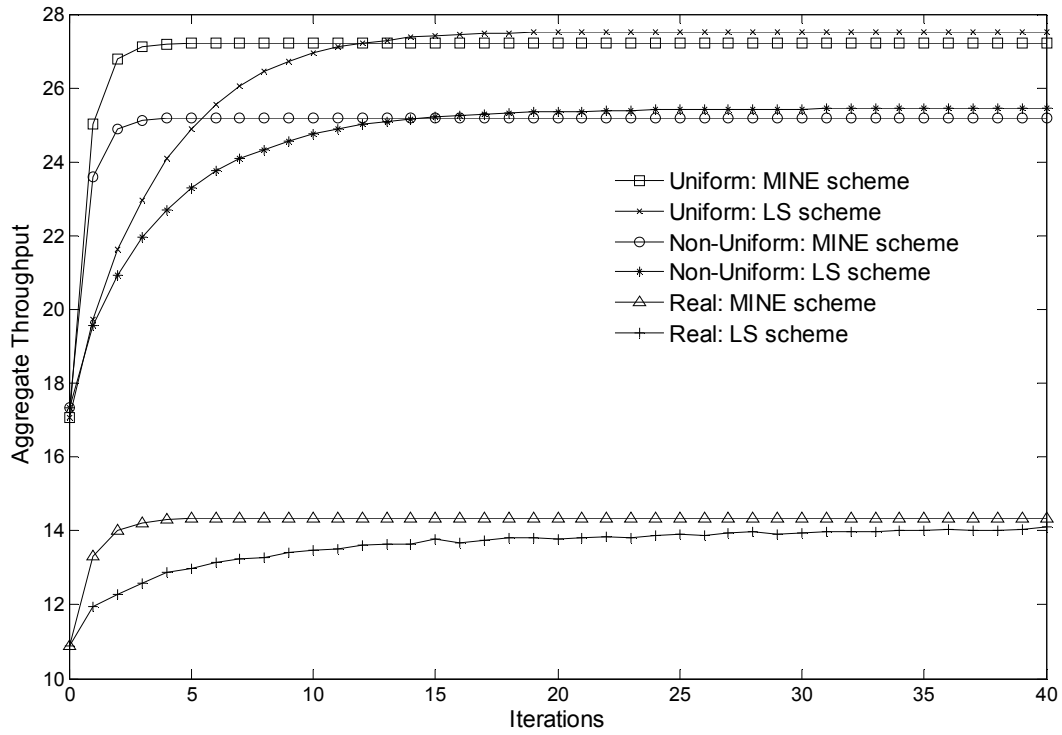


Figure 3.11: Aggregate throughput for MINE scheme and LS scheme with various non-uniformity for IEEE 802.11b.

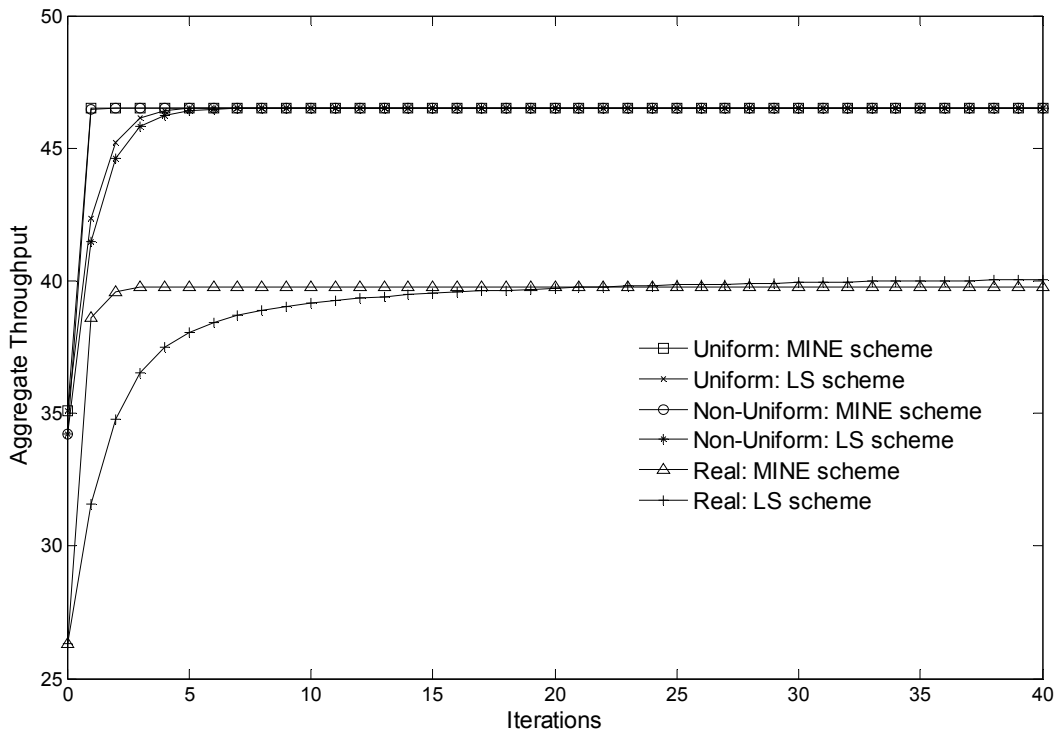


Figure 3.12: Aggregate throughput for MINE scheme and LS scheme with various non-uniformity for IEEE 802.11a.

Thirdly, there is also degradation in the throughput gain of both schemes over the random scheme (note that the throughput at the zeroth iteration reflects the performance of the random scheme since the initial channels are assigned randomly). The throughput gains of the MINE scheme in the case of IEEE 802.11b are 59%, 45% and 31% for uniform, non-uniform and real topologies respectively. As non-uniformity increases from the uniform to real topology, the interference reaches saturation point where all available channels are overloaded and any channel assignment scheme's ability to produce a gain over a simple random scheme is diminished. However, a meaningful gain can still be achieved, even for the real topology.

3.2.5 Dynamic Topologies

Traffic demands in actual WLANs deployments are known to be time-varying. Studies on WLAN traffic characterization have shown that it is not uncommon to have a large number of APs idle for substantial periods of time with daily or even weekly trends [68]. For example, in an office environment, heavy traffic demands occur during office hours but there is virtually no traffic outside of work hours and at weekends.

The unavailability of traffic can be attributed to two main factors. Firstly, taking a home environment as an example, traffic may be only available after office hours (time factor). Secondly, idle periods depend on the location of APs (location factor). For example, APs located in meeting rooms and auditoriums have traffic only when there is a scheduled event. The lack/availability of traffic at different times can be effectively represented by APs switching "on/off", which creates a highly dynamic topology scenario. In view of this, it is imperative to determine if the proposed MINE scheme is still able to provide acceptable performance in dynamic topology scenarios.

The number of APs that are switched on/off is modeled by the Poisson distribution with differing values of λ , the expected number of AP on/off switches per iteration. The probability that there are ζ number of switches is given by the probability mass function

$$f_{PMF}(\zeta) = \frac{\lambda^\zeta e^{-\lambda}}{\zeta!} \quad (3.2.1)$$

where e is the base of the natural logarithm and $\zeta \in \{0, 1, 2, \dots\}$. The values for λ are taken from the set $\{0, 0.5, 1, 1.5, 2\}$ which is reasonable considering the large number of APs in our topology and that the lack/availability of traffic in APs does not change too often in a relatively small time interval. The particular APs that are switched on/off are chosen randomly and they are toggled between the on/off states. We have also used the real topology of Fig. 3.10(c), which is based on an actual WLAN deployment.

In Fig. 3.13, the aggregate throughput of both the MINE scheme and LS scheme for $\lambda = 0$ (static topology) and $\lambda = 2$ (dynamic topology) for IEEE 802.11b are shown. Although the throughput performance of both schemes exhibits only a marginal difference between static topology and dynamic topology, an evident performance gap between the MINE scheme and LS scheme can be seen in the dynamic topology. The improved throughput performance of the MINE scheme is due to its shorter convergence time, which allows it to track the changes in the network topology better than the LS scheme. We expect the MINE scheme to outperform the LS scheme even more with larger values of λ .

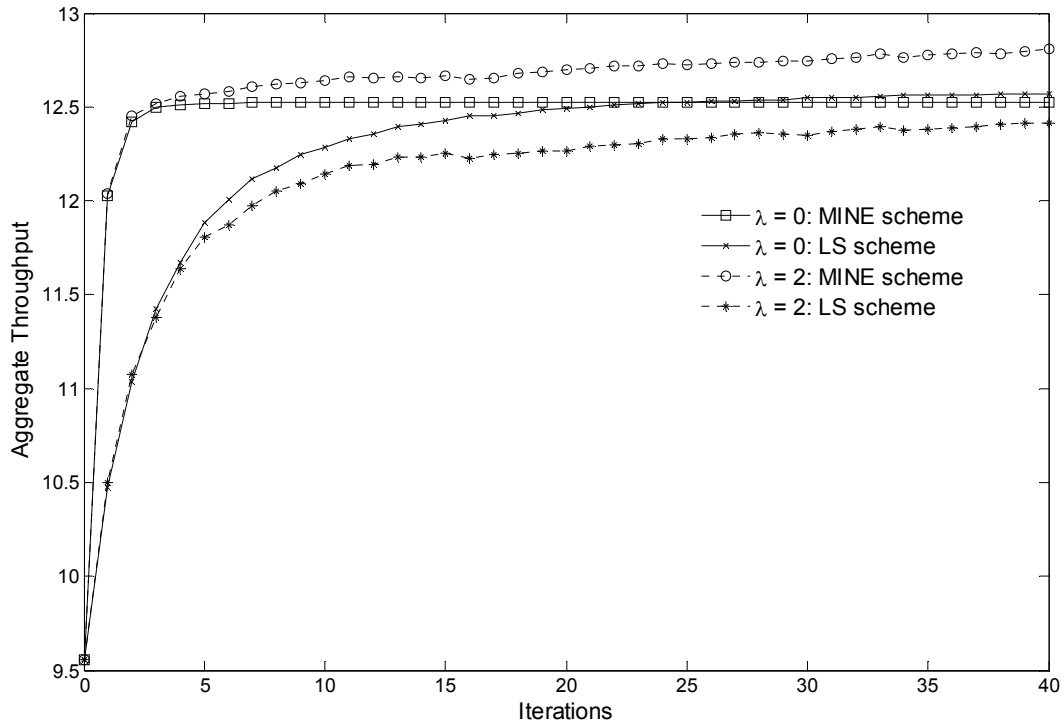


Figure 3.13: Aggregate throughput for MINE scheme and LS scheme in dynamic topology.

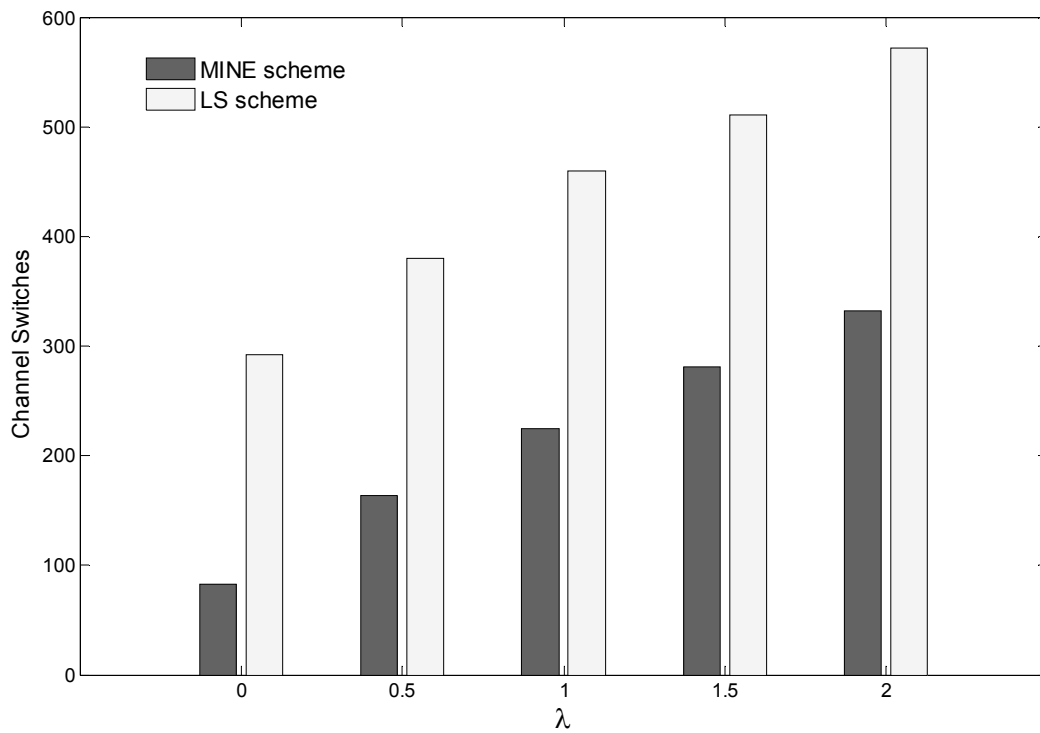


Figure 3.14: Channel switches required for convergence with various dynamic topologies.

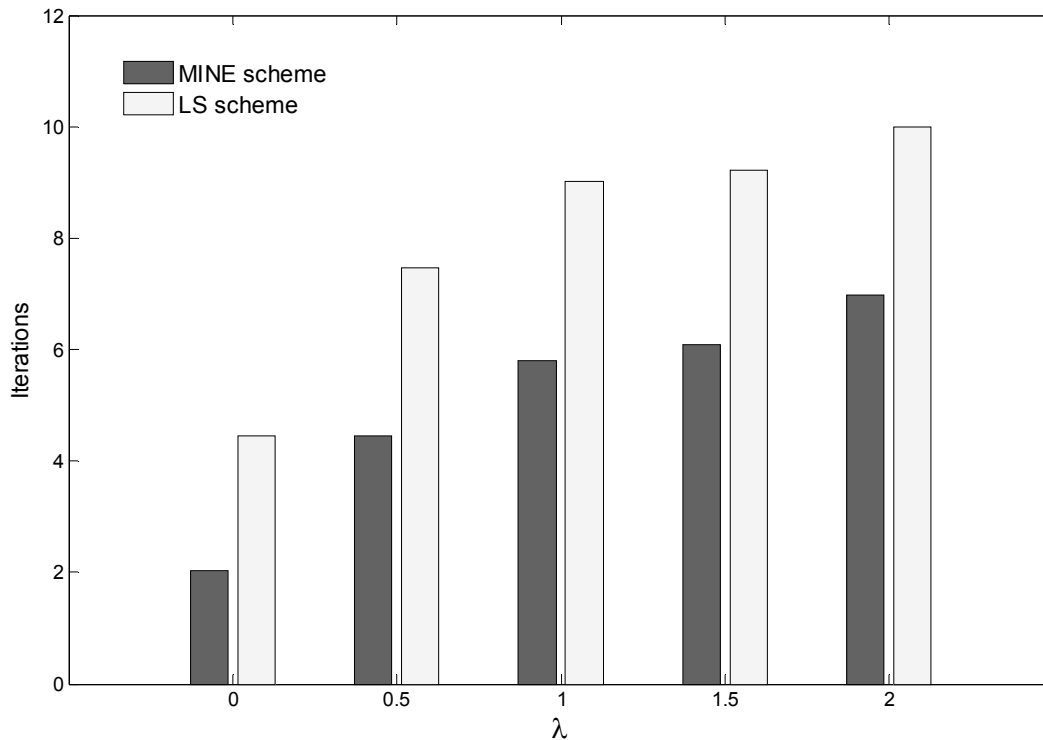


Figure 3.15: Iterations required for convergence with various dynamic topologies.

Fig. 3.14 and Fig. 3.15 show the number of channel switches and iterations required for “convergence” with various dynamic topologies. In a strict sense, channel assignment schemes do not converge in a dynamically changing topology. However, the term is loosely used here to indicate the first instance it reaches 90% of the maximum throughput. Note that both schemes “converge” to a relatively constant throughput in Fig. 3.13.

It is clear in both figures that as the value of λ increases, the number of channel switches and iterations required for convergence increases as well. This is expected since more APs will change their channels and a longer time is needed for tracking when the topology changes at a higher rate. Although the gain in percentage decreases as λ increases, the MINE scheme is still able to maintain meaningful margins of improvement over the LS scheme, which are 41% and 30% for the number of channel

switches and iterations respectively at $\lambda = 2$. Although not shown, similar robust performance has been observed for IEEE 802.11a.

3.2.6 Heterogeneous Networks

The majority of the dense WLAN networks encountered today are deployed by different entities, resulting in equipment from various vendors. Based on data obtained from actual WLANs deployment in several US cities, APs from at least 10 different WLANs vendors can be found [13]. Furthermore, channel assignment is a non-standardized feature so vendors are left to develop their own proprietary schemes. These imply that at best only a certain percentage of all APs will implement a certain channel assignment scheme and that multiple channel assignments schemes implemented by different vendors have to co-exist in the same network.

However, previous studies on channel assignment in WLANs almost always assume that all APs employ the same channel assignment scheme, which is clearly unrealistic. On the other hand, to the best of our knowledge, the interaction between different channel assignment schemes has also not been studied before. In view of this, we evaluate the effectiveness of the proposed MINE scheme in heterogeneous WLAN networks where i) only a certain percentage of all APs employ the MINE scheme and ii) when there are multiple channel assignment schemes implemented by APs in the same network. These heterogeneous network scenarios are expected in practice as WLAN AP vendors implement their own proprietary channel assignment schemes. With this in mind, a good channel assignment scheme should be robust enough to provide gains across all percentages of APs implementing it as well as when it co-exists with other channel assignment schemes.

In order to determine the effectiveness of the MINE scheme when co-existing with other channel assignment schemes in the same network, we have implemented the DSATUR scheme, described in Section 2.3.2. This scheme is chosen because of its simplicity and hence its attractiveness for practical implementation. Although the scheme is intended for small and isolated centralized WLAN networks, it can still be deployed in a heterogeneous network where a group of APs belong to the same owner while the rest of the APs belong to various owners. An example of this is an office block where a big enterprise occupies several floors while other floors are occupied by many smaller firms.

Throughput gains are calculated by taking the convergence throughput over the initial throughput which represents the gains when APs implement the MINE scheme instead of the default random channel assignment scheme. Results are only shown for IEEE 802.11b which is representative of denser scenarios (with $D = 3$ channels and $Y = 8$ interfering APs). The percentage of APs that implement the MINE scheme is varied from $P_M = 0\%$ to 100% . The remaining APs remain on their initial randomly assigned channels throughout the simulation duration (random channel assignment scheme).

Fig. 3.16 shows the aggregate throughput for various P_M percentages of APs that implement the MINE scheme. There is an evident throughput improvement across all percentages with higher gains seen when more APs implement the MINE scheme. Fast convergence times of less than four iterations are also seen across all percentages. The throughput decomposition gains for APs that implement the MINE scheme and the remaining APs (random scheme) are shown in Fig. 3.17. The performance of the MINE scheme is very commendable in that the total throughput gain increases linearly with P_M with up to almost 60% improvement when $P_M = 100\%$. Furthermore, APs that implement the MINE scheme can expect at least 50% improvement in their throughputs

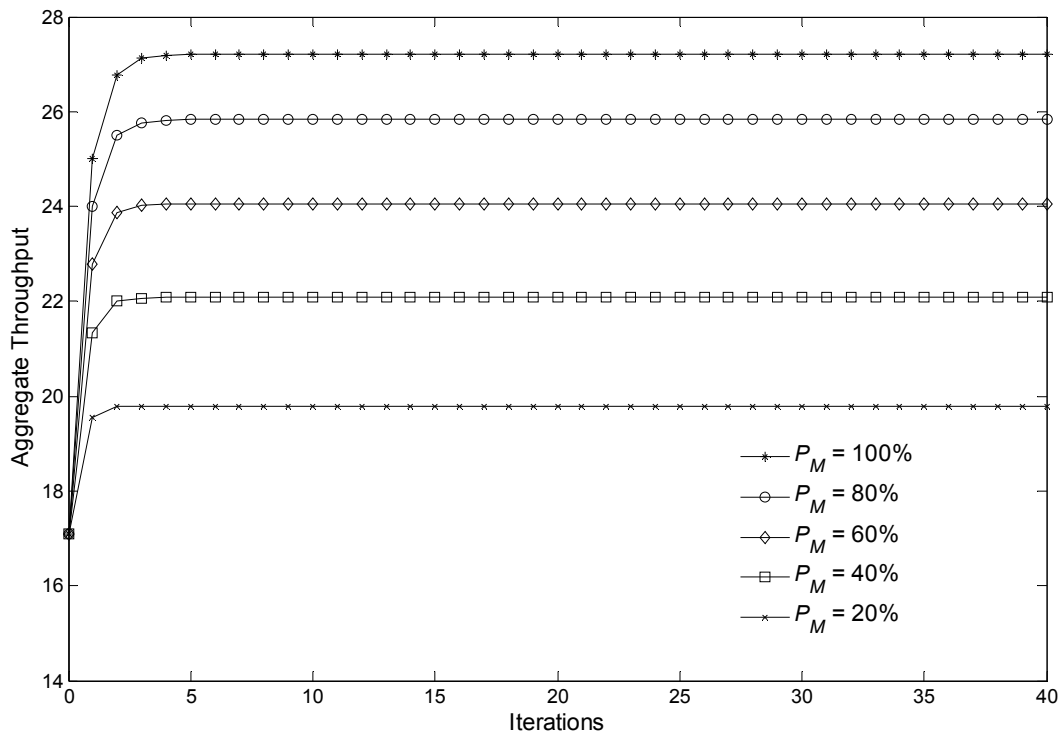


Figure 3.16: Aggregate throughput for various percentages of APs that implement MINE scheme.

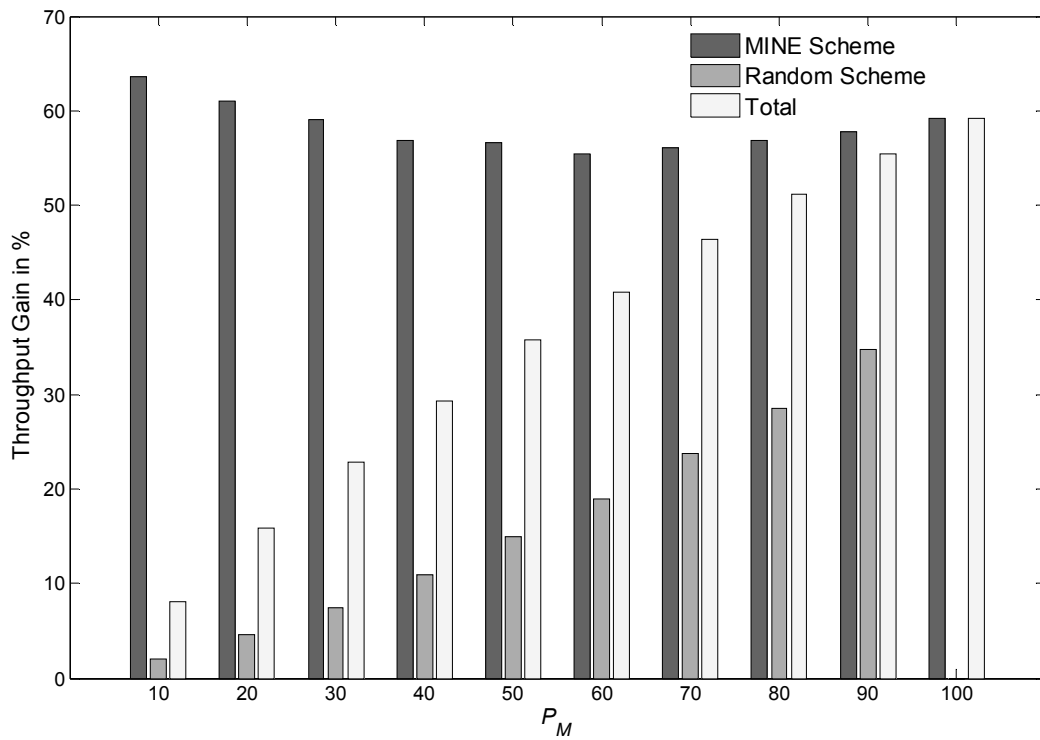


Figure 3.17: Throughput decomposition gains for various percentages of APs that implement MINE scheme.

irrespective of how many APs are implementing the scheme in the network. It is equally important to note that even APs that do not implement the MINE scheme also benefit when APs that implement the MINE scheme are present in the network. Their throughput is seen to increase up to 30% with higher gains seen for higher values of P_M .

The interaction of the MINE scheme with the DSATUR scheme is presented here. Initially, the percentage P_D of APs that implement the DSATUR scheme is set. Due to the centralized nature of this scheme, an algorithm is designed that ensures that the APs chosen to implement the DSATUR scheme are connected to each other. The first AP is chosen randomly. The next AP is chosen randomly from all possible neighbour APs of the reference AP (which is set as the previously chosen AP). In the event that all neighbour APs have already been chosen, the reference AP is selected randomly from the set of previously chosen APs. This process is repeated until the desired number of APs is chosen. After the DSATUR APs have been chosen, the APs that implement MINE scheme are chosen randomly from the rest of the APs. The remaining APs implement the random channel assignment scheme.

Fig. 3.18 shows the throughput decomposition for various percentages P_M of APs that implement the MINE scheme when $P_D = 10\%$ of APs implement the DSATUR scheme. Note the increase in aggregate throughput as more APs implement the MINE scheme. Of particular interest is when $P_M = 40\%$ which means $P_R = 50\%$ (P_R is the percentage of APs that implements the random channel assignment scheme and $P_M + P_R + P_D = 100\%$). Even though the number of APs that implement the MINE scheme is lesser, their throughput is higher than APs that implement the random scheme. The throughput decomposition gains for various percentages P_M of APs that implement the MINE scheme when $P_D = 10\%$ of APs implement the DSATUR scheme is shown in Fig. 3.19. Similar to the case when only the MINE scheme is implemented by a percentage of APs

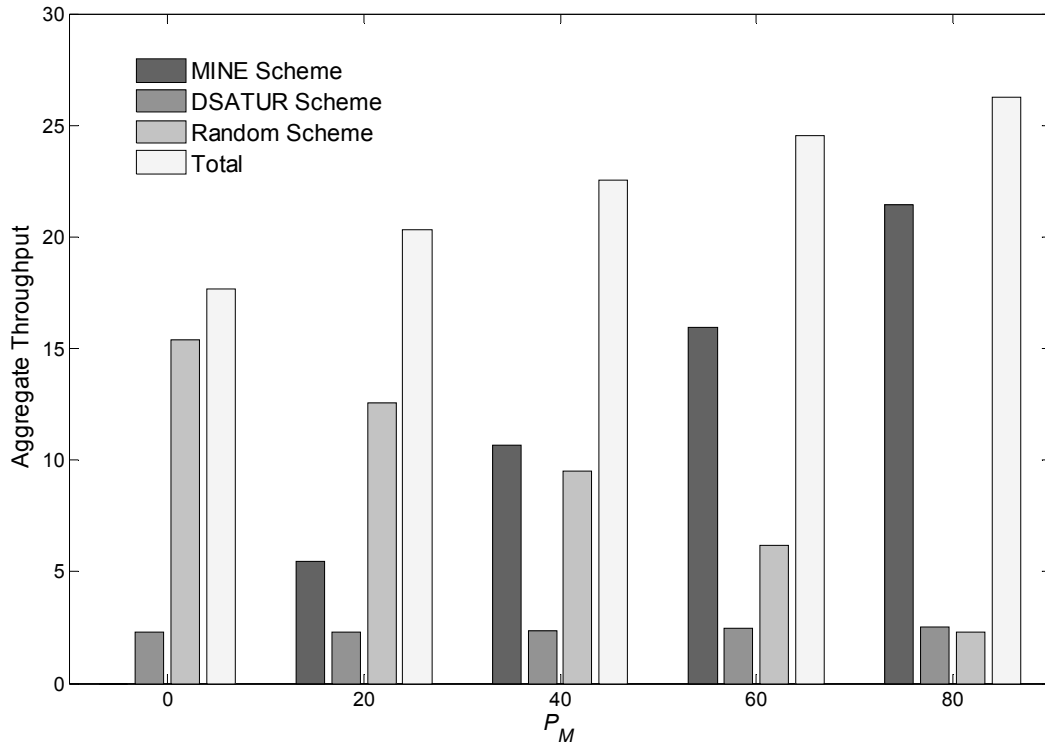


Figure 3.18: Throughput decomposition for various percentages of APs that implement MINE scheme when 10% of APs implement DSATUR scheme.

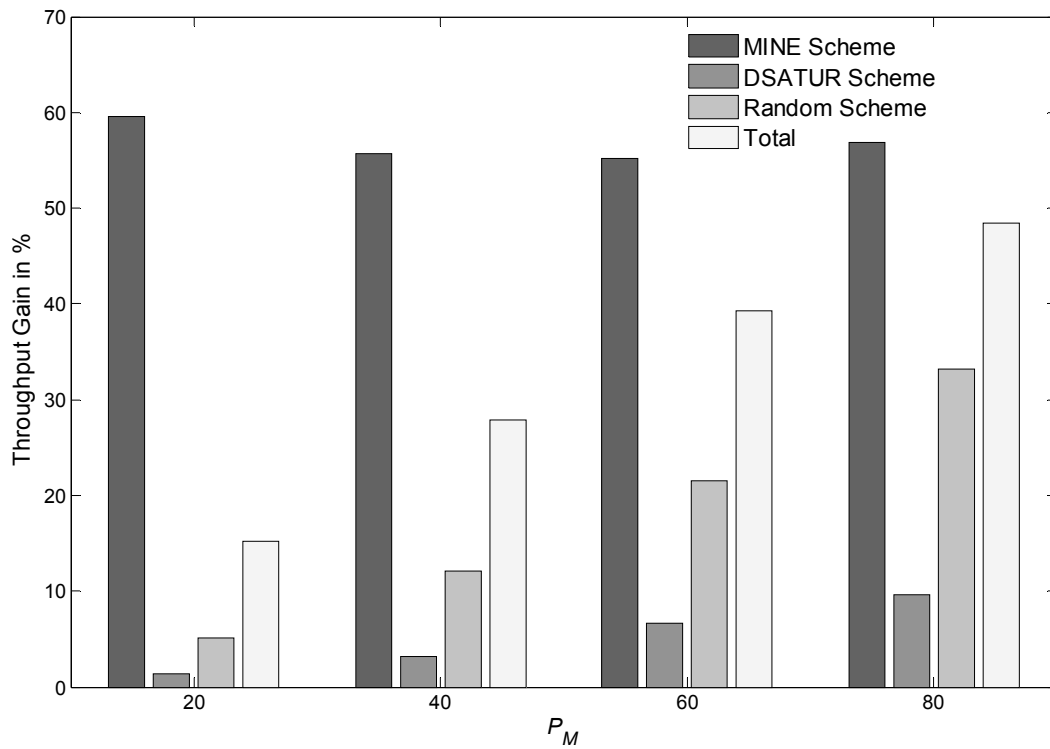


Figure 3.19: Throughput decomposition gains for various percentages of APs that implement MINE scheme when 10% of APs implement DSATUR scheme.

in the network, the robust performance of the MINE scheme can be seen from total throughput gains of up to almost 50%. Furthermore, throughput gains of not less than 50% can be noted for the MINE scheme APs across all values of P_M . Last but not least, the presence of APs that implement the MINE scheme results in throughput gains for APs that implement other channel assignment schemes such as the DSATUR scheme and the random scheme. This is because the MINE scheme maximizes its own throughput by minimizing interference, which benefits neighbouring APs as well. Although not shown, similar gains can also be seen for different values of P_D which reflect networks with a higher percentage of APs that implement the DSATUR scheme.

3.3 Summary

In this chapter, the MINE scheme has been proposed. It has several key features. Firstly, it does not require knowledge of the throughput function. Secondly, it is asynchronous. Third and finally, it has a much lower complexity. It has been shown that in order to maximize throughput, each AP only needs to choose the channel with the minimum number of active neighbour nodes.

Simulation results have shown that the MINE scheme not only converges significantly faster and requires less channel switches, but also achieves better throughput in dynamic load scenarios. Furthermore, extensive performance evaluation of the MINE scheme has been carried out across a wide variety of realistic scenarios by considering the effects of the number of channels, deployment densities, non-uniform topologies, dynamic topologies and heterogeneous networks. In all of these scenarios, the performance of the MINE scheme has been shown to be highly robust with significant gains in terms of throughput, channel switches and convergence time.

Hence, due to its low complexity and robust performance, the MINE scheme is highly attractive from a practical point of view. However, for practical implementation, the assumption that APs broadcast their number of associated nodes may be highly unrealistic and inadequate. This is due to two reasons. Firstly, it involves changes to the existing MAC protocol that are likely to be backwards incompatible. Secondly, the number of formally associated nodes can be very different from the number of active nodes that have packets to send at any instant of time. In view of this, the estimation of the number of neighbour nodes in each channel becomes a critical task, which will be dealt with in the next chapter.

MINIMUM NEIGHBOUR WITH EKF ESTIMATOR SCHEME

In the previous chapter, we have proposed and described the MINE scheme. It was shown that in order to maximize throughput, each AP only needed to choose the channel with the minimum number of neighbour nodes. The MINE scheme not only converged significantly faster and required less channel switches, but also achieved better throughput in dynamic load scenarios when compared to the LS scheme. Extensive performance evaluation showed that it is highly robust across a wide variety of realistic scenarios.

However, the application of the MINE scheme to practice depends critically on its ability to estimate the number of neighbour nodes in each channel. In view of this, an extended Kalman filter (EKF) estimator and an estimate of the number of nodes by AP are proposed in this chapter. These not only provide fast and accurate estimates but can also exploit channel switching information of neighbouring APs. The integration of the EKF estimator into the MINE scheme gives rise to the minimum neighbour with EKF estimator (MINEK) scheme. Extensive packet level simulation results show that the MINEK scheme is highly scalable and can provide significant throughput improvement over other channel assignment schemes [69].

This chapter is organized as follows. In Section 4.1, the EKF estimator of the total number of nodes is described. This is followed by the estimation of the number of neighbour nodes in Section 4.2. In Section 4.3, the complete MINEK scheme is described. Next, extensive performance evaluation of the MINEK scheme is presented in Section 4.4. Finally, the chapter is summarized in Section 4.5.

4.1 Estimation of the Total Number of Nodes

The strategy for estimating the number of neighbour nodes begins with the estimation of the total number of nodes. Intuitively, a node that observes the transmissions in the channel can determine the prevailing level of contention. Utilizing this information, the total number of nodes can be estimated because a higher number of nodes causes higher contention and vice versa. Using this idea, an EKF was proposed in [70] to estimate the total number of contending nodes in a channel. The motivation for this work is twofold. Firstly, throughput performance can be optimized by setting operating parameters such as backoff window size and RTS threshold [71-74]. Secondly, the knowledge of the estimated total number of nodes can be used in load balancing and handover algorithms for better network utilization [75-78].

However, this EKF cannot be applied to the MINE scheme directly, for two reasons. Firstly, it does not effectively capture the changes in the number of nodes whenever any AP switches into or out of the channel. Secondly, it can only estimate the total number of nodes but not the number of neighbour nodes that is required in the MINE scheme. It might appear that the number of neighbour nodes can be obtained trivially by subtracting the number of nodes formally associated to the AP from the estimated total number of nodes. However, the number of formally associated nodes is generally very

different to the number of active/contending associated nodes at any instant in time.

Active nodes are nodes that have packets to send.

Therefore, in this section, we propose a modified EKF, which addresses the above deficiencies. Based on the two-dimensional Markov Chain model presented in Section 2.1.3, a non-linear function, $n = g(p)$ is derived that relates p , the conditional collision probability, with n , the total number of nodes. Given a particular level of conditional collision probability (which can be measured by observing the channel), function $g(p)$ allows the determination of the corresponding number of nodes. For the derivation of this function, it is useful to remember that p is equal to the probability that at least one of the remaining $n-1$ nodes transmits,

$$p = 1 - (1 - \tau)^{n-1}. \quad (4.1.1)$$

Furthermore, recall that the probability τ that a node transmits in a randomly chosen time slot for two distinct cases is given by:

Case i) $m \leq m'$,

$$\tau = \frac{2(1-2p)(1-p^{m+1})}{W(1-p)(1-(2p)^{m+1}) + (1-2p)(1-p^{m+1})}. \quad (4.1.2)$$

Case ii) $m > m'$,

$$\tau = \frac{2(1-2p)(1-p^{m+1})}{W[(1-p)(1-(2p)^{m'+1}) + 2^{m'} p^{m'+1}(1-p^{m-m'})(1-2p)] + (1-2p)(1-p^{m+1})}. \quad (4.1.3)$$

These equations have been repeated here for convenience. Substituting τ from (4.1.2) and (4.1.3) into (4.1.1) and rearranging for n , we have:

Case i) $m \leq m'$,

$$n = g(p) = 1 + \frac{\log(1-p)}{\log\left(1 - \frac{2(1-2p)(1-p^{m+1})}{W(1-p)(1-(2p)^{m+1}) + (1-2p)(1-p^{m+1})}\right)}. \quad (4.1.4)$$

Case ii) $m > m'$,

$$n = g(p) = 1 + \frac{\log(1-p)}{\log\left(1 - \frac{2(1-2p)(1-p^{m+1})}{\left[W(1-(2p)^{m+1})(1-p) + (1-2p)(1-p^{m+1})\right] + W \cdot 2^m p^{m+1} (1-2p)(1-p^{m-m'})}\right)}. \quad (4.1.5)$$

The corresponding functions $g(p)$ are shown in Fig. 4.1 Since each node can measure p from observing channel activity, an estimate of the total number of nodes can be obtained by using the function $g(p)$.

For an on-line estimate of n , a discrete time measurement p_k of the conditional collision probability in the channel is taken at each time step k . The time step refers to the instant when the EKF is updated. Each time step k consists of B time slots, where B is a predefined constant value. Thus,

$$p_k = \frac{1}{B} \sum_{i=(k-1)B}^{kB-1} c_i \quad (4.1.6)$$

where $c_i = 0$ if there is no transmission or a successful transmission and $c_i = 1$ if there is a collision or the channel is busy in the i^{th} time slot. Because there are only two possible outcomes and B number of trials, p_k is a binomial random variable with

$$Pr\left(p_k = \frac{\beta}{B}\right) = \binom{B}{\beta} p^\beta (1-p)^{B-\beta} \quad \beta \in (0, B). \quad (4.1.7)$$

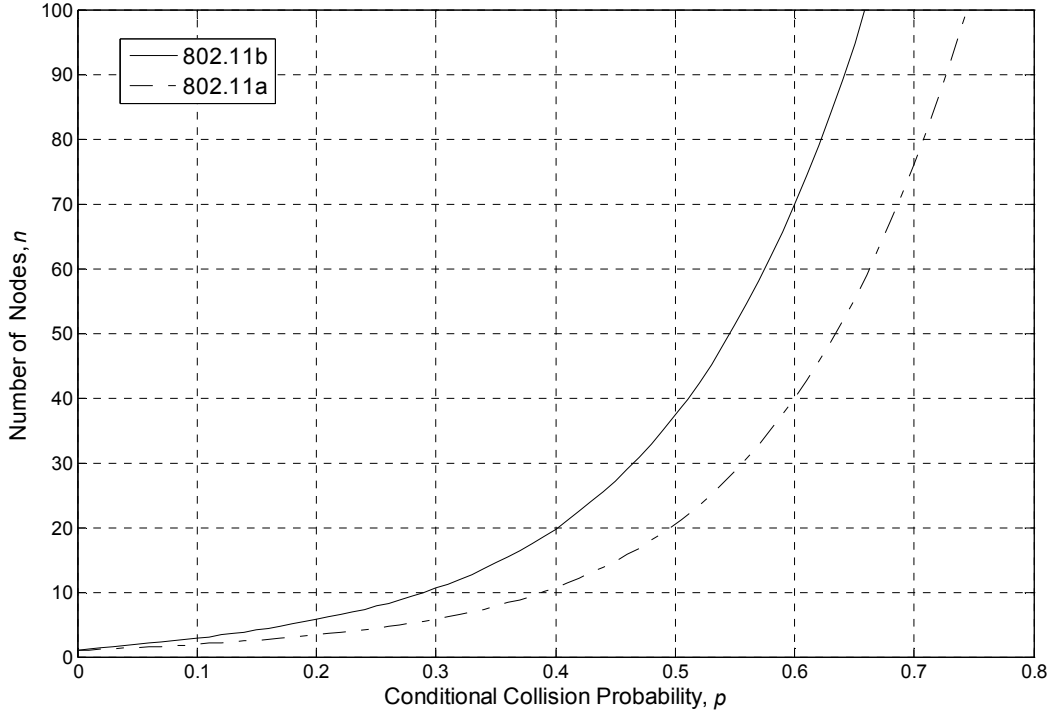


Figure 4.1: Function $n = g(p)$ for IEEE 802.11b and IEEE 802.11a.

The mean and variance of p_k are p and $p(1-p)/B$ respectively. Note that a higher B reduces the variance of p_k at the expense of a longer time between consecutive EKF updates.

The EKF is defined by its state model, which consists of the state and measurement equations. The state equation is

$$n_k = n_{k-1} + u_k + w_k \quad (4.1.8)$$

where n_k and n_{k-1} are the total number of nodes in the occupied channel at time k and $k-1$ respectively, u_k is the net difference in number of nodes due to AP channel switches and w_k is the state noise with zero mean and variance Q_k . The variance Q_k can be used to model changes due to nodes that have activated/terminated. The model for w_k is not

assumed and the selection for the value of Q_k will be discussed at the end of this section.

On the other hand, the measurement equation is

$$p_k = g^{-1}(n_k) + v_k = h(n_k) + v_k \quad (4.1.9)$$

where $p = h(n)$ is the inverse function of $g(p)$ and v_k is a binomial random variable with zero mean and variance

$$\text{var}(v_k) = \frac{h(n_k) \cdot [1 - h(n_k)]}{B}. \quad (4.1.10)$$

The measurement equation is obtained by expressing p_k in (4.1.7) with two terms, a constant and a random variable, that represent its mean and variance respectively.

The design of an EKF lies mainly in the formulation of the state model. Once the state model is defined, the EKF equations can be derived from basic principles. The estimated total number of nodes at time k ,

$$\hat{n}_k = \hat{n}_{k-1} + \hat{u}_k + K_k z_k \quad (4.1.11)$$

where K_k is the Kalman gain and z_k is the innovation. Note that although u_k is normally a known deterministic input, its value is approximated here by its estimate \hat{u}_k and any mismatch that rarely occurs will be compensated by the change detection filter, which is described at the end of this section. The innovation z_k , which gives the difference between the predicted and actual measurement value, is given by

$$z_k = p_k - h(\hat{n}_{k-1}). \quad (4.1.12)$$

The Kalman gain, which represents the relative importance of the new measurement when compared to the previous estimate,

$$K_k = \frac{(P_{k-1} + Q_k)h_k}{(P_{k-1} + Q_k)h_k^2 + R_k} \quad (4.1.13)$$

where Q_k is the variance of the state noise w_k in (4.1.8), R_k is the estimated variance of the measurement p_k , h_k is the sensitivity of the measurement, and P_k is the error variance of the new estimate. R_k is obtained using (4.1.10) with n_k approximated by its estimate \hat{n}_{k-1} ,

$$R_k = \frac{h(\hat{n}_{k-1}) \cdot [1 - h(\hat{n}_{k-1})]}{B}. \quad (4.1.14)$$

The sensitivity of the measurement, h_k linearized at the previous state estimate, \hat{n}_{k-1} is given by

$$h_k = \left. \frac{\partial h(n)}{\partial n} \right|_{n = \hat{n}_{k-1}}. \quad (4.1.15)$$

Finally, the error variance of the new estimate P_k , is calculated recursively by

$$P_k = (1 - K_k h_k)(P_{k-1} + Q_k). \quad (4.1.16)$$

The inverse function of $g(p)$ given in (4.1.4) and (4.1.5), $h(n)$ is not readily expressible in closed form. Furthermore, its derivative function $\partial h(n)/\partial n$ is also needed in the EKF operation. In view of this, the data set that relates n and p is generated using function $g(p)$ and inversed by swapping its coordinates. The inversed data set, which reflect the function $h(n)$, are plotted and curve fitted as shown in Fig. 4.2. The Fourier series fit is found to provide very high goodness of fit for these functions. In particular, the root mean squared errors (RMSE) of both fits are less than 10^{-3} . Its derivative $\partial h(n)/\partial n$ is

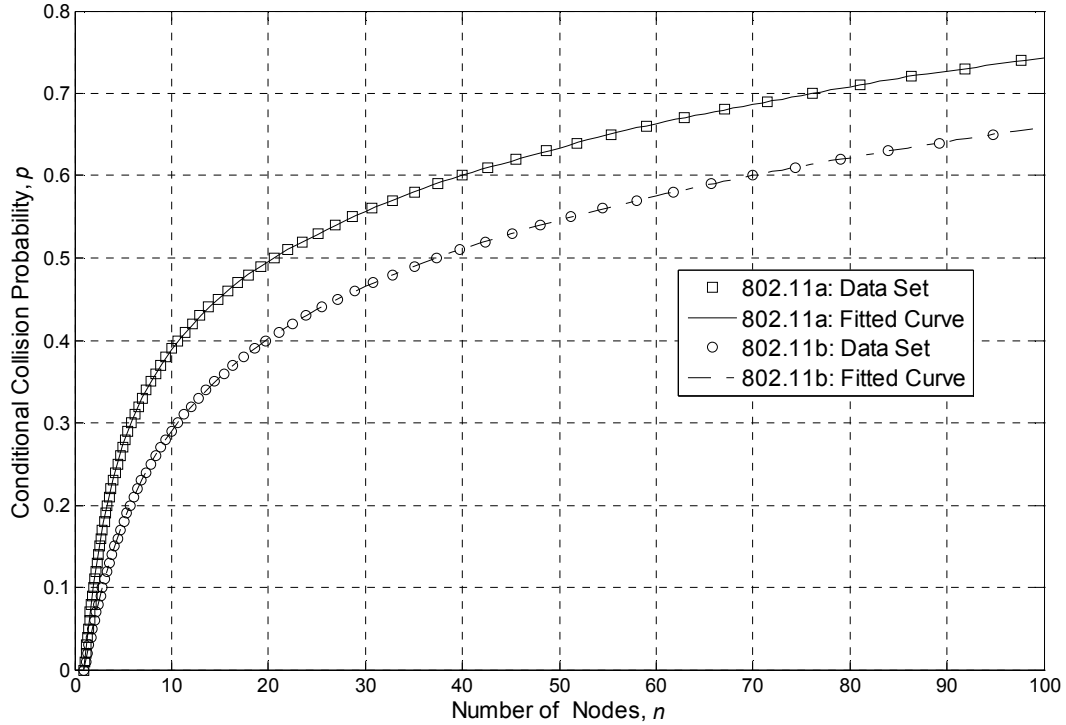


Figure 4.2: Function $p = h(n)$ data set and curve fitting for IEEE 802.11b and IEEE 802.11a.

easily obtained from derivation of the fitted curve's analytical expression. These procedures are performed offline and they help to reduce the computational requirements of the EKF.

In some applications, it is generally assumed that the state noise w_k in (4.1.8) is a stationary process with a constant variance Q_k . However, having a fixed variance trades tracking ability for estimation accuracy. In view of this, a change detection filter is used alongside the EKF to automate the selection of Q_k [70]. The change detection filter raises an alarm each time it detects a network state change. The network state may change due to activated/terminated nodes. The network state change can be detected by examining the innovation, z_k , given in (4.1.12). When the network state is static, the innovation is a white process with zero mean. Therefore, a network state change can be detected if the innovation indicates a nonzero mean.

A change detection filter based on the cumulative summary (CUSUM) test is used due to its simplicity and performance. The innovation, normalized to its standard deviation is used for convenience, with

$$z_k^\sigma = \frac{z_k}{\sqrt{(P_{k-1} + Q_k)h_k^2 + R_k}}. \quad (4.1.17)$$

The CUSUM test is based on two filtered versions of the normalized innovation, g_k^+ and g_k^- given as

$$\begin{cases} g_k^+ = \max(0, g_{k-1}^+ + z_k^\sigma - \nu) \\ g_k^- = \min(0, g_{k-1}^- - z_k^\sigma + \nu) \end{cases} \quad (4.1.18)$$

where ν is the drift parameter. The drift parameter, ν is a filter design parameter that determines the sensitivity of the test. A smaller ν makes the test processes more sensitive towards changes in the z_k^σ process. Initially, g_k^+ and g_k^- are set to zero. When there is a network state change, either one of g_k^+ or g_k^- will increase indefinitely. Note that from (4.1.18), the mean of z_k^σ has to be larger than ν before the test processes begins to diverge. In addition, an alarm is sent if $g_k^+ > a$ or $g_k^- < -a$, where a is the alarm threshold. After an alarm is sent, both g_k^+ and g_k^- are reset back to zero. The selection of a is a trade off between faster detection time and lower probability of a false alarm.

The alarm from the change detection filter is used to set Q_k to a high value for that time step, otherwise Q_k is set to zero. It is found that the exact value set for Q_k when an alarm is raised is not critical to the performance of the filter. If the network change is larger than that provided by the Q_k value, subsequent alarms will be raised until the EKF converges to the new network state. Therefore, the change detection filter aids the EKF

in adapting promptly to any network state changes while maintaining high estimation accuracy when the network state is static.

4.2 Estimation of the Number of Neighbour Nodes

An estimate of the total number of nodes has been obtained in the previous section. However, the number of neighbour nodes is still to be determined. Toward this goal, we propose a related parameter, the estimated number of nodes by an arbitrary AP, which apportions the estimated total number of nodes to each AP. An AP and its associated nodes, which form a BSS, switch channel as a collective unit. Thus, it is not only natural but also beneficial to have estimates of the number of nodes by AP. This is because even after any AP has switched channels, the estimates of the number of nodes by AP are still valid. Using this estimate, channel switching information of neighbouring APs can be exploited. Complemented by information of channels occupied by each AP, the number of neighbour nodes can be estimated accurately.

As has been seen, distributed schemes use only local information to determine which channel they should occupy. Inevitably, measurements need to be obtained from all available channels, either by the APs or their associated nodes. However, whenever any neighbouring APs switch into or out of the occupied channel, these schemes generally employ one of two options. They either obtain new measurements from all available channels or continue averaging the measurements. The former incurs costly overheads, is time consuming and its measurements may become invalidated if there are any subsequent channel changes during the measurement period. As for the latter, this results in inaccurate and erroneous estimates. On the contrary, by employing the estimated number of nodes by AP, only the occupied channel of the AP that switched

channels needs to be updated. To the best of our knowledge, the MINEK scheme is the first that exploits channel switching information of neighbouring APs in order to obtain accurate and timely measurement estimates.

After obtaining an estimate of the total number of nodes \hat{n}_k , the estimated number of nodes by AP, $\hat{n}_{k,i}$ is derived. Here, i is used to reference each AP uniquely and can be the BSS identifier (BSSID). In the derivation of this parameter, the fact that every contending node has an equal opportunity in accessing the channel is used. The implication of this fact is that the number of nodes from each AP is proportional to the average number of successful transmissions that it makes. Consider n_k nodes contending for a channel and let γ_i be the ratio of the number of successful transmissions by an arbitrary AP over the total number of successful transmissions, $\gamma_i = s_i/S$. Since the probability for a successful transmission in a random time slot is the same for every node, γ_i is a binomial random variable with

$$Pr\left(\gamma_i = \frac{s_i}{S}\right) = \binom{S}{s_i} q_i^{s_i} (1 - q_i)^{S - s_i} \quad s_i \in (0, S). \quad (4.2.1)$$

where $q_i = n_{k,i}/n_k$ is the actual ratio of the number of nodes associated with AP- i over the total number of nodes in the channel. The mean and variance of γ_i are q_i and $q_i(1 - q_i)/S$ respectively. Using the estimate \hat{n}_k from the EKF, $\hat{n}_{k,i}$ is proportional to γ_i ,

$$\hat{n}_{k,i} = \hat{n}_k \cdot \gamma_i = \hat{n}_k \cdot \frac{s_i}{\sum_{j \in M_d} s_j} \quad (4.2.2)$$

where M_d is the set of APs that is using channel d . Subsequently, each AP keeps a channel assignment information table that has entries of BSSID, successful transmission

TABLE 4.1

Channel assignment information

BSSID (i)	No. of Successful Transmissions (s_i)	Estimated No. of Nodes by AP ($\hat{n}_{k,i}$)	Channel Occupied (d)
1	200	2	1
2	800	8	1
3	0	6	2
4	0	4	3

count by each AP, the estimated number of nodes by AP and channel occupied for each neighbouring AP as shown in Table 4.1.

Finally, an AP can determine the channel with the least number of neighbour nodes by summation of all $\hat{n}_{k,i}$ for each channel. In other words, the minimum neighbour algorithm in (3.1.2) can be implemented as

$$\begin{aligned}
 d_{\max}(i) &= \arg \min_{d \in C} N_d(i) \\
 &= \arg \min_{d \in C} \sum_{j \in M_d} \hat{n}_{k,j}
 \end{aligned} \tag{4.2.3}$$

Furthermore, whenever any AP switches into or out of the channel, the estimated net difference in the number of nodes can be determined as

$$\hat{u}_k = \sum_{i \in M_d} \hat{n}_{k,i} - \sum_{j \in M_d^*} \hat{n}_{k,j} \tag{4.2.4}$$

where M_d^* and M_d are the sets of APs using channel d before and after any channel switching respectively.

The rationale for choosing the EKF estimator is twofold. Firstly, the Kalman filter is well known for its superior performance in estimating the state of dynamical systems from noise perturbed measurements. It is the optimal estimator when the state noise and

measurement noise are zero-mean, Gaussian and white. Even if the noise is non-Gaussian, it is still the optimal linear filter. For nonlinear systems such as the one described here, the EKF approximates the optimal solution [79]. As mentioned earlier, the EKF with change detection filter can provide both high estimation accuracy and superior tracking ability.

Secondly, although generally known to be more computationally expensive, the EKF proposed here has a low complexity due to its zeroth order and scalar state [80]. With a zeroth order, there is no numerical integration needed for projecting states forward while a scalar state means that there is no complex matrix inversions required. Moreover, its memory requirements are undemanding due to its recursive nature and the computation involved in each time step only requires several multiplication and addition operations. To reduce the computational requirements further, the function $h(n)$ can be curve fitted offline with very high goodness of fit and its derivative $\partial h(n)/\partial n$ subsequently obtained. Therefore, the EKF estimator's superior performance and low complexity makes it an ideal candidate for practical implementation.

4.3 Minimum Neighbour with EKF Estimator Scheme

In the previous sections, an EKF estimator and the estimate of the number of nodes by AP have been described. These enable the determination of the number of neighbour nodes in each channel, which is critically needed for the application of the MINE scheme. The EKF estimator not only provides fast and accurate estimates but can also exploit channel switching information of neighbouring APs. In this section, the MINEK scheme, which is the combination of the MINE scheme and EKF estimator, is fully

described. The operation of the MINEK scheme is illustrated and several important issues are also discussed.

The MINEK scheme runs continuously at each AP, and its pseudo code is given below.

Algorithm 8: MINEK

```

1: if Time_Slots =  $xB$  then
2:    $\hat{n}_k \leftarrow \text{EKF\_Update}(\hat{n}_{k-1}, \hat{u}_k, p_k, P_{k-1}, Q_k, R_k)$ 
3:   if  $S_{count} > S_{TH}$  then
4:      $\hat{n}_{k,i} \leftarrow \text{Nodes\_AP\_Update}(\hat{n}_k, s_i)$ 
5:      $d_{\max} \leftarrow \text{Channel\_Min\_Neigh\_Nodes}(N_d)$ 
6:     if  $(d_{\max} \neq d) \ \& \ (N_{d_{\max}} < N_d + N_{HYS}) \ \& \ (\Delta T > T_{WAIT})$  then
7:        $d \leftarrow d_{\max}$ 
8:        $\hat{u}_k \leftarrow \text{Nett\_Diff\_Nodes}(\hat{n}_{k,i}, M_d, M_d^*)$ 
9:        $S_{count} \leftarrow 0$ 
10:       $\Delta T \leftarrow 0$ 
11:     end if
12:   end if
13: end if
14:
15: if AP_Changed_Into_or_Out_of_Channel = true then
16:    $\hat{u}_k \leftarrow \text{Nett\_Diff\_Nodes}(\hat{n}_{k,i}, M_d, M_d^*)$ 
17: end if

```

A new measurement of the conditional collision probability, p_k , is obtained every B time slots. Using the new measurement, the EKF estimator outputs an updated estimate of the total number of nodes, \hat{n}_k (Lines 1-2). If the total number of successful packet transmissions is more than a predetermined threshold, S_{TH} , the estimated number of nodes by AP, $\hat{n}_{k,i}$ is updated and the channel with the minimum number of neighbour nodes, d_{\max} is determined (Lines 3-5). The number of successful transmissions threshold, S_{TH} , is employed to ensure that a statistically sound number of observations have been made before the estimated number of nodes by AP is updated and any channel change is considered.

There are three conditions that must be met before a channel change is undertaken. Firstly, the new channel with the minimum number of neighbours has to be different to the currently occupied channel. Secondly, the difference between the number of neighbour nodes of the new and current channels must be more than N_{HYS} . This provides hysteresis and prevents channel changes due to insignificant differences in the number of neighbour nodes. Thirdly, the elapsed time since the last channel change needs to be more than T_{WAIT} . The reason for this is to allow enough time for an AP to obtain an accurate estimate after any channel change. If all three conditions are satisfied, the AP switches from the current channel to the new channel (Lines 6-7). Once an AP switches to a new channel, it calculates the corresponding estimated net difference in the number of nodes, \hat{u}_k which will be used in the next EKF update. In addition, the counter for the number of successful packet transmissions and the timer are reset as well (Lines 8-10). On the other hand, whenever an AP detects other APs switching into or out of the channel, it also calculates the corresponding estimated net difference in the number of nodes used to update the EKF (Lines 15 -17).

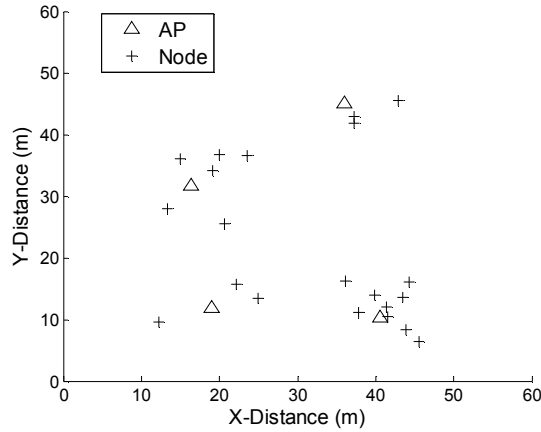
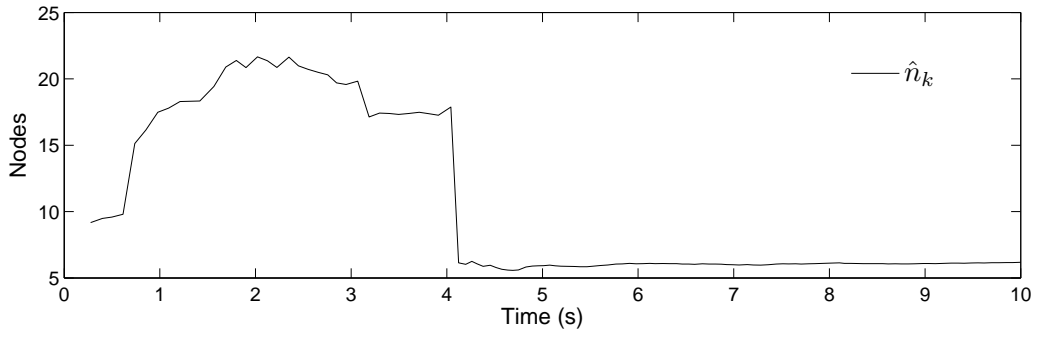


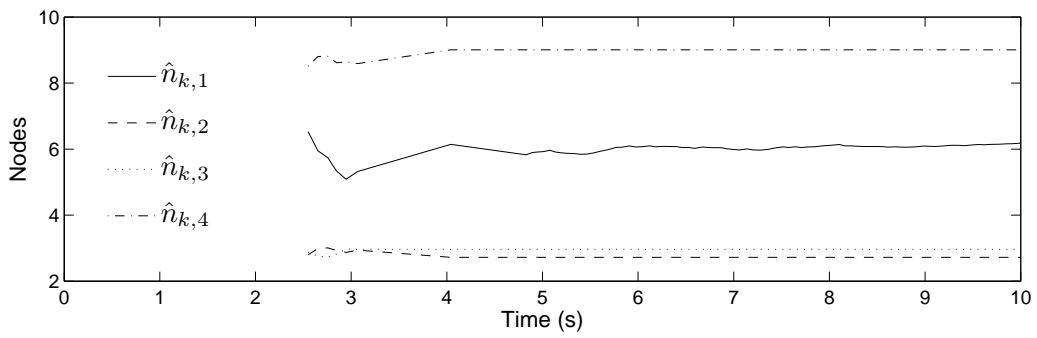
Figure 4.3: A simple topology of four APs used to illustrate the MINEK scheme.

In order to demonstrate the mechanism of the MINEK scheme, an illustrative example is used. Consider the simple topology consisting of four APs shown in Fig. 4.3. The number of nodes associated with AP1, AP2, AP3 and AP4 are 6, 3, 3, 9 nodes respectively. All APs are within transmission range of each other. Moreover, all APs are assigned to Channel 1 initially and there are $D = 3$ channels. This topology is simulated using the OPNET network simulator. Details of OPNET will be described in the next section. Several parameters of interests obtained from the simulation run are shown in Fig. 4.4. For instance, Fig. 4.4 shows the total number of nodes and number of nodes by AP estimates from AP1. It also shows the channel assignment and the aggregate throughput of all APs.

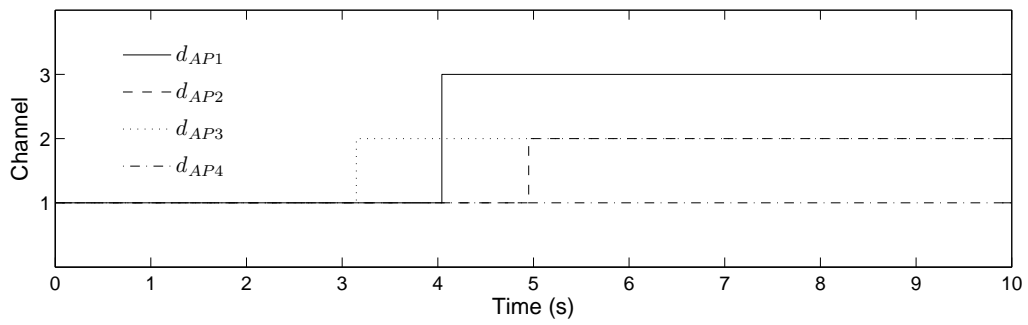
From the perspective of AP1, firstly it obtains an estimate of the total number of nodes. Fig. 4.4(a) shows that AP1 is able to estimate the total number of nodes accurately (21 nodes) in less than 2s. Next, by using this estimate, it apportions the total number of nodes to each AP. Accurate estimates of the number of nodes by AP for all APs are obtained by AP1, as shown in Fig. 4.4(b). A while later, AP3 switches to Channel 2 at around $t = 3$ s because there are no neighbour nodes in that channel, as shown in Fig. 4.4(c). Realizing this, AP1 is able to use the estimated number of nodes



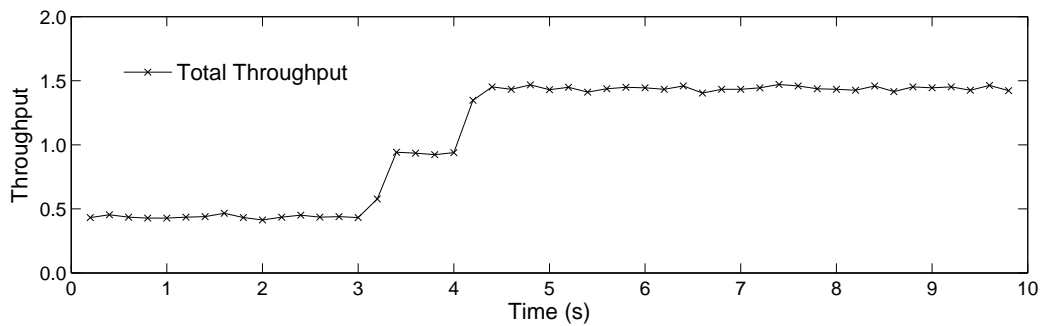
(a) Total number of nodes estimate



(b) Number of nodes by AP estimate



(c) Channel assignment



(d) Aggregate throughput

Figure 4.4: An illustration of the MINEK scheme.

by AP information to update the total number of nodes from 21 to 18 nodes. After some time, AP1 decides to switch to Channel 3 at around $t = 4s$ because the channel also has no neighbour nodes. After switching channels, AP1 is able to correctly update the total number of nodes from 18 to 6 nodes. Next, AP2 switches to Channel 2 which has the minimum number of neighbour nodes. Fig. 4.4(c) shows that the MINEK scheme converges to the optimal channel assignment (Channel 1: AP4, Channel 2: AP2 and AP3 and Channel 3: AP1) with only three channel switches and in less than 5s. Finally, the significantly improved aggregate throughput can be clearly seen in Fig. 4.4(d).

In the formulation of the MINEK scheme so far, the effects of different packet lengths and different offered loads have not been considered. For the former, it is important to note that packet length does not affect the estimation of the number of nodes, as is shown in (4.1.4) and (4.1.5). However, the throughput obtained is directly related to packet length, which was shown in Section 2.1.3. For example, nodes with higher average packet lengths have longer transmission and collision durations when compared to nodes with lower average packet lengths. This implies that an AP that occupies different channels with the same number of neighbour nodes may or may not obtain the same throughput depending on their relative packet lengths. Furthermore, for each AP, it is more useful to consider the average packet lengths of that AP and all its associated nodes since they change channels as a group. Such an average packet lengths of different APs may not differ greatly.

Nevertheless, the MINEK scheme can be easily adapted to include the effect of packet length. A packet length weight proportional to the ratio of the average packet length of the neighbour AP over the reference AP can be incorporated (more complex expressions can be used if needed). These weights are then multiplied to the corresponding number of nodes by AP before being summed in (4.2.3). The MINEK scheme then chooses the

channel with the minimum number of “weighted” neighbour nodes. For simplicity, it is assumed that the average packet lengths of all APs are the same.

The MINEK scheme also has the ability to discriminate against the difference in offered loads. A node contends for the channel only when it has packets to send and stays idle otherwise. A node with a lower load will be contending less often when compared to a node with a higher load. Any change in contention is captured by the measurements collected by the EKF over a small duration of B time slots in (4.1.6). For example, a node that is saturated always contends for the channel and will be estimated as 1 node. On the other hand, a node that has a lower load may only contend for some of the duration, which is estimated as a value between 0 and 1 node. This has been observed in the simulations and also in [70]. In other words, the EKF is able to provide the average number of contending nodes (a real number) when there is a change in the instantaneous number of contending nodes due to differences in offered loads. The performance of MINEK scheme with different packet lengths and unequal loads can be found in the next section.

4.4 Performance Evaluation

In this section, extensive performance evaluation of the MINEK scheme will be presented. The performance evaluation of the MINEK scheme can be obtained through packet level simulations using OPNET. For this purpose, several critical features that were lacking in OPNET were implemented. The detailed description of the simulation developments carried out in OPNET can be found in Appendix A. Subsequently, packet level simulations have been performed to evaluate the performance of the MINEK scheme in large and arbitrary topologies. Its performance is determined across several

important performance metrics and factors. These include upper bound performance, normalized density, non-saturated loads, unequal loads, fairness and scalability.

The OPNET simulator implements the complete IEEE 802.11a/b standards and additional parameters in Table 2.1. The EKF and change detection filter parameters used are shown in Table 4.2. These parameter values provide a good balance between estimation accuracy and tracking speed. Two sets of scenarios are defined: moderate density and high density in which each node on the average will have $Y = 4$ and 8 APs within its transmission range of 50m respectively. Each topology consists of 50 APs and the number of associated nodes is randomly selected from 1 to 10. The locations of APs are randomly distributed while the associated nodes are randomly located around the AP in order to create a hotspot-like topology. Unless mentioned otherwise, all nodes are saturated and generate packets that have a fixed size of 1024 bytes. Each topology is simulated for a duration of 120s in which more than 2×10^6 packets are received successfully. Each simulation run takes around 150 minutes on an Intel Core 2 Duo Processor running at 2.33 GHz with 2 GB of memory. A total of 10 topologies are randomly generated for each scenario and the average results are shown. A topology realization for moderate density scenario is shown in Fig. 4.5.

TABLE 4.2

MINEK scheme parameters

No. of Timeslots, B	200
State Noise Variance, Q_k without Alarm	0
State Noise Variance, Q_k with Alarm	5
Drift Parameter, v	0.5
Alarm Threshold, a	10
No. of Successful Transmissions Threshold, S_{TH}	500
Difference in the Minimum No. of Neighbour Nodes, N_{HYS}	0.99
Time Since Last Channel Change, T_{WAIT}	3s

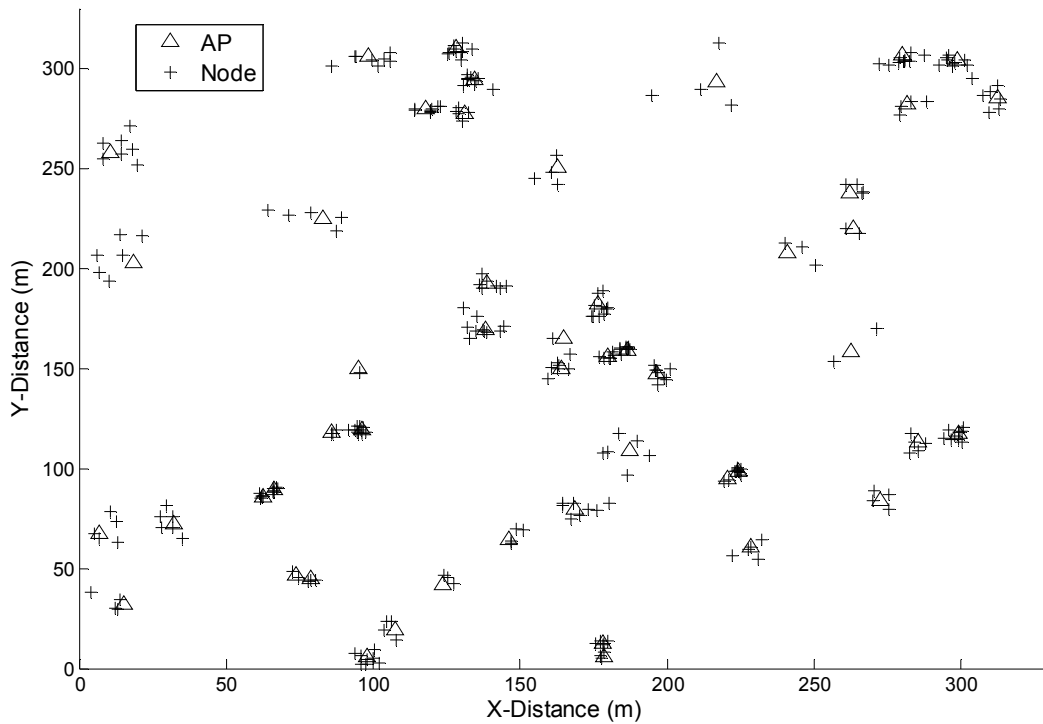


Figure 4.5: A topology realization for moderate density scenario.

4.4.1 Upper Bound Performance

The ratio of the average number of interfering APs over the number of channels, Y/D can be used as a measure of normalized densities when comparing different scenarios. At normalized densities near to unity, where the number of channels are equal to the number of interfering APs, the performance of a good channel assignment scheme should be near to that of the ideal interference free case. The upper bound performance represented by the ideal interference free case is when all APs occupy channels without any interference from any other APs. Furthermore, the performance of the MINEK scheme in estimating the number of neighbour nodes can be benchmarked against the performance when the number of nodes is assumed to be known a priori. This represents a different upper bound performance, one that is due to the estimation of the number of nodes.

The performance of the MINEK scheme when compared to both upper bounds is shown in Fig. 4.6. These are generated for the scenario of IEEE 802.11a with high density that has a normalized density of $Y/D = 8/12$. It can be seen that the performance of the MINEK scheme is very close to the ideal interference free case. In fact, its performance is as much as 96.2% of the ideal throughput. On the other hand, the MINEK scheme's performance in estimating the number of neighbour nodes is also excellent. The performance of the MINEK scheme is virtually identical to that with the number of neighbour nodes perfectly known.

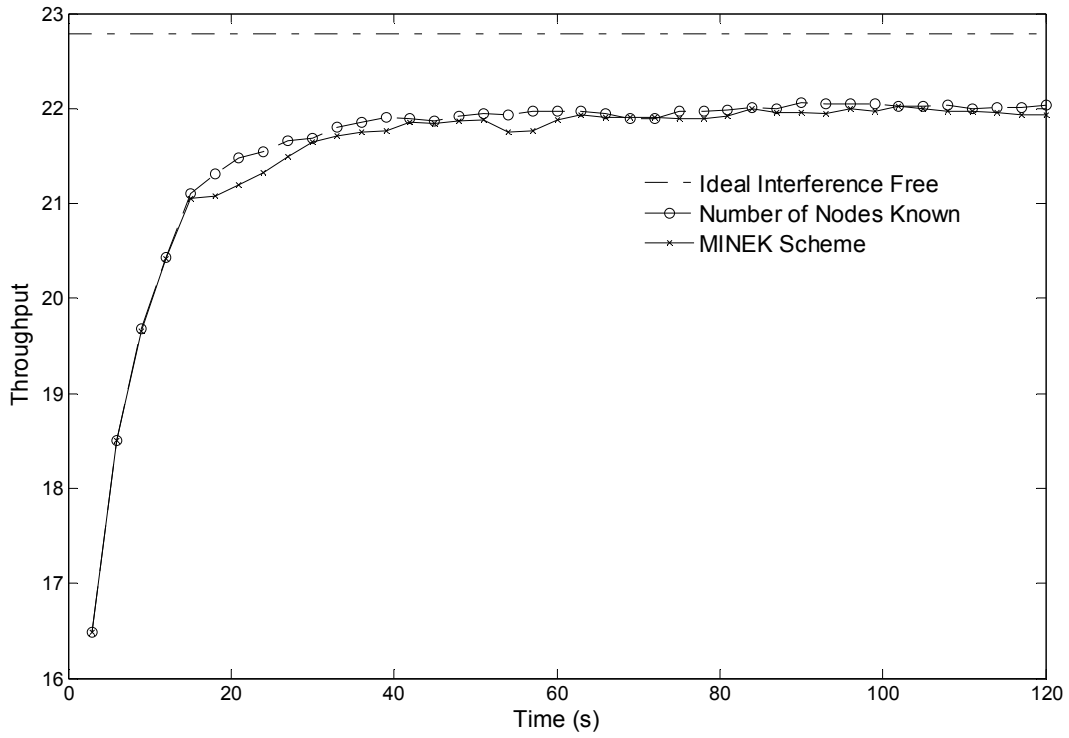


Figure 4.6: Performance of MINEK scheme benchmarked against upper bounds.

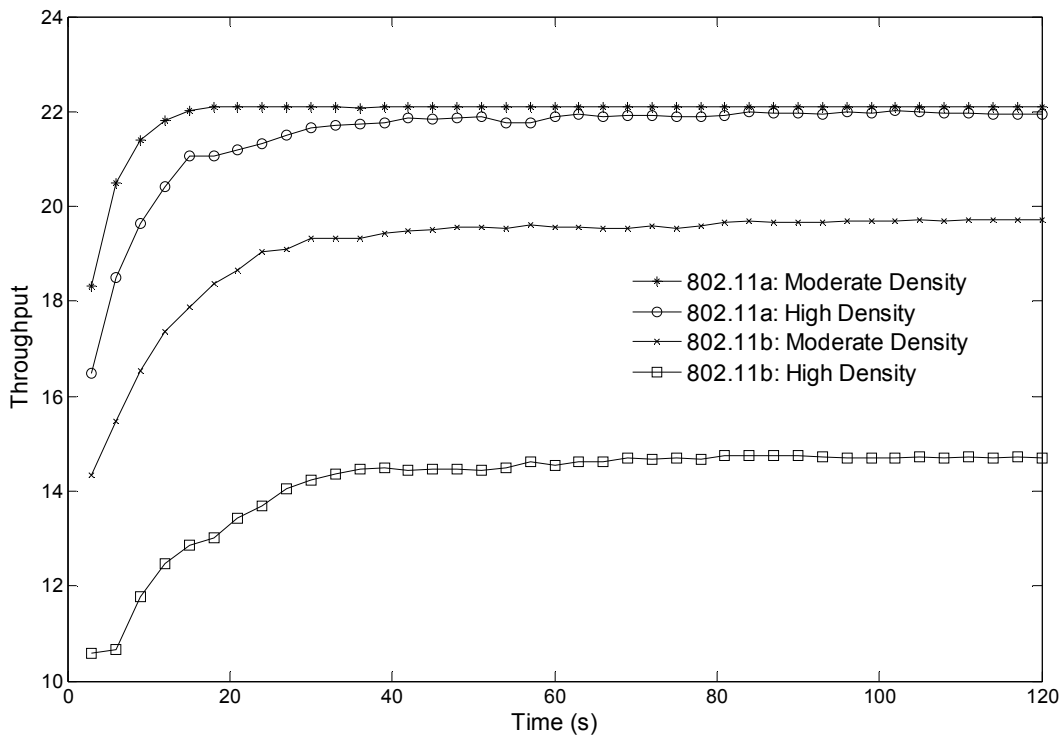


Figure 4.7: Throughput of MINEK scheme for IEEE 802.11a and IEEE 802.11b.

4.4.2 Normalized Density

The throughput performance of the MINEK scheme over time for IEEE 802.11b and IEEE 802.11a is shown in Fig. 4.7. For IEEE 802.11b, the throughput gains over random channel assignment are 37.3% and 38.8% for the moderate and high density scenarios respectively. Note that the performance of random channel assignment is taken from the initial throughput value since channels are initially randomly assigned. Similarly, for IEEE 802.11a, throughput gains of 20.6% and 33.1% over random channel assignment can be seen for moderate and high density scenarios respectively.

These results show that meaningful gains can be obtained by employing the proposed MINEK scheme. Furthermore, the trend of increasing throughput gains for topology scenarios with higher normalized density can be noted. For example, the throughput gain increases from IEEE 802.11a with moderate density, $Y/D = 4/12$ to IEEE 802.11b with high density, $Y/D = 8/3$. It is also interesting to see that the scheme can achieve more than 90% of the final throughput in the short duration of the first 20s over such a large network.

4.4.3 Non-Saturated Load

So far, only saturated load condition has been considered. In order to determine its performance across a wide range of operating conditions, varying levels of offered loads below saturation have been introduced. The packets arrival of each node is Poisson distributed with equal means and a queue buffer size of 50 packets is used. Fig. 4.8 shows the throughput of MINEK and other channel assignment schemes with various offered loads for IEEE 802.11b with high density. The offered loads shown are normalized to the number of APs and the reciprocal of normalized density, D/Y .

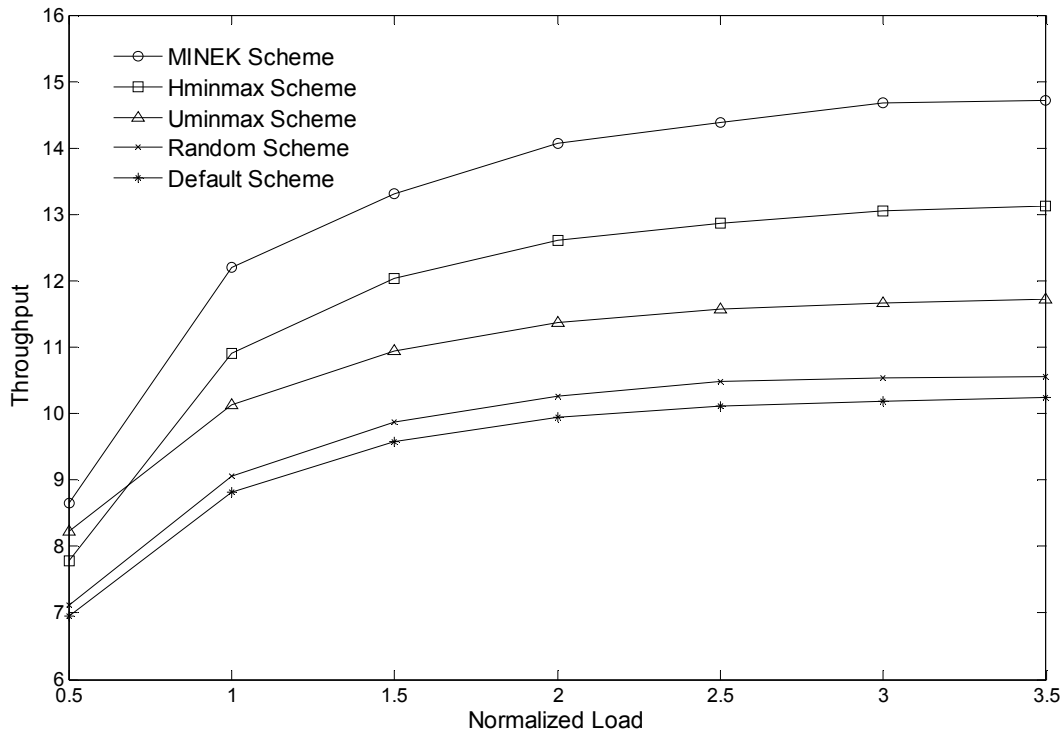


Figure 4.8: Throughput of MINEK and other schemes with various offered loads for IEEE 802.11b with high density.

Hminmax and Uminmax are channel assignment schemes that are more frequently cited in the literature. Both schemes have been described in Section 2.4.1 and Section 2.3.1 respectively. The default scheme replicates the channel distribution taken from a real WLAN network from Pittsburgh. The channel distribution is as follows: Channel 1: 15.71%, Channel 2: 56.63% and Channel 3: 27.66% [13].

The figure shows that the MINEK scheme outperforms all other channel assignment schemes. Furthermore, respectable throughput gains can be obtained over all other schemes and across all non-saturated and saturated offered loads. The MINEK scheme's throughput gain over the Hminmax scheme is relatively constant across all offered loads, with an average gain of 11.46%. On the other hand, the throughput gain over Uminmax increases with higher offered loads. The throughput gain at a normalized load

of 0.5 is 5.07% but this rapidly increases to 20.43% at a normalized load of 1.0. Similarly, even at a low normalized load of 0.5, a throughput gain of 21.7% over the random scheme can be seen. The throughput gain quickly increases to 34.6% for a normalized load of 1.0 and higher gains can be seen for higher loads. These results show that the MINEK scheme can provide significant throughput improvement over other channel assignment schemes.

It can be noted that the performance of the default scheme is only marginally lower than the random scheme. In the simulations, although the channel distributions have been replicated for the default scheme, the APs were still randomly chosen. In reality, the performance of a real WLAN can be worse due to the clustering of APs with similar channels. This implies that the potential throughput improvement by employing MINEK scheme in actual WLAN networks can be higher than those shown here. Finally, these results show that although the MINEK scheme was formulated with saturated load assumptions, the scheme is still able to maximize throughput by minimizing the average number of active neighbour nodes for the non-saturated case.

4.4.4 Unequal Load

Thus far, only the case where every node generated an identical traffic has been considered. Furthermore, a fixed packet size has been used. On the other hand, several studies on the characterization of real WLAN network usage have shown that traffic loads can vary across APs and that meaningful differences in packet size distributions can exist between uplink and downlink [49, 53, 81]. Therefore, it will be interesting to determine the performance of the MINEK scheme in these unequal load conditions, which reflect more realistic networks.

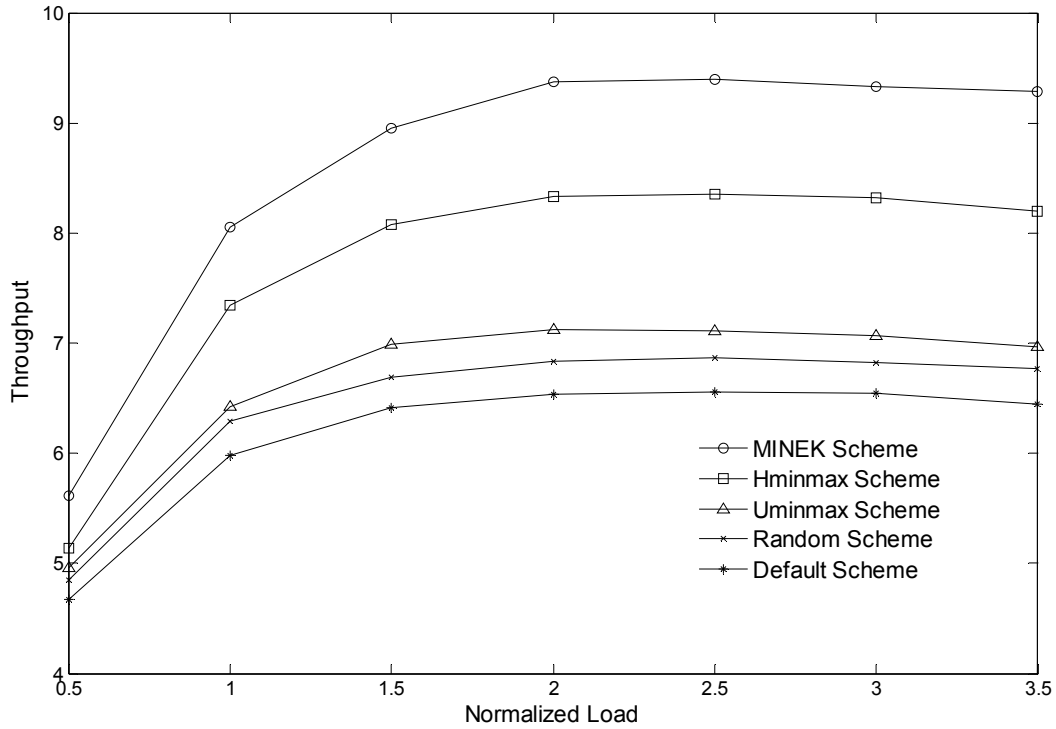


Figure 4.9: Throughput of MINEK and other schemes with unequal loads for IEEE 802.11b with high density.

A Pareto distribution is used to approximate the empirical throughput across APs in [53]. The mean of this distribution is set to be equal to the average offered load per AP. The ratio of uplink to downlink traffic is assumed to be 0.5. In order to model the differences in packet size distributions for uplink and downlink, a uniform distribution with different means is used. APs have packet sizes with a mean of 1024 bytes. The associated nodes are divided equally into high load and low load nodes. High and low load nodes have packet sizes with means of 512 and 256 bytes respectively. The mean packet arrival rate of high load nodes is twice that of low load nodes. Hence, high load nodes generate four times as much traffic as low load nodes.

Fig. 4.9 shows the throughput of MINEK and other channel assignment schemes with unequal loads for IEEE 802.11b with high density. The general trend seen here is very

similar to the case with equal loads shown in Fig. 4.8. However, on an absolute basis, there is an approximately 35% reduction in the obtained throughputs for all schemes when compared to the case with equal loads. This is due to the overloading of several APs that have limited transmission opportunities while other underloaded APs underutilize their transmission opportunities in the channel.

More importantly, it can be seen that the MINEK scheme still outperforms all other channel assignment schemes, even with unequal load conditions. Significant throughput gains are obtained over other schemes across all levels of offered load. Its throughput gain over other schemes increases rapidly from a normalized load of 0.5 to 2.0 and becomes relatively stable for higher loads. Throughput gains over Hminmax, Uminmax, random and default schemes of up to 13.24%, 33.18%, 37.22% and 43.98% respectively have been observed. These results show that the MINEK scheme can still provide significant throughput improvement over other channel assignment schemes, even with unequal traffic loads and different packet sizes.

4.4.5 Fairness

Apart from aggregate throughput, the relative throughputs obtained by APs should also be considered. In this respect, a fairness measure can be used to determine whether APs are receiving a fair share of the aggregate throughput in the network. Fairness can be determined at the individual node level or the AP level. Due to the unlicensed operation of WLANs, there should not be any prioritization between APs employed by differing entities. Therefore, it is more appropriate to measure fairness at the AP level. The well known quantitative fairness measure, Jain's fairness index, is used to measure the fairness in the throughputs obtained by APs [82]. Jain's fairness index is defined as

$$I_{Jain} = \frac{|\sum_{i=1}^n x_i|^2}{n \sum_{i=1}^n x_i^2} \quad (4.5.1)$$

and its value lies within $[0, 1]$. An index of 1 means total fairness which is the case if all APs obtain an equal share of the aggregate throughput, while an index of 0 means total unfairness.

Fig. 4.10 shows the fairness index for MINEK and other schemes across various offered loads for IEEE 802.11b with high density. The figure shows that the MINEK scheme has the highest fairness for high normalized loads. For low loads, the Uminmax scheme gives the highest fairness. However, the fairness of the MINEK scheme is only marginally lower than the Uminmax scheme at lower loads. Both MINEK and

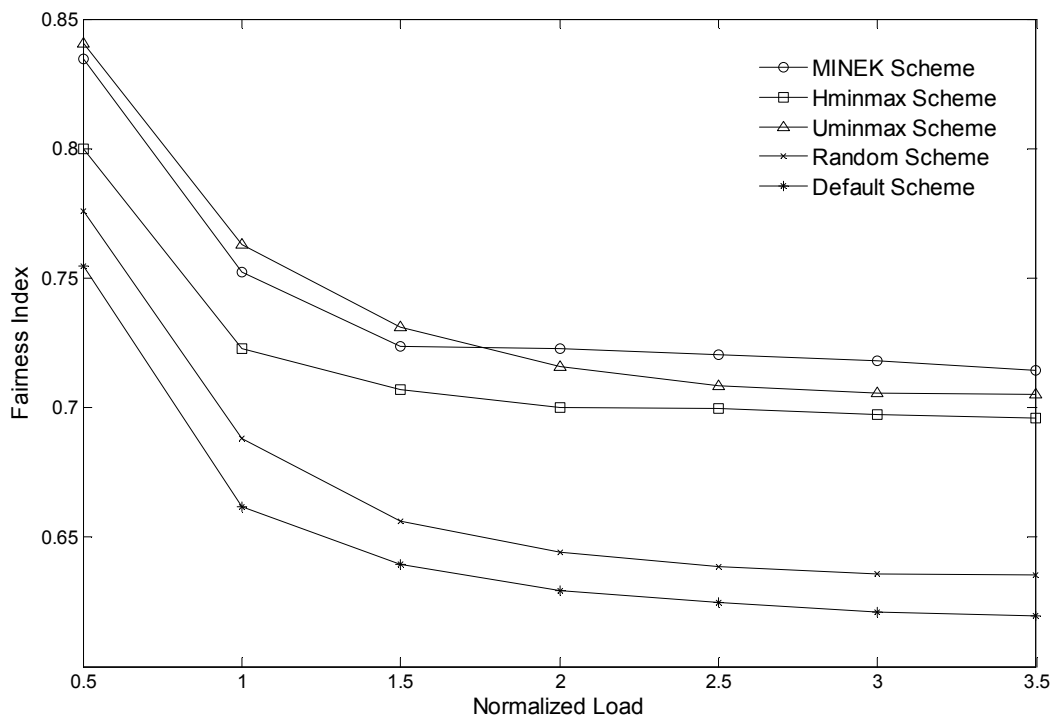


Figure 4.10: Fairness of MINEK and other schemes with various offered loads for IEEE 802.11b with high density.

Uminmax schemes have commendable fairness indices that are always above 0.7 across the loads considered. The Hminmax scheme has acceptable fairness at high loads but suffers at low loads. As expected, both random and default schemes are the most unfair schemes, especially at high loads. Although MINEK and Uminmax schemes are considered the fairest, when aggregate throughput (as in Fig. 4.8) is taken into account, it is clear that the MINEK scheme is the superior scheme.

4.4.6 Scalability

Another important practical performance consideration is the scalability of the MINEK scheme. In a network where APs belong to multiple owners, it is likely that the MINEK scheme is only employed by a subset of APs. Therefore, it is imperative to determine its throughput performance when the percentage of APs that employ the MINEK scheme, P_A , is varied. For example, $P_A = 0\%$ refers to the case where none of the APs employ the MINEK scheme. This is the case if the MINEK scheme is not used at all in the network. On the other hand, $P_A = 100\%$ refers to the case when all APs employ the MINEK scheme. This can happen if all owners in the network deploy APs that employ the MINEK scheme. The MINEK scheme can be implemented through firmware upgrade or by purchasing new APs. The other APs that do not employ the MINEK scheme stay on their randomly selected channel.

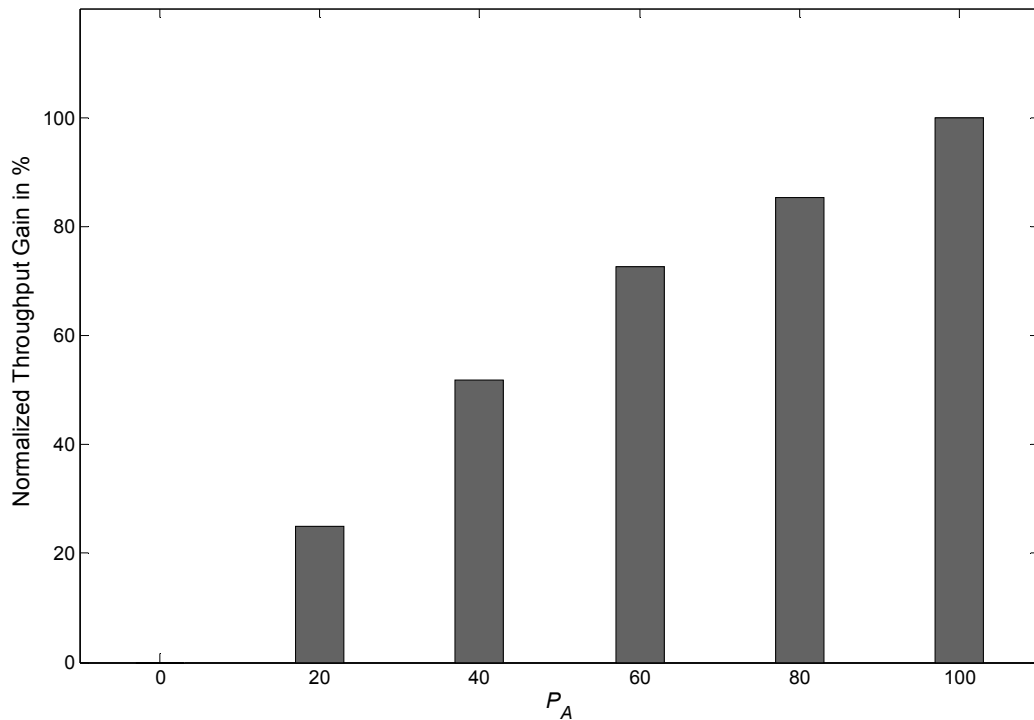


Figure 4.11: Normalized throughput gain when a percentage of all APs employ the MINEK scheme.

Fig. 4.11 shows the performance when the percentage of APs that deploy the MINEK scheme, $P_A = 0\%$ to 100% . For ease of comparison, the percentage gain in throughput is normalized to the throughput gain at $P_A = 100\%$. The figure shows that the proposed scheme is highly scalable with a slightly better than linear corresponding normalized throughput performance. In other words, higher gains are achieved as more APs become MINEK-enabled.

4.5 Summary

In the MINE scheme, an AP selects the channel with the minimum number of active neighbour nodes in order to maximize throughput. However, its application depends critically on its ability to estimate the number of neighbour nodes. In view of this, an

EKF estimator and the number of nodes by AP estimate have been proposed in this chapter, giving rise to the MINEK scheme. This approach successfully exploits channel switching information of neighbouring APs, resulting in fast and accurate estimates of the number of neighbour nodes.

Extensive packet level simulation results show that the MINEK scheme can provide significant throughput improvement over other channel assignment schemes. Throughput gains over other channel assignment schemes of up to almost 40% can be obtained in a short duration of less than 20s. For certain scenarios where the normalized density is close to unity, it has been shown that its performance is very close to the ideal interference free case with only 4% degradation. In addition, it showed negligible performance difference when compared to the case where the number of neighbour nodes is known a priori.

Furthermore, the MINEK scheme's performance is robust across a wide range of non-saturated and saturated load conditions. Equally important is its ability to maintain very high fairness while achieving these high throughputs. Last but not least, it is shown that the proposed scheme is highly scalable. Even when only a certain percentage of all APs can implement the scheme, proportional incremental improvement in throughput can still be obtained.

Thus far, the channel assignment schemes that were proposed have only utilized the AP's measurement. Due to their location around the AP, clients actually have the potential to help their AP to obtain an extended view of the network. Whether, how and under what conditions clients can assist APs in making better decisions on channel selection are just some of the questions that can be explored. Therefore, client assisted channel assignment will be investigated in the next chapter.

CLIENT ASSISTED MINIMUM CONFLICT PAIRS SCHEME

The MINEK scheme was described in the previous chapter. In order to estimate the number of neighbour nodes, an EKF estimator and the number of nodes by AP estimate were proposed. This approach successfully exploited channel switching information of neighbouring APs, which resulted in fast and accurate estimates. Extensive performance evaluation showed that the MINEK scheme provided significant throughput improvement over other channel assignment schemes.

In this chapter, client assisted channel assignment is investigated. A study on the impact of interference on throughput with multiple APs is undertaken using a novel approach that determines the possibility of parallel transmissions. Insights obtained are used to design the client assisted channel assignment scheme. A metric with a good correlation to the throughput, the number of conflict pairs is used in the client assisted minimum conflict pairs (MICPA) scheme. In this scheme, measurements from clients are used to assist the AP in determining the channel with the minimum number of conflict pairs in order to maximize its expected throughput. Simulation results show that the client assisted MICPA scheme can provide meaningful throughput improvements over other schemes that only utilize the AP's measurements.

This chapter is organized as follows. In Section 5.1, the impact of interference on throughput with multiple APs is presented. Next, the number of conflict pairs metric and the client assisted MICPA scheme are described in Section 5.2. In Section 5.3, extensive performance evaluation of the MICPA scheme and comparisons with other schemes are shown. Finally, the chapter is summarized in Section 5.4.

5.1 Impact of Interference on Throughput with Multiple APs

It is useful to recall that a detailed description of Bianchi's model for the performance analysis of DCF was given in Section 2.1.3. Although the model can provide very accurate throughput predictions, it assumes that all nodes can hear each other. Subsequently, Bianchi's model was extended to account for hidden nodes in [83]. However, a symmetric network is also assumed where every node sees the same number of hidden and contending nodes.

More recently, several efforts have been made to model the throughputs in non-symmetric networks or arbitrary topologies. A complex analytical model was proposed that allows the determination of link throughputs in [84]. In [85], a simple algorithm known as the back-of-the-envelope method for estimating link throughputs is described. However, these schemes cannot be utilized for our purpose for the following reasons. Firstly, these models require information of every node in the network, which is not possible in a distributed scheme. Secondly, there is no straightforward way to extend these models to the case where the links are not static as in the case where APs can send packets to any of its clients. Thirdly, their complexity grows exponentially due to the NP-hard operation that is involved. Therefore, an analytical approach that is likely to be

complex and has many limiting assumptions may not be the best way to extract useful insights into high density WLAN deployments with multiple APs.

In this section, a study on the impact of interference on throughput with multiple APs is undertaken. Firstly, a useful classification of commonly found interference scenarios is given. Secondly, the impact of interference on throughput for each class is investigated based on a novel approach that determines the possibility of parallel transmissions. Interestingly, results have shown that in some topologies, increased interference can lead to higher throughput and vice versa [86].

The proposed interference classes are by no means exhaustive but they are sufficient in that they i) are simple to identify even in a dense network, and ii) lend themselves to natural and systematic groupings when investigating the impact of interference on throughput. It is worth mentioning that only interference from within the transmission range is considered. This is because interference from the carrier sensing range cannot be known deterministically. Packets originating from the carrier sensing range have signal strengths that are too low for the correct decoding of packets. In order to account for interference from the carrier sensing range, measurements of their blocking periods and/or energy levels can be made in each channel. These measurements can then be used to augment the interference information obtained from within the transmission range. However, the average levels of interference from the larger sensing range may not be very different across different channels in a high density WLAN deployment scenario. Because of this reason and for simplicity, it is assumed that their impact on each channel is the same.

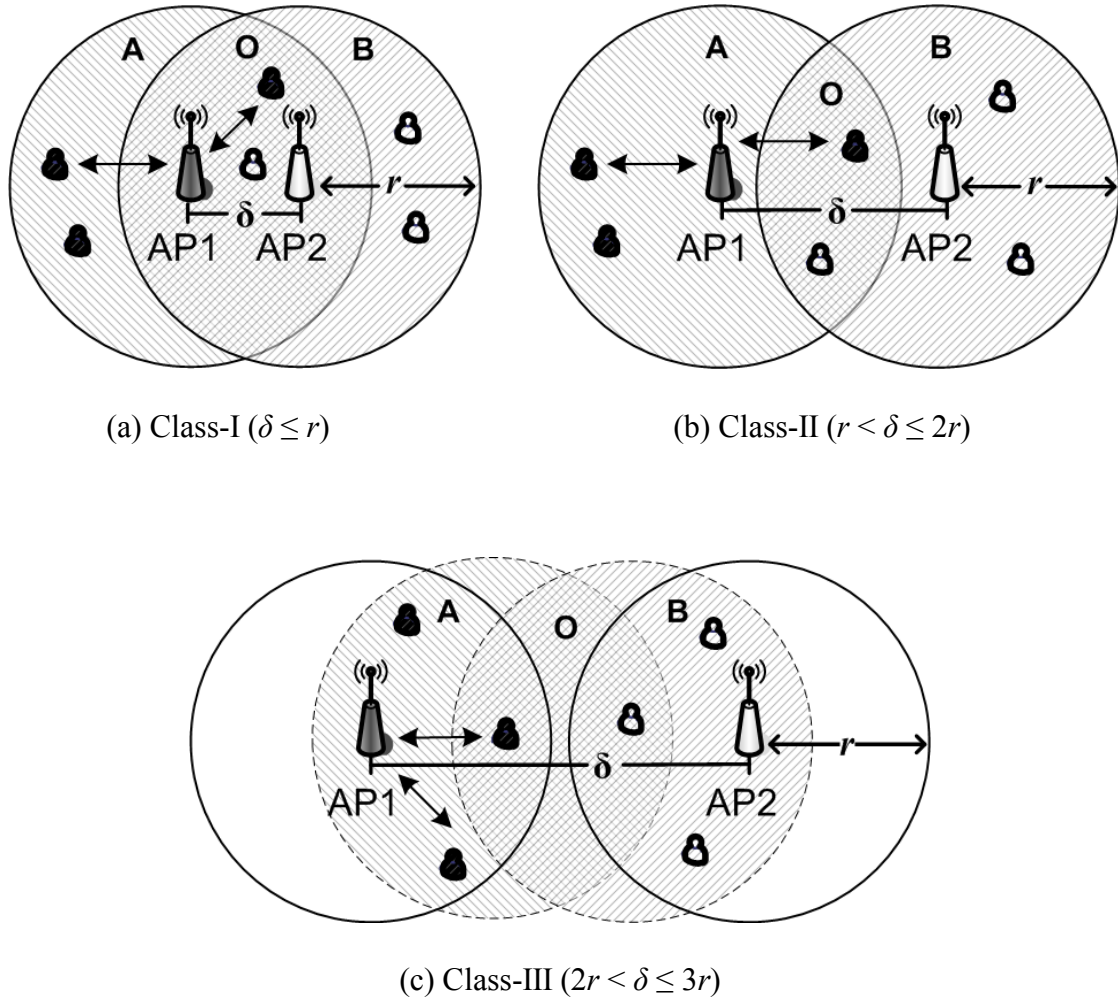


Figure 5.1: Classification of interference scenarios.

A BSS is said to be interfered by another BSS if any of its members (AP or clients) suffers from interference due to transmissions originating from any member of the interfering BSS. The interference scenarios are classified by the distance, δ between the APs. As shown in Fig. 5.1, Class-I, Class-II and Class-III interference scenarios correspond to $\delta \leq r$, $r < \delta \leq 2r$ and $2r < \delta \leq 3r$ respectively, where r is the transmission range of the AP and clients. Note that the maximum distance between the APs when both BSSs can still interfere with each other occurs when AP-to-client, client-to-interfering_client and interfering_client-to-interfering_AP are all separated by distance r . Therefore, for $\delta > 3r$, is no interference between both BSSs.

Before delving further into the characteristics of each interference class, several helpful notations are introduced. Using Fig. 5.1 as a reference, the region of interest can be divided into 3 regions, namely region A, region B and the overlapping region O. AP1 and its clients are located in region A or region O while AP2 and its clients are located in region B or region O. Note that region A and region B are only that part of the area within the respective circles without region O. In other words, region A and region B are represented by the areas with only a single shading respectively while region O refers to the area with the cross shading. Transmissions from ap_x to clients in region y will be denoted by $Trn(ap_x, cl_y)$ and transmissions from clients in region y to ap_x will be denoted by $Trn(cl_y, ap_x)$. For example, transmissions from AP1 to clients in region A will be denoted by $Trn(ap_1, cl_A)$.

Furthermore, even in the same interference class, different topologies can be formed depending on the location of the clients. A convenient way to refer to different topologies will be to specify the number of clients from each BSS that is in the overlapping region O, in the form $Class_i_nco1_nco2$ where i is the interference class, $nco1 \in \{0, 1, \dots, nc1\}$ and $nco2 \in \{0, 1, \dots, nc2\}$ are the number of clients in region O that are associated with AP1 and AP2 respectively. For example, the topology in Fig. 5.1(a) will be denoted as $Class_I_1_1$. In this study, the case where $nc1 = nc2 = 3$ clients has been used, where $nc1$ and $nc2$ are the total number of clients belonging to AP1 and AP2 respectively.

In Class-I, an AP can receive direct transmissions from the interfering AP and some or all of its clients. The problem faced by the Class-I interference scenario is that its own clients, and the interfering AP and its clients, can become potential hidden nodes to the ongoing transmission. For example, as shown in Fig. 5.1(a), when there are $Trn(cl_A, ap_1)$ transmissions, AP2 and some clients in region O become hidden nodes.

On the other hand, for $Trn(ap_1, cl_O)$ transmissions, some clients of AP2 in region B become hidden nodes. For $Trn(cl_O, ap_1)$ transmissions, some of its own clients in region A become hidden nodes.

For Class-II, the APs are not within transmission range of each other and therefore cannot receive each other's transmitted packets. However, the APs can hear from the clients of the interfering AP. The possibility of its own clients, and the interfering AP and its clients becoming hidden nodes is also present here. Referring to Fig. 5.1(b), for $Trn(cl_A, ap_1)$ transmissions, clients in region O become hidden nodes. In $Trn(ap_1, cl_O)$ transmissions, AP2 and some clients in region B become hidden nodes. For $Trn(cl_O, ap_1)$ transmissions, its own clients in region A become hidden nodes.

Finally in Class-III, the AP cannot hear transmission from the interfering AP or its clients. Only its clients can hear the interfering clients. This means that only the interfering clients can become potential hidden nodes. In Fig. 5.1(c), it can be seen that AP2's clients in region O are hidden nodes for $Trn(ap_1, cl_O)$ transmissions.

Thus far, common interference scenarios have been classified and the characteristics of each interference class have been presented. Although the approach used was to highlight transmissions with potential hidden nodes, the throughput of various interference scenarios in dense WLANs with multiple APs cannot be obtained from just extending the results from the analysis of classical hidden node problem. This is due to the fact that i) the potential hidden nodes in multiple AP scenarios behave differently from classical hidden nodes, and ii) the AP is either the source or the destination in all transmissions. For example, in the former, as is shown in Fig. 5.1(b), AP2's clients in region O are hidden nodes for $Trn(cl_A, ap_1)$ transmissions but they have a high probability of being prevented from transmitting due to parallel $Trn(ap_2, cl_B)$ transmissions.

Therefore, we adopt an approach that focuses on the possibility of parallel transmissions to predict the impact of interference on throughput in a qualitative manner. Parallel transmissions can result in the doubling of throughputs and this is expected to be the most important factor in determining the impact of interference on throughputs in a multiple APs scenario. Consequently, the following condition for parallel transmissions is given.

Condition 5.1: Parallel transmissions can take place if there exist at least two unique pairs of source and destination that are not within transmission range of each other.

By its definition, both APs in Class-I are within each other's transmission range. Using the fact that the AP must be either the source or destination in all transmissions, it can be deduced that Condition 5.1 is always not satisfied. This proves that parallel transmissions are not possible in Class I for all topologies. In other words, this means that at most, only a single transmission can take place successfully at any time. On the other hand, based on the characteristics of Class-I, hidden nodes are reduced when the number of clients in region A and region B are reduced. Therefore, the throughput is expected to increase from Class_I_0_0 to Class_I_3_3 topology as the total number of clients in region O increases. In fact, hidden nodes are eliminated completely in the case where all clients are in region O. The corresponding topology, Class_I_3_3 as shown in Fig. 5.2(a), is expected to give the maximum throughput for Class-I interference scenarios.

In Class-II, note that clients in region O cannot be part of the two unique pairs of source and destination in Condition 5.1 because they are in the transmission range of both APs. Therefore, the unique pairs of source and destination must be found from

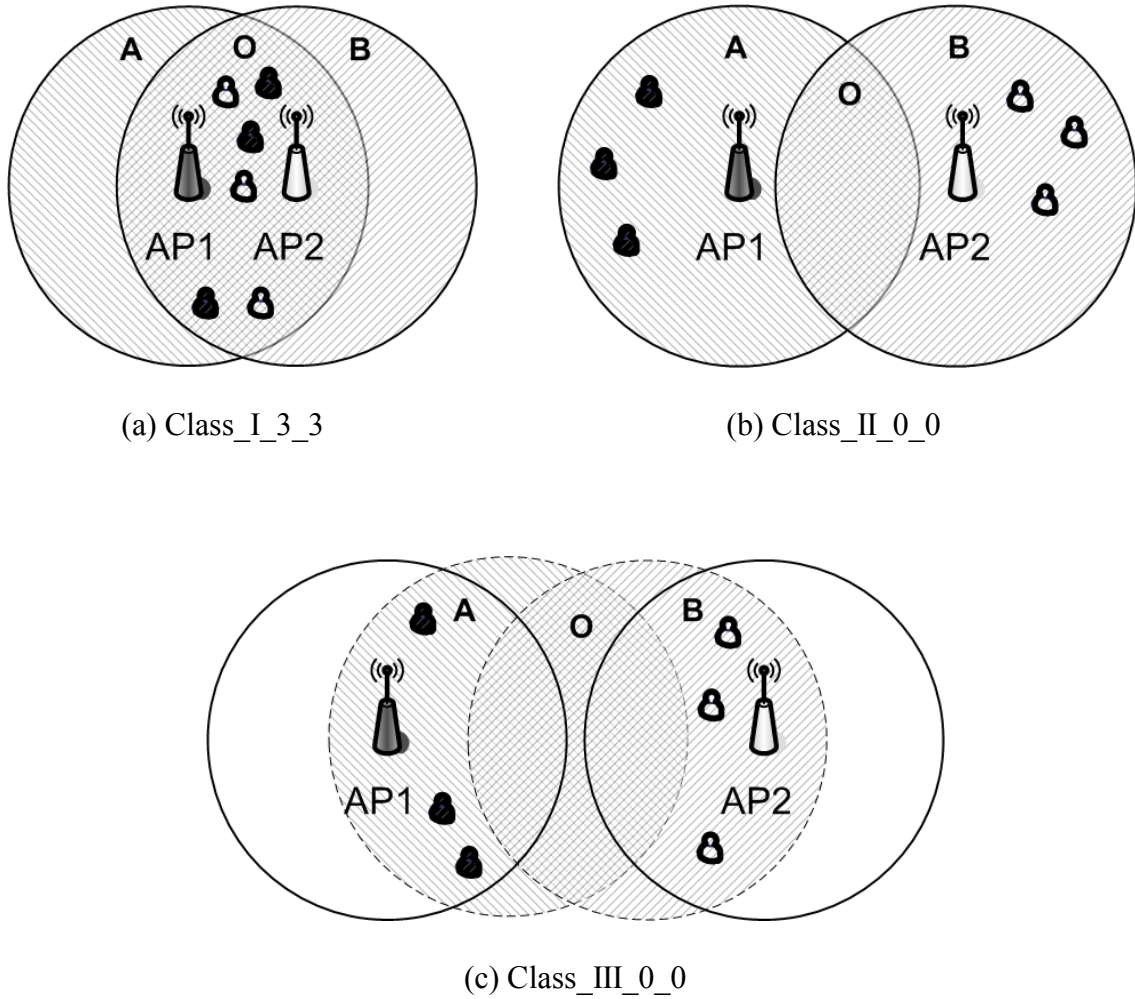


Figure 5.2: Topologies with expected maximum throughput for each interference class.

$P(ap_1, cl_A)$ and $P(ap_2, cl_B)$ where $P(ap_x, cl_Y)$ refers to ap_x and cl_Y source and destination pair. This leads us to deduce that Condition 5.1 is satisfied if there is at least one pair of $P(ap_1, cl_A)$ and at least one pair of $P(ap_2, cl_B)$. This is equivalent to saying that parallel transmissions are possible if not all of AP1's clients and not all of AP2's clients are in region O or mathematically $(nc1 \neq nc1) \wedge (nc2 \neq nc2)$. For Class-II topologies, hidden nodes are reduced if there are lesser clients in region O. Therefore, within each subset of topologies that have possible parallel transmissions and those that do not, the throughput is expected to decrease from Class_II_0_0 to Class_II_2_2 topology and from Class_II_3_0 to Class_II_3_3 topology respectively as the total number of clients in

region O increases. Consequently, when there are no clients in region O, there are no hidden nodes. This corresponds to Class_II_0_0 topology shown in Fig. 5.2(b) that is expected to give the maximum throughput for Class-II interference scenarios. The discussion above runs counter to the widely held assumption that throughput is always a monotonically decreasing function of interference. For example, Class_II_2_2 experiences higher interference than Class_II_3_0 topology but it is predicted that the former's throughput will be higher than the latter's.

Finally, for Class-III, recall that only the clients in region O can interfere with each other. This means that clients in region O from both APs cannot both be part of the two unique pairs of source and destination at the same time. However, even if all clients from one AP are in region O, Condition 5.1 can still be satisfied from $P(ap_1, cl_O)$ and $P(ap_2, cl_B)$ or $P(ap_1, cl_A)$ and $P(ap_2, cl_O)$ pairs. Clearly, $P(ap_1, cl_A)$ and $P(ap_2, cl_B)$ pairs can also satisfy Condition 5.1. From this, it can be deduced that the only Class-III topology where parallel transmissions are not possible is the Class_III_3_3 topology. As mentioned before, clients in region O are hidden nodes. Therefore, throughputs are expected to decrease from Class_III_0_0 to Class_III_3_3 topology as the number of clients in region O increases. Class_III_0_0 topology as shown in Fig. 5.2(c) is expected to give the maximum throughput for Class-III interference scenarios.

Packet-level simulations using OPNET have been performed to validate the observations made above. The IEEE 802.11b DSSS specifications and additional parameters as shown in Table 2.1 have been used in the simulations. All nodes are in saturated condition. Each topology has been simulated for 30 seconds for which more than 10000 packets have been successfully received. All throughputs shown are normalized to the data rate. Unless mentioned otherwise, the basic access mechanism of the DCF has been used. This is because the RTS/CTS mechanism has been shown to be

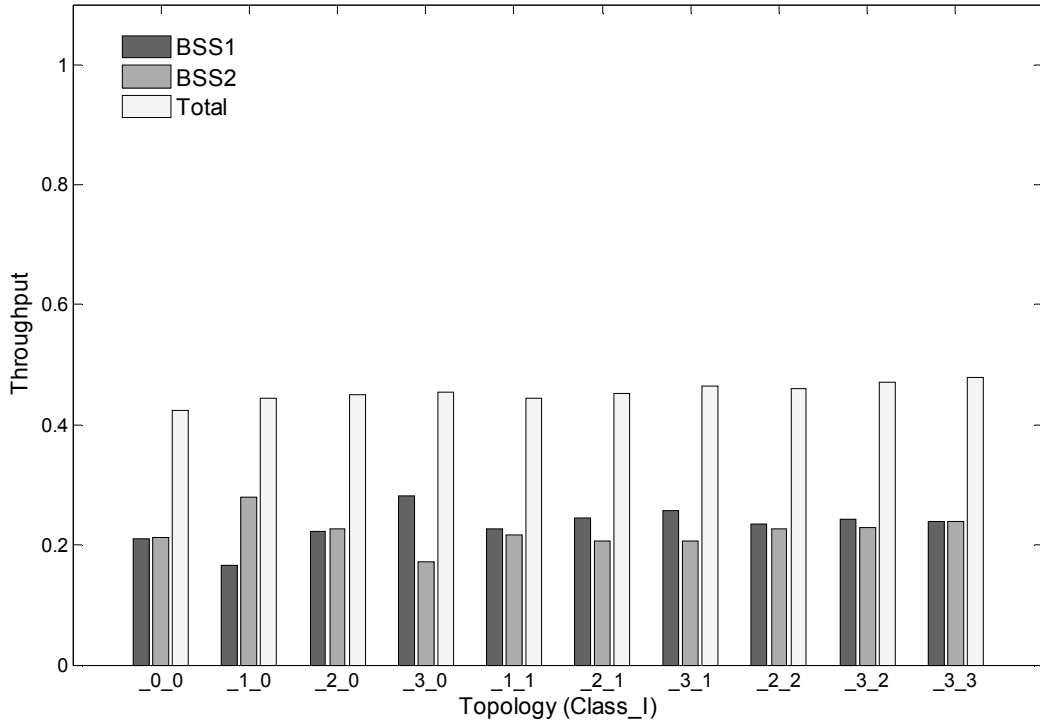


Figure 5.3: Throughput for Class-I interference topologies.

inferior when used in high speed WLANs where the data rate is significantly higher than the control rate, even in the presence of hidden nodes [38].

Fig. 5.3 shows the throughput for all unique Class-I interference topologies. Note that certain topologies such as $Class_I_0_1$, $Class_I_0_2$, $Class_I_0_3$, $Class_I_1_2$, $Class_I_1_3$ and $Class_I_2_3$ are not shown because they are symmetrical to $Class_I_1_0$, $Class_I_2_0$, $Class_I_3_0$, $Class_I_2_1$, $Class_I_3_1$ and $Class_I_3_2$ topologies respectively. It can be seen that the total throughput is relatively constant for all topologies. This is as expected because for Class-I, parallel transmissions are not possible for all topologies. Upon closer inspection of the throughputs of both BSS, it can be noted that any throughput decrease of one BSS is complemented by the throughput increase in the other BSS. This is because any transmissions opportunities

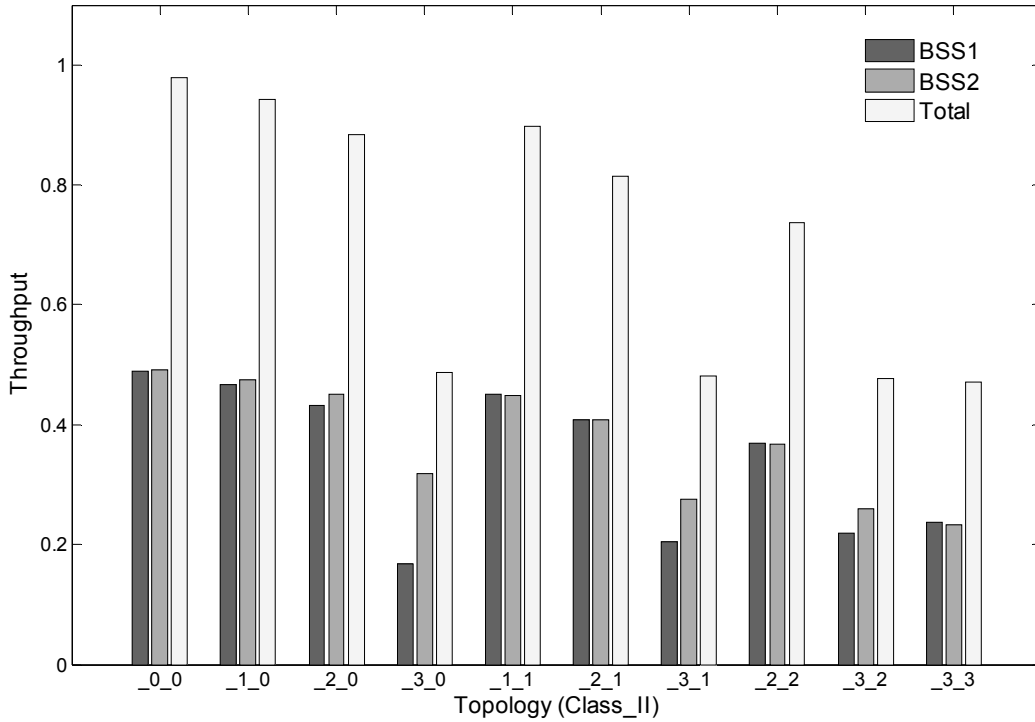


Figure 5.4: Throughput for Class-II interference topologies.

not used by one BSS are fully utilized by the other BSS as both are contending for the only available single transmission.

The throughput for all unique Class-II interference topologies is shown in Fig. 5.4. The distinct difference in the total throughput for certain topologies is evident in the figure. Class_II_3_0, Class_II_3_1, Class_II_3_2 and Class_II_3_3 topologies have a significantly lower total throughput than the other topologies. This observation is consistent with our expectation that parallel transmissions are only possible if not all of AP1's clients and not all of AP2's clients are in region O. Note that all the topologies with lower total throughputs have all of AP1's clients in region O, hence have only single transmission.

Another observation is that the throughputs of both BSS1 and BSS2 are similar in topologies with parallel transmissions but are quite different in topologies with only

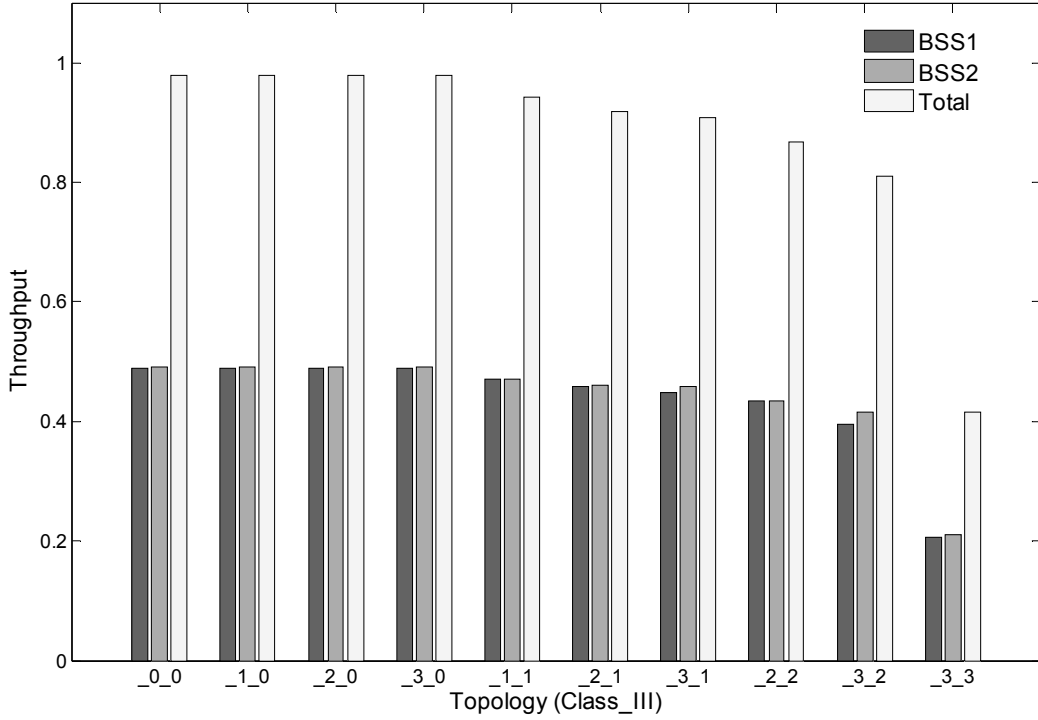


Figure 5.5: Throughput for Class-III interference topologies.

single transmission (except Class_II_3_3, which is a symmetric topology). This phenomenon may be due to the high collisions as a result of hidden nodes which in the latter affect all the possible pairs of the BSS that has all its clients in region O, while the other BSS can transmit unhindered to its clients that are not in region O.

Fig. 5.5 shows the throughput for all unique Class-III interference topologies. Similarly, it can be noted that Class_III_3_3 topology shows a significantly lower total throughput in comparison to all the other topologies. This observation concurs with our expectation because the only Class-III topology that does not have parallel transmissions is the one where both APs have all their clients in region O. Furthermore, for the rest of the topologies, the throughputs of both BSSs are very similar due to the availability of other possible pairs for transmissions even though clients in region O suffer from collisions due to hidden nodes.

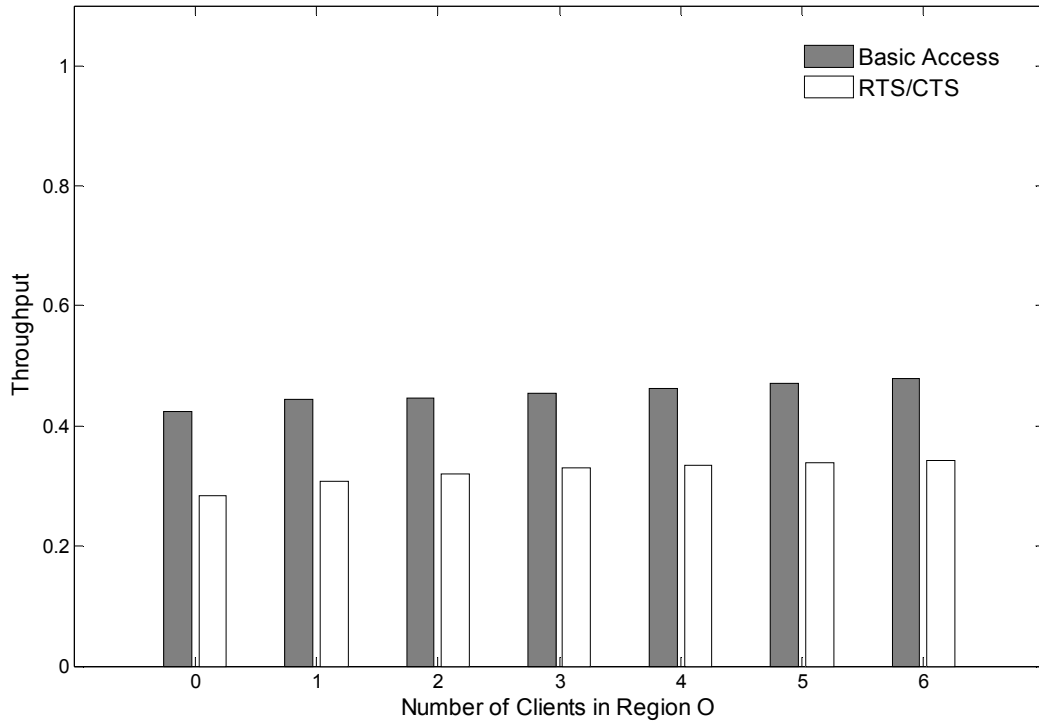


Figure 5.6: Aggregate throughput for Class-I interference topologies for basic access and RTS/CTS mechanisms.

In order to see the trends in the throughput more clearly, the topologies are grouped into those that have parallel transmissions and those that have only single transmission. In addition, the aggregate throughputs of topologies are plotted against the total number of clients in region O, nco , where $nco = nco1 + nco2$. The number of clients in region O generally indicates the severity of hidden nodes.

In Fig. 5.6, the aggregate throughput of Class-I topologies against the total number of clients in region O is shown for both basic access and RTS/CTS mechanisms. For example, $nco = 1$ corresponds to the Class_I_1_0 topology. For $nco = 2, 3$ and 4, we have shown the average total throughput for (Class_I_2_0 and Class_I_1_1), (Class_I_3_0 and Class_I_2_1), and (Class_I_3_1 and Class_I_2_2) topologies respectively. From the figure, it is clear that the basic access mechanism gives superior throughput when compared with the RTS/CTS mechanism for all possible topologies,

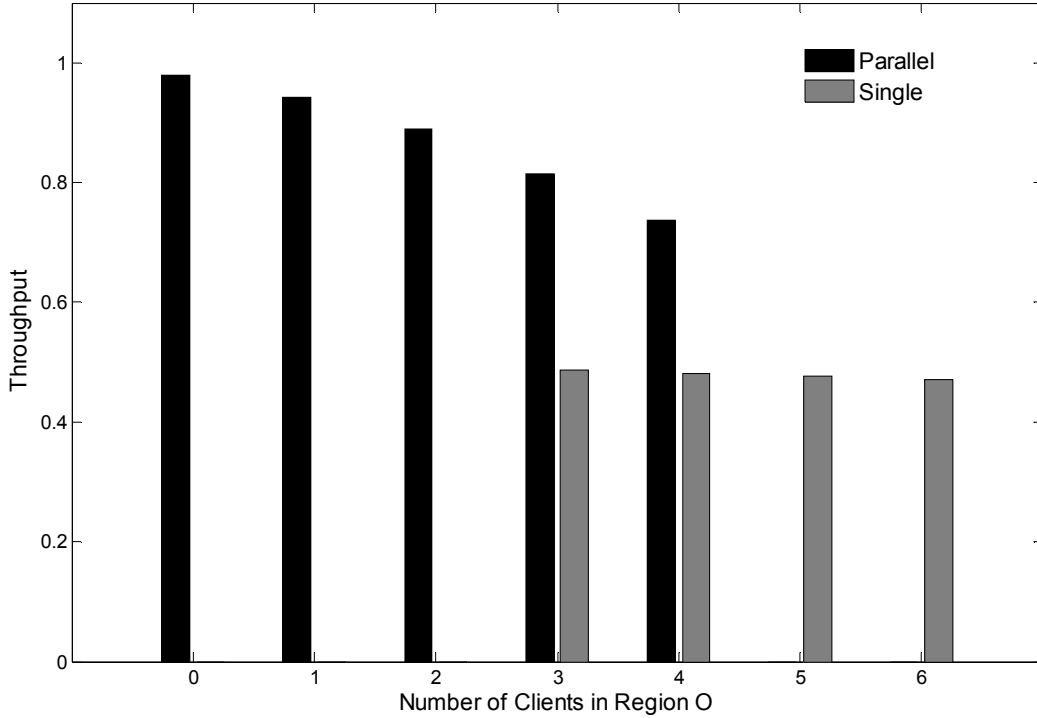


Figure 5.7: Aggregate throughput for Class-II interference topologies with parallel and single transmissions.

which is consistent with existing research studies. Furthermore, for Class-I, parallel transmissions are not possible for all topologies and the throughput is expected to increase for topologies with higher nco . Although quite marginal, it can be observed from the figure that higher throughputs are obtained for topologies with higher nco for both access mechanisms.

The aggregate throughput of Class-II topologies against the total number of clients in region O is shown in Fig. 5.7. In this figure, one can see the two groups of topologies, those that have possible parallel transmissions and those that do not. For Class-II, topologies that do not have all its clients from either BSSs in region O have possible parallel transmissions while others have only single transmission. As an example, for the single transmission topologies, $nco = 3, 4, 5$ and 6 corresponds to Class_II_3_0,

Class_II_3_1, Class_II_3_2 and Class_II_3_3 topologies respectively. From the figure, it can be clearly seen that topologies that have possible parallel transmissions have much higher throughputs than those with only single transmission. The throughputs of the former can be as high as twice the latter's.

When a comparison is made within each group of topologies, the throughputs decrease for topologies with higher nco , as expected. The results also show that the throughput for Class_II_2_2 (parallel transmissions group, with $nco = 4$) is evidently higher than Class_II_3_0 topology (single transmissions group with $nco = 3$), which validates our assertion that the assumption that throughput is a monotonically decreasing function of interference may not be always true.

Furthermore, it is also interesting to note that the throughput decrements in the parallel transmissions group are much higher than the single transmission group as nco increases. This can be explained by the number of unique pairs of source and destination for parallel transmissions. As nco increases, the number of unique pairs of source and destination for parallel transmissions decreases, which in turn decreases the probability of parallel transmissions. However, having additional clients in region O does not have such a serious effect on the single transmission group.

In Fig. 5.8, the throughput of Class-III topologies with various nco is shown. A similar observation can be made that throughputs are significantly higher for topologies that have parallel transmissions when compared to those with only single transmission. For Class-III, recall that only Class_III_3_3 topology does not have possible parallel transmissions, which explains the single bar in the single transmission group.

Furthermore, as is similar to Class-II, it can be noted that the throughputs decrease for topologies with higher nco , which is as predicted previously. However, the throughput decrements as nco increases are evidently smaller when compared to Class-II. Again,

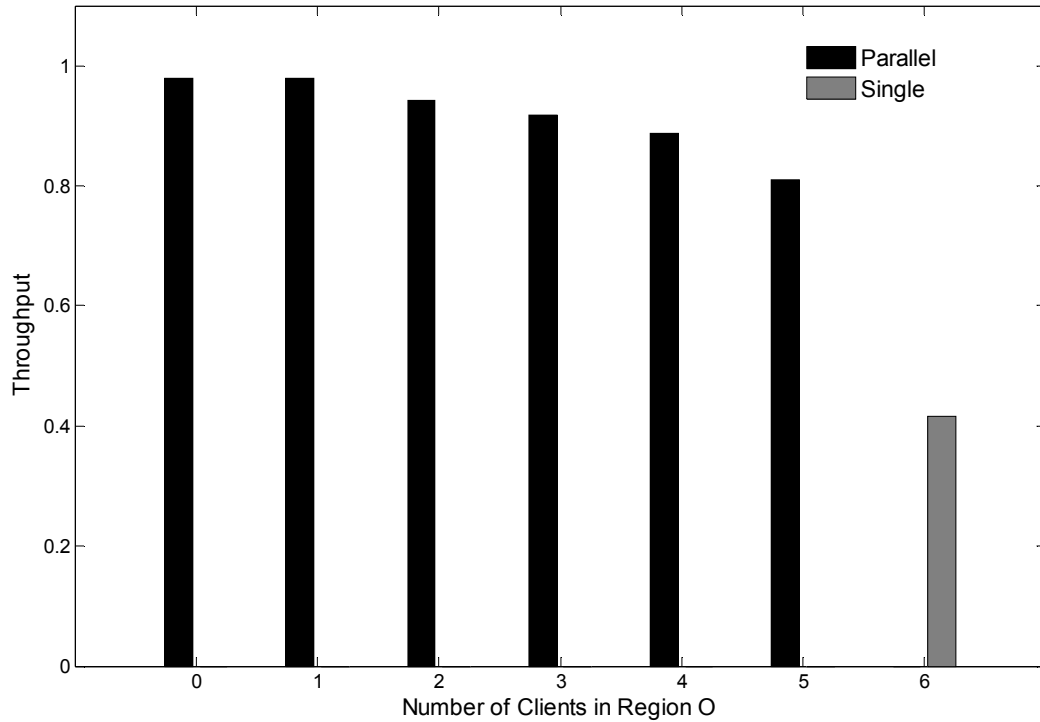


Figure 5.8: Aggregate throughput for Class-III interference topologies with parallel and single transmissions.

this can be explained by considering the number of unique pairs of source and destination for parallel transmissions. Consider the case when a client is moved from region A/B to region O. In Class-II, it ceases to be a candidate for the unique pairs of source and destination because it is in the transmission range of both APs. On the other hand, in Class-III, it can still be a candidate for unique pairs as long as the other pair does not consist of another client in region O. Therefore, Class-III topologies suffer less throughput degradation when compared to Class-II topologies when n_{co} increases.

5.2 Minimum Conflict Pairs Scheme

In this section, a client assisted channel assignment scheme is described. Insights obtained from the study on the impact of interference on throughput in the previous section are used in identifying a metric that can give a good indication of the expected throughput. The number of conflict pairs metric is not only intuitive but also simple to determine even in high density networks. Employing this metric, the client assisted MICPA scheme is proposed. In this scheme, each AP maximizes its expected throughput by selecting the channel with the minimum number of conflict pairs.

Before the client assisted channel assignment scheme can be developed, a metric that correlates with the expected throughput across all three interference classes is needed. Towards this end, the number of conflict pairs, XP , has been identified as a suitable metric. Conflict pairs are defined as two source and destination pairs that cannot transmit in parallel without interfering with each other. In other words, at most only a single transmission can take place among the conflict pairs. A larger number of conflict pairs indicates a higher proportion of source and destination pairs that can be prevented from transmitting simultaneously. On the other hand, a smaller number of conflict pairs means that source and destination pairs that are not blocked have more opportunities to transmit in parallel. Because of this, it is expected that the number of conflict pairs can be used as a good indicator of the expected throughput.

Another advantage of using the number of conflict pairs lies in its simplicity. As will be seen, the number of conflict pairs can be easily determined even for high density networks. To illustrate this, the number of conflict pairs for each interference class is now described using the interference topologies from the previous study. The number of unique source and destination pairs for any two interfering BSSs (BSS1 and BSS2) is

$nc1 \times nc2$. For Class-I, because parallel transmissions are not possible for all topologies, all source and destination pairs are conflict pairs, that is

$$XP = nc1 \times nc2. \quad (5.2.1)$$

In Class-II, only a single transmission can take place if either all of AP1's clients or all of AP2's clients are in region O. This means that for these topologies, all source and destination pairs are conflict pairs. Therefore the number of conflict pairs for these topologies are the same as those for Class-I, as given in (5.2.1). Otherwise, for topologies that have parallel transmissions, the number of conflict pairs is dependent on the number of clients from each AP in region O. Recall that in Class-II, clients in region O from one AP prevents transmissions from all clients of the other AP. Hence, the number of conflict pairs for Class-II topologies with parallel transmissions can be given as

$$XP = nco1 \times nc2 + nco2 \times nc1 - nco1 \times nco2. \quad (5.2.2)$$

In (5.2.2), the first term represents the conflict pairs between each of AP1's clients in region O with all of AP2's clients, the second term represents the conflict pairs between each of AP2's clients in region O with all of AP1's clients, and the last term accounts for conflict pairs that appear in both the first and second terms.

Finally, for Class-III, only clients in region O can interfere with each other. Therefore, the number of conflict pairs is simply the product of the clients from each BSS that is in region O, that is

$$XP = nco1 \times nco2. \quad (5.2.3)$$

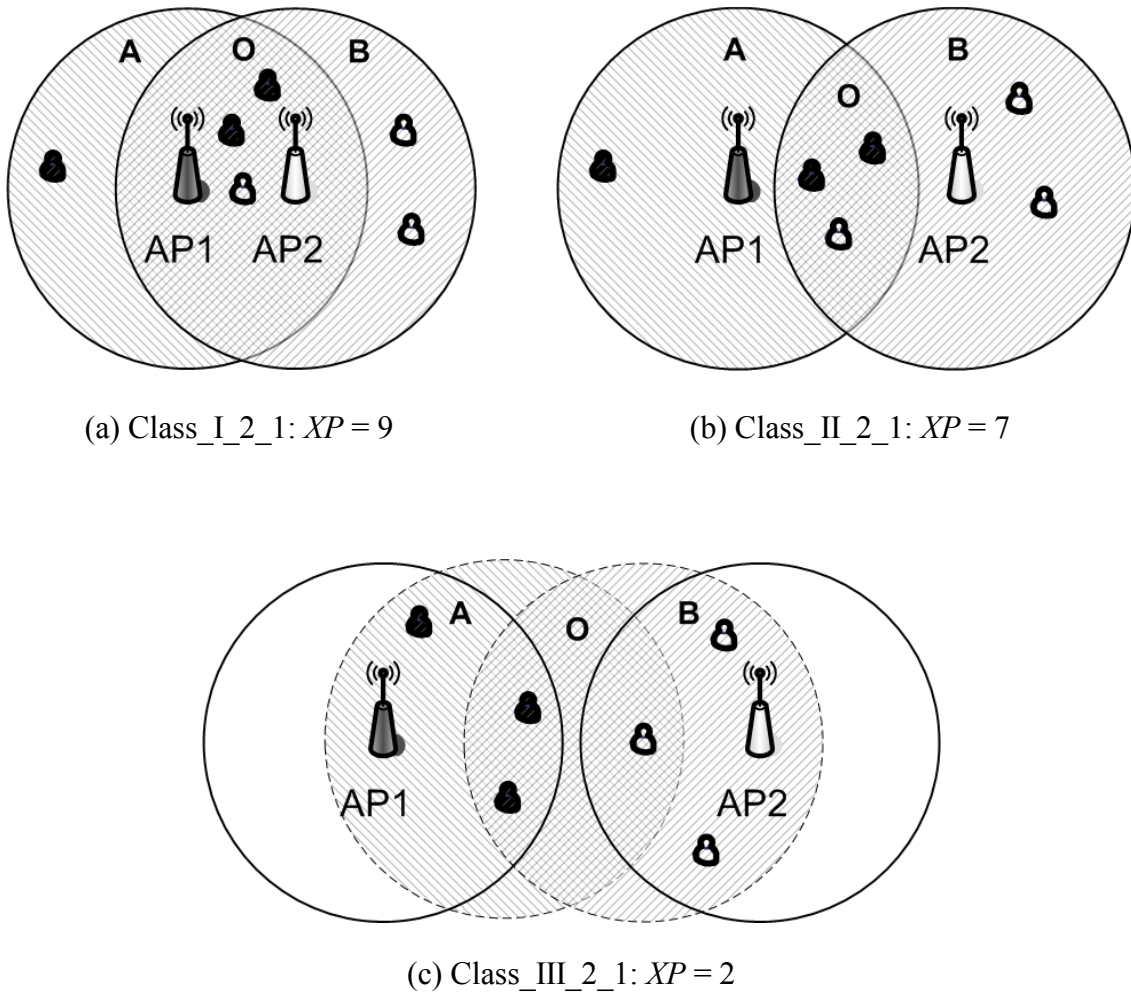


Figure 5.9: Number of conflict pairs for each interference class.

Fig. 5.9 shows the number of conflict pairs for the topology with $nco1 = 2$ and $nco2 = 1$ from each of the interference classes.

For the purpose of verifying the relation between the number of conflict pairs and the expected throughput, the throughputs obtained from each of the interference classes are plotted against the number of conflict pairs, as shown in Fig. 5.10. For each of the interference classes, it can be seen that the throughput obtained is inversely related to the number of conflict pairs. In other words, higher throughputs can be achieved by selecting topologies that have a lower number of conflict pairs.

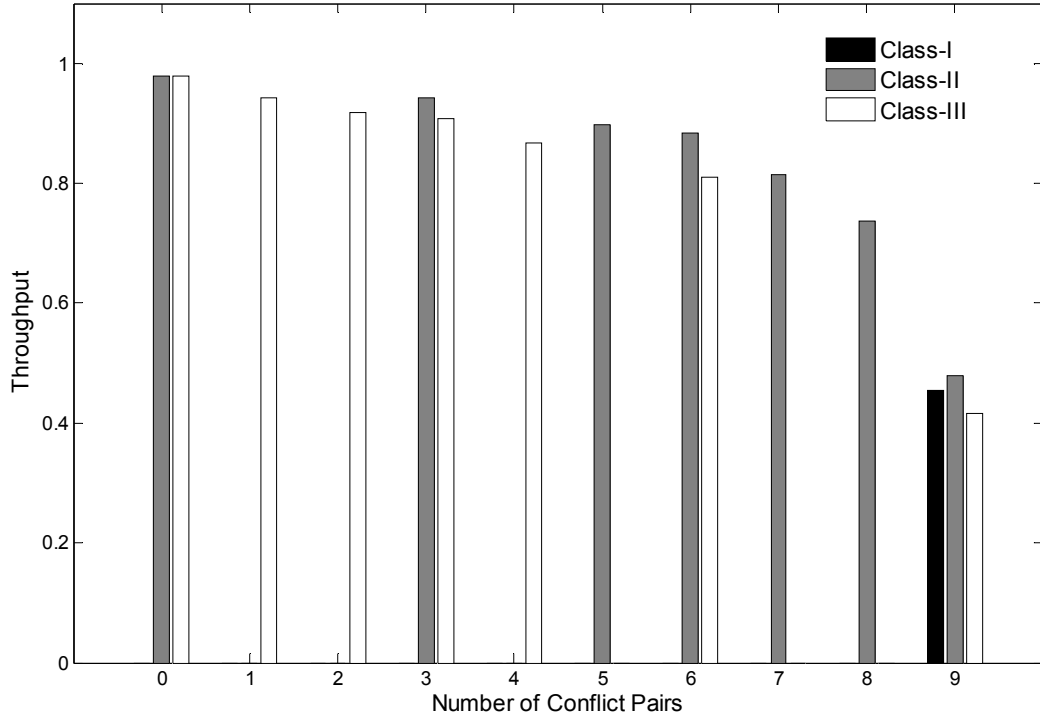


Figure 5.10: Relation between the number of conflict pairs and throughput for all interference classes.

Therefore, in the MICPA scheme, each AP- i maximizes its expected throughput by choosing the channel d_{\min} that has the minimum number of conflict pairs, as given by

$$d_{\min}(i) = \arg \min_{d \in C} XP_d(i). \quad (5.2.4)$$

The MICPA scheme, which is run at each AP, can be described as follows:

Algorithm 9: MICPA

- 1) The AP performs its own measurements by sensing the presence of interfering APs and their clients.
- 2) The AP broadcasts the interference information (which is the collated measurements from the AP and all clients in the previous iteration) to all of its clients periodically and requests them to perform similar measurements at specified intervals.
- 3) The clients perform the measurements and report back to the AP.
- 4) The AP combines and uses this information to determine the channel with the minimum number of conflict pairs. If a new channel is found, it switches into that channel. Otherwise, it stays on its current channel.
- 5) Steps 1 – 4 are repeated at specific intervals.

Overheads incurred by the transmission of measurement reports from clients are an important factor that needs to be considered. To minimize the number of measurements that needs to be transmitted to the AP, the AP broadcasts the updated interference information that it and its clients have sensed. Now the clients compare this information with its measurements and only feedback measurements that are different to those of the AP. This reduces the amount of information that needs to be relayed back to the AP, ensuring that any overheads incurred are only for the transmissions of useful information. Furthermore, since the location of APs and its clients is usually constant in a short period of time, most clients will not need to send reports at every interval.

On the other hand, APs can also over time identify and only request measurements from clients that are located farther from themselves. These clients have a higher probability of sensing interference that is uncorrelated to the AP. Finally, to further

minimize overheads, the interference information that needs to be broadcasted can be appended to beacon frames that are already transmitted by APs periodically.

5.3 Performance Evaluation

Performance evaluation of the MICPA scheme will be presented in this section. Hybrid simulations consisting of high-level simulations in MATLAB and packet-level simulations in OPNET have been performed. In MATLAB, the performance of the MICPA scheme in terms of the number of conflict pairs is evaluated. The channel assignment obtained from MATLAB is then exported to the packet-level OPNET simulator in order to determine the scheme's throughput performance. The performance of the client assisted MICPA scheme will be compared to the AP-only MINE scheme. Recall that in the MINE scheme, it is assumed that the APs have perfect knowledge of the number of neighbour nodes.

5.3.1 Number of Conflict Pairs

High-level simulations in MATLAB were carried out to evaluate the performance of the MICPA scheme. A network consisting of 100 APs is used and the number of clients is randomly selected from 1 to 10. Each node has an average of Y interfering APs within its transmission range of 50m while the number of channels for IEEE 802.11b and IEEE 802.11a are $D = 3$ and $D = 12$ respectively. Three levels of client spread have been used, which are low, moderate and high client spreads. All results shown are obtained using the average of 1000 independent realizations with randomly generated initial channels and number of clients.

The levels of client spread are expected to have a considerable impact on the

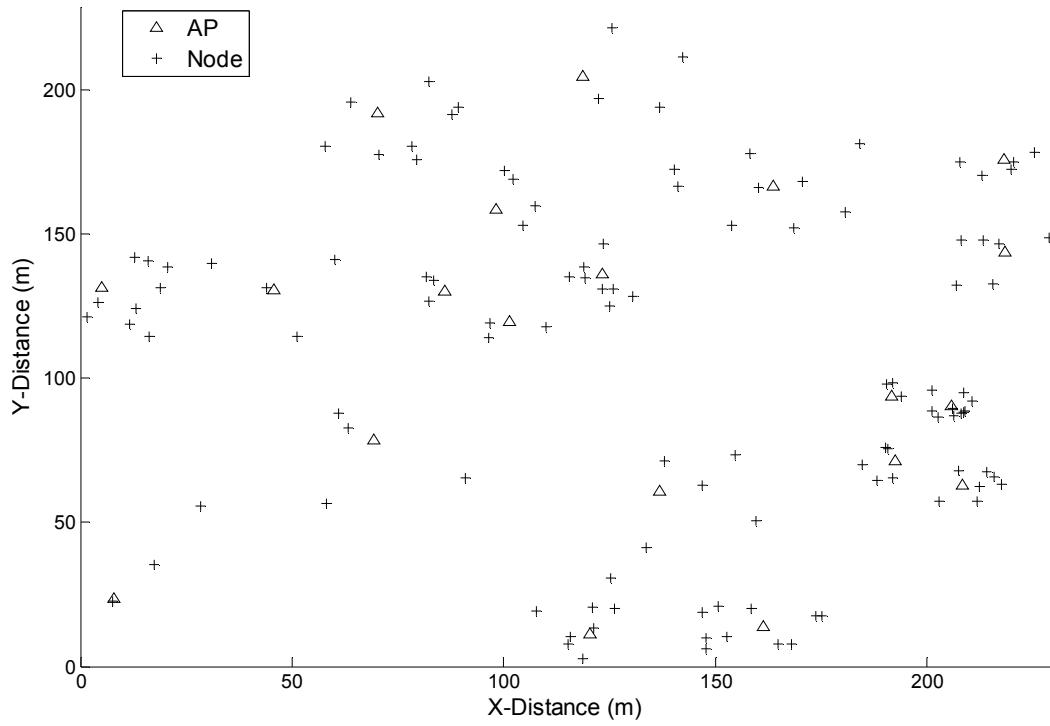
performance of the client assisted MICPA scheme. The exact impact of client spread will be investigated in this section. The clients' locations are Gaussian distributed around the AP with a specified standard deviation in order to create a hotspot-like topology. For all levels of client spread, the maximum distance of clients from their AP is limited by half the transmission range.

In addition, for the low client spread, the clients' maximum distance from their AP is further limited by half the distance between their AP to the nearest neighbour AP. For moderate client spread, all clients have to be located nearer to their own APs when compared to all neighbouring APs. No such additional conditions apply for high client spread. Table 5.1 summarizes the characteristics of the levels of client spread while Fig. 5.11 illustrates the different levels of client spread for a small topology of 20 APs.

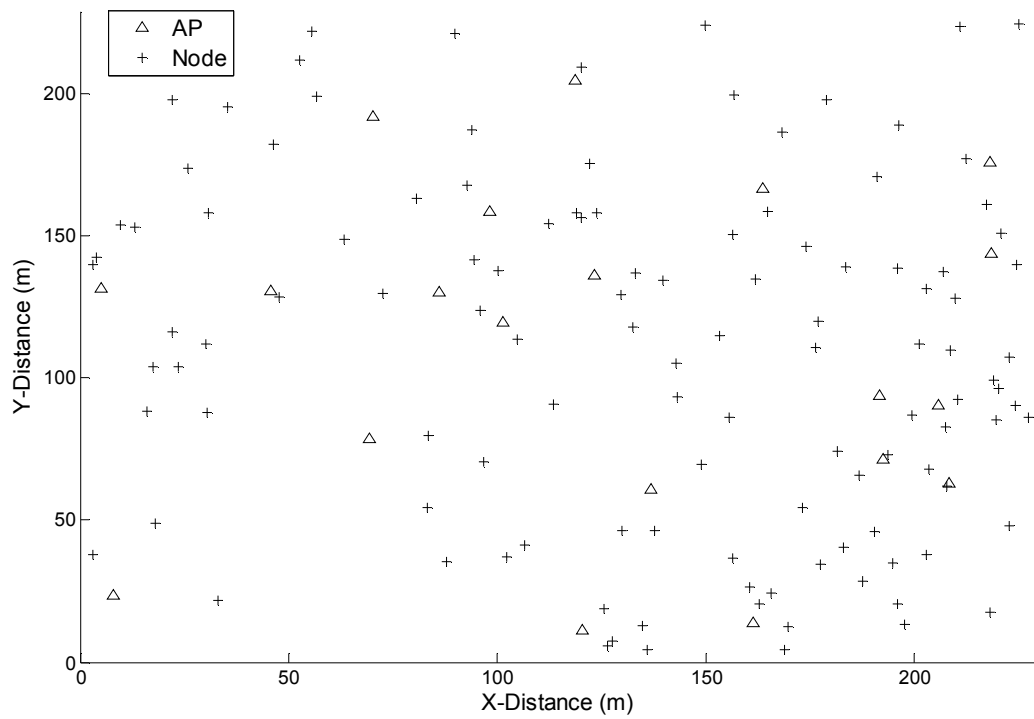
TABLE 5.1

Characteristics of the levels of client spread

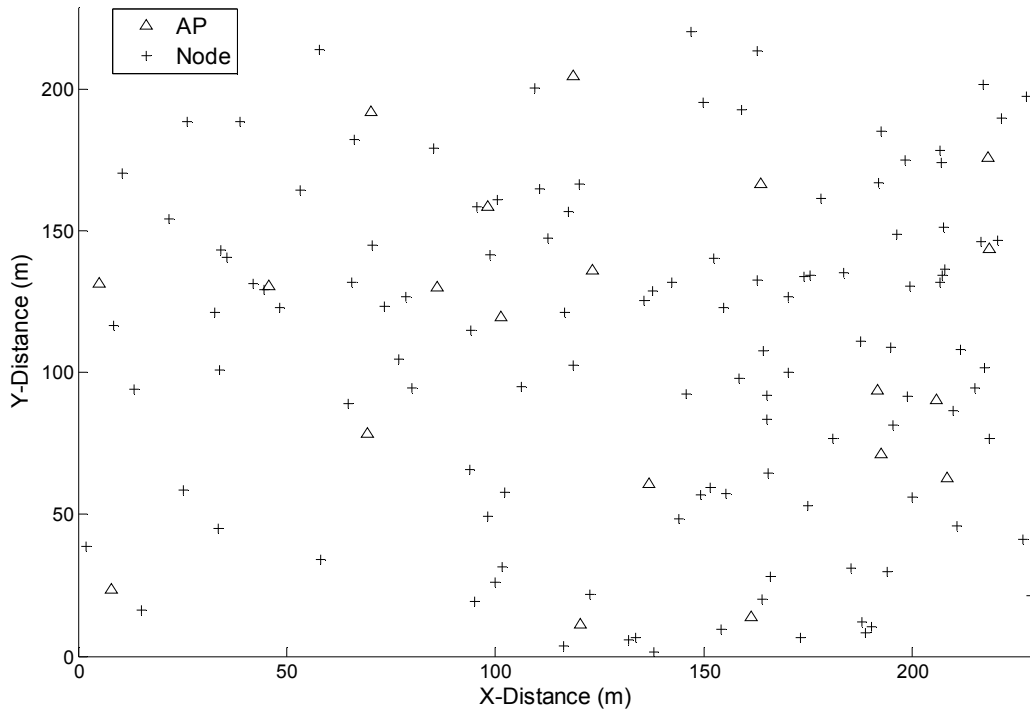
Client Spread	Standard Deviation	Conditions
Low	0.5 x Range	Limited to $\frac{1}{2}$ of distance between the AP to the nearest neighbour AP
Moderate	1.5 x Range	Clients must be nearer to its own AP than other APs
High	3 x Range	No condition



(a) Low client spread



(b) Moderate client spread



(c) High client spread

Figure 5.11: Different levels of client spread for a 20 AP topology.

The number of conflict pairs against the number of iterations for both the MICPA scheme and the MINE scheme are shown in Fig. 5.12. These results have been generated for IEEE 802.11a and IEEE 802.11b with a normalized density $Y/D = 1$, and with high client spread. From the figure, it is clear that the MICPA scheme outperforms the MINE scheme with a significant reduction in the number of conflict pairs. In fact, Table 5.2 shows that reductions of up to 81% for the number of conflict pairs can be achieved by the MICPA scheme over the MINE scheme. When compared to the random scheme (note that the number of conflict pairs at the zeroth iteration reflects the performance of the random scheme since the initial channels are assigned randomly), an even more impressive reduction of 93% can be seen.

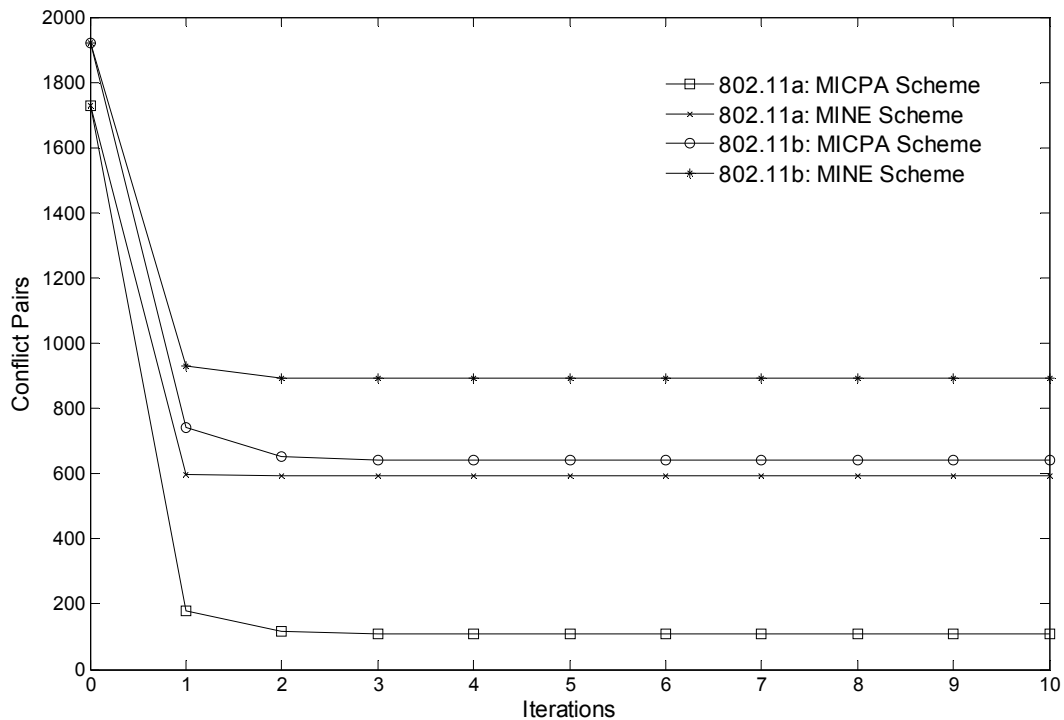


Figure 5.12: Number of conflict pairs for MICPA scheme and MINE scheme with high client spread.

TABLE 5.2

Number of conflict pairs for MICPA scheme and MINE scheme

	MINE Scheme	MICPA Scheme	% Change
802.11a	592.52	108.78	-81.64
802.11b	891.34	641.11	-28.07

Fig. 5.13 shows the number of conflict pairs for both the MICPA scheme and the MINE scheme with different levels of client spread for IEEE 802.11a with a normalized density $Y/D = 1$. For both schemes, it can be noted that the number of conflict pairs is increased as client spread increases. This is expected because clients that are located further away from their AP not only are more exposed to but also create more interference to other APs. Nevertheless, significant reductions in the number of conflict

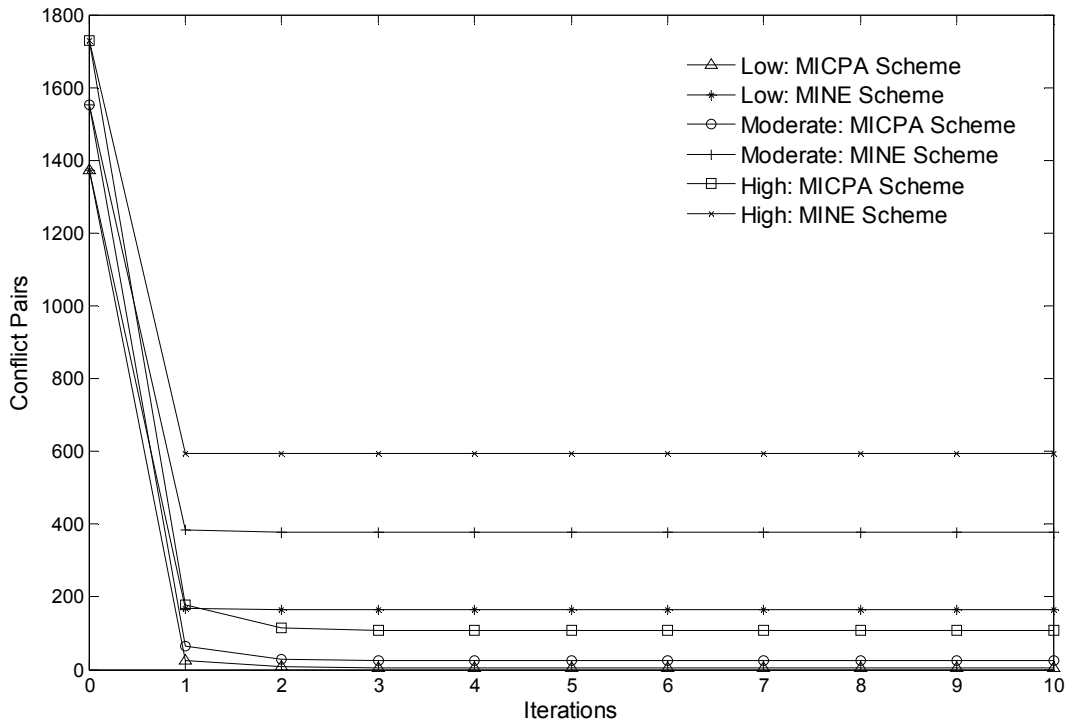


Figure 5.13: Number of conflict pairs for MICPA scheme and MINE scheme with different levels of client spread for IEEE 802.11a.

pairs can still be obtained by the MICPA scheme over the MINE scheme across all levels of client spread. Reductions in the number of conflict pairs of 96%, 93% and 81% have been observed for low, moderate and high client spread respectively. Although not shown here, a similar trend has also been seen for IEEE 802.11b.

The number of conflict pairs for both the MICPA scheme and the MINE scheme with different deployment densities for IEEE 802.11a with high client spread is shown in Fig. 5.14. From the figure, it can be seen that the number of conflict pairs for both schemes is larger when the deployment density is higher. This is because when the deployment density is increased by reducing the size of the topology, distances between APs are also reduced. Interfering BSSs that were in Class-II now become Class-I while those in Class-III now become Class-II, which causes an increase in the number of conflict pairs. Nonetheless, meaningful reductions in the number of conflict pairs of

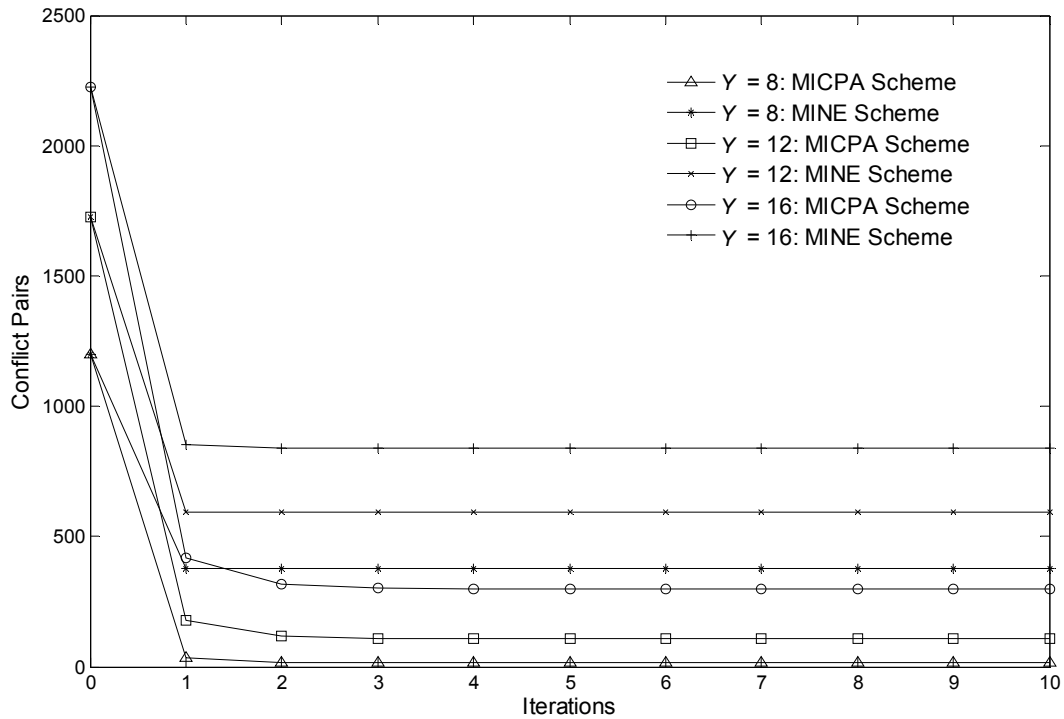


Figure 5.14: Number of conflict pairs for MICPA scheme and MINE scheme with different deployment densities for IEEE 802.11a.

58%, 81% and 64% by the MICPA scheme over the MINE scheme can still be observed for $Y = 8$, $Y = 12$ and $Y = 16$ respectively.

5.3.2 Throughput

The channel assignments obtained from the MATLAB simulations were then exported to the packet-level OPNET simulator in order to determine the throughput performance of the MICPA scheme. The OPNET simulator implements the complete IEEE 802.11a/b standards and additional parameters as shown in Table 2.1. Topologies consisting of 20 APs have been used. The locations of APs and clients are generated in the same way as described earlier in this section. All nodes are saturated and generate packets with a constant size of 1024 bytes. A total of 10 topologies are randomly generated for each

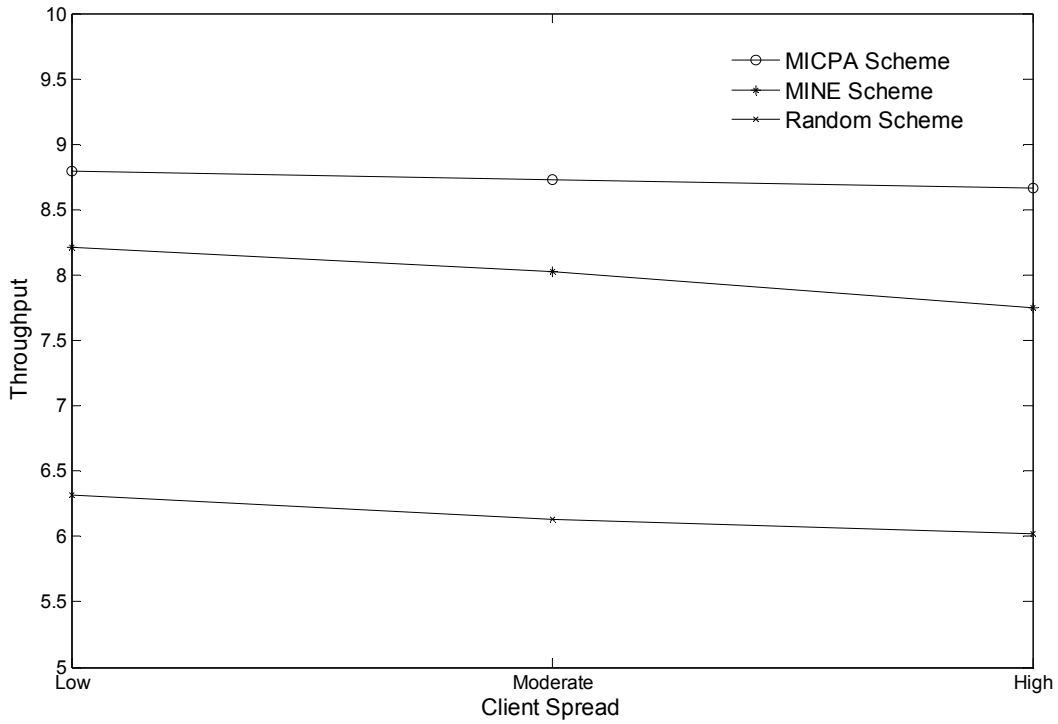


Figure 5.15: Throughput of MICPA, MINE and random schemes with different levels of client spread for IEEE 802.11a.

TABLE 5.3

Throughput of MICPA scheme and MINE scheme with different levels of client spread

Client Spread	MINE Scheme	MICPA Scheme	% Change
Low	8.21	8.79	7.06
Moderate	8.03	8.73	8.72
High	7.75	8.66	11.74

scenario and the average results are shown.

Fig. 5.15 shows the throughput of the MICPA, the MINE and the random schemes with different levels of client spread for IEEE 802.11a with a normalized density of $Y/D = 1$. Firstly, it can be noted that the MICPA scheme outperforms both the MINE and random schemes across all levels of client spread. Throughput gains of more than

10% can be obtained over the MINE scheme. In addition, throughput gains of around 40% over the random scheme across all levels of client spread is achieved. Secondly, as client spread increases, it can be seen that the throughput of all three schemes decreases, which is expected because a higher client spread results in higher interference suffered by both the AP and its clients. Nevertheless, as is shown in Table 5.3, the throughput gain over the MINE scheme actually increases for higher levels of client spread. The reason for this lies in the correlation between the clients and the AP's sensing. With low client spread, the clients' sensing is highly correlated to the AP's sensing due to their close proximity. On the other hand, a high client spread means that clients will be able to sense interference that the AP cannot sense by itself.

The throughput of the MICPA, the MINE and the random schemes with different deployment densities for IEEE 802.11a with high client spread is shown in Fig. 5.16. It is clear that the MICPA scheme gives the highest throughput among all schemes across all deployment densities. Meaningful throughput improvements of over 10% and 40% can be obtained by the MICPA scheme over the MINE scheme and the random scheme respectively. Moreover, as is shown in Table 5.4, the throughput gain over the MINE scheme increases to a maximum before it decreases as the deployment density is increased. The maximum throughput gain is achieved when $Y = 12$, which corresponds to a normalized density of unity ($Y/D = 1$). A similar observation has also been made for the case of IEEE 802.11b.

Although seemingly strange, there is a satisfactory explanation for this peculiar trend. When the deployment density is low, the utility of the clients' sensing is also low because there are not many interfering APs in its vicinity. This utility increases when the deployment density increases, by the same reasoning. However, with further increases in

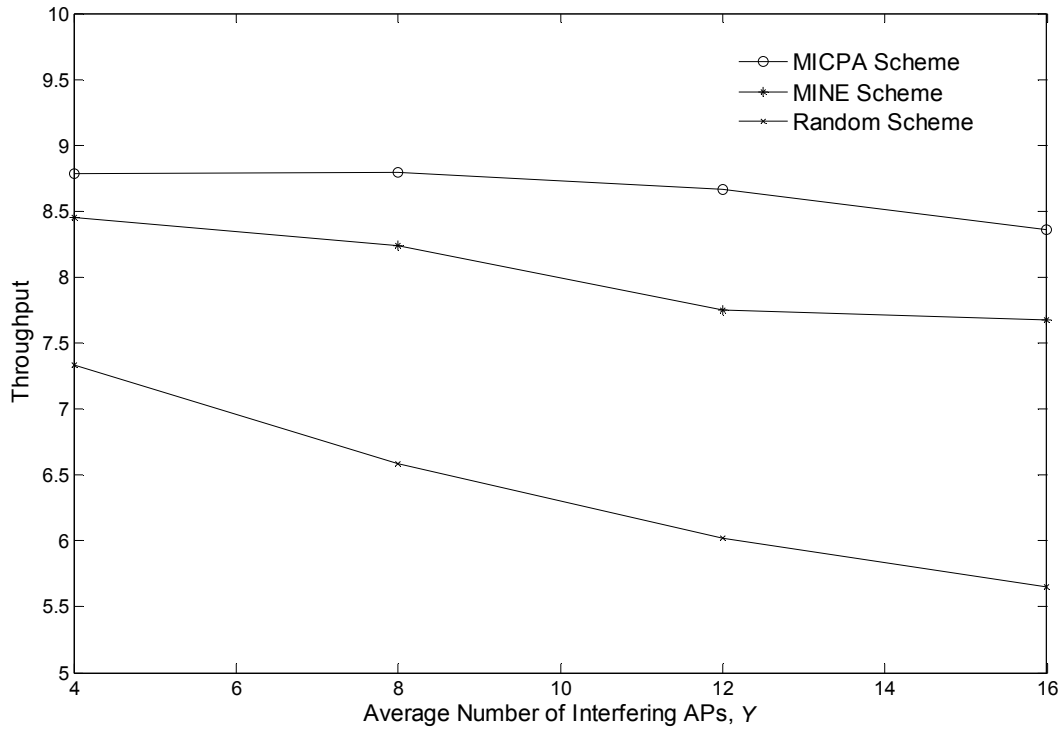


Figure 5.16: Throughput of MICPA, MINE and random schemes with different deployment densities for IEEE 802.11a.

TABLE 5.4

Throughput of MICPA scheme and MINE scheme with different deployment densities

Avg. No. of Interfering APs (Y)	MINE Scheme	MICPA Scheme	% Change
4	8.45	8.78	3.90
8	8.23	8.78	6.68
12	7.75	8.66	11.74
16	7.67	8.35	8.86

the deployment density, the number of interfering APs that can be sensed directly by the AP also increases. It is important to remember that this is a Class-I interference, which has the highest contribution towards the total number of conflict pairs when compared to Class-II or Class-III interference. In other words, beyond a certain point, the high

interference suffered by the AP becomes the dominant factor in higher deployment densities. This effectively reduces the performance gain of the client assisted MICPA scheme over the AP-only MINE scheme.

5.4 Summary

In this chapter, a study on the impact of interference on throughput with multiple APs has been undertaken. In the study, a useful and practical classification of interference scenarios has been presented. The impact of interference on throughput has been investigated for each interference class based on a novel approach that determines the possibility of parallel transmissions. It has been found that topologies with parallel transmissions exhibit significantly higher throughputs than those that only have single transmission. Also interestingly, results have shown that in some topologies, increased interference can lead to higher throughput and vice versa.

Insights gained from this study were used in designing the client assisted channel assignment scheme. A useful metric, the number of conflict pairs, has been identified and was shown to have a good correlation to the throughputs obtained across all interference classes. The number of conflict pairs is not only intuitive but also easily determined, even for complicated topologies. Employing this metric, the client assisted MICPA scheme was proposed. In this scheme, measurements from clients are used to assist the AP in determining the channel with the minimum number of conflict pairs in order to maximize its expected throughput.

Extensive simulation results have shown that the MICPA scheme can provide a significant reduction of up to 80% in the number of conflict pairs when compared to the MINE scheme across different levels of client spread and deployment densities.

Furthermore, meaningful gains of more than 10% and 40% in throughput were achieved over the AP-only MINE and the random schemes respectively. On the other hand, the effects of client spread and deployment densities on the performance of the MICPA scheme were also investigated. It was found that the MICPA scheme is best deployed in high client spread and moderate deployment density (normalized density close to unity) scenarios. These findings show that channel assignment schemes which utilize client's measurements such as the MICPA scheme have the potential to provide enhanced throughput performance in high density WLAN deployments.

CONCLUSIONS AND FUTURE WORK

6.1 Conclusions

In this thesis, we set out to investigate and develop practical channel assignment schemes in high density WLANs that can provide enhanced throughputs. In recent years, the popularity and mass adoption of WLAN technology has resulted in its high density deployments around the world. On one hand, the proliferation of high density WLAN deployments brings with it the potential of increased capacity, extended coverage and exciting new applications. On the other hand, the corresponding increase in contention and interference, which can significantly degrade throughputs, has posed new challenges in channel assignment. With the growth of WLANs expected to persist well into the future, channel assignment in high density WLANs is an important and challenging problem that requires immediate attention.

An introduction to WLANs in general and channel assignment in particular was given. The advent of high density WLAN deployments as the consequence of its success and growth was highlighted. The traditional methods used for channel assignment in WLANs were described. While these methods were acceptable for planned or sparsely deployed WLANs, their inadequacies when used in high density WLAN deployments were exposed. These provided the motivation for the research.

Next, the foundation for the research was laid through a critical review of the relevant background information. The IEEE 802.11 standards and its medium access mechanisms were introduced and the performance analysis of DCF was shown. The latter was used to demonstrate the expected throughputs for different combinations of data and control rates for both basic access and RTS/CTS mechanisms. The characteristics of high density WLAN deployments were investigated. It was shown that high density WLAN deployments have already become the norm in most cities. Furthermore, most APs were found to have a significant number of neighbouring APs. Existing WLAN channel assignment schemes were critically reviewed. A useful classification of these schemes into centralized and distributed schemes was proposed. Due to the lack of communication and cooperation, it was established that only distributed schemes can be applied in high density WLANs. However, distributed schemes have their own set of challenges, for example, the availability of only local information and lack of control over other APs. In view of this, and adopting a practical approach, we aspired to develop low complexity schemes that are able to provide acceptable and robust performance.

Following this, the MINE channel assignment scheme was proposed. It was shown that in order to maximize throughput, each AP only needed to choose the channel with the minimum number of active neighbour nodes. The MINE scheme has several key features. It does not require knowledge of the throughput function, it is asynchronous and it has low complexity. Extensive simulations were performed and these have shown that the MINE scheme not only converged significantly faster and required less channel switches, but also achieved superior throughputs with dynamic loads. Furthermore, robust performance was exhibited when the MINE scheme was applied in various realistic scenarios which included different numbers of channels, different deployment

densities, non-uniform topologies, dynamic topologies and heterogeneous networks.

The application of the MINE scheme to practice requires the estimation of the number of neighbour nodes. In view of this, the MINEK channel assignment scheme was proposed. In the MINEK scheme, an EKF estimator was formulated to estimate the total number of nodes. The number of nodes by AP estimate, which allowed the estimation of the number of neighbour nodes, was derived next. It was shown that the MINEK scheme not only provided fast and accurate estimates but also successfully exploited channel switching information of neighbouring APs. In order to determine the performance of the MINEK scheme, considerable developments were undertaken in the OPNET simulator. Extensive packet level simulations were performed and results have shown that the MINEK scheme was able to provide significant throughput improvement of up to almost 40% over other channel assignment schemes. Marginal degradation of only 4% from the ideal case, and negligible difference from the case when the number of neighbour nodes is known a priori, were observed for scenarios where the normalized density is close to unity. Furthermore, robust performance gains were seen across a wide range of non-saturated and saturated load conditions. The MINEK scheme also exhibited high fairness while achieving these high throughputs. Finally, the MINEK scheme was shown to be highly scalable, with proportional improvement in throughput even when only a subset of all APs had implemented it.

Thus far, only the AP's measurements were utilized in the proposed channel assignment schemes. Subsequently, client assisted channel assignment was investigated. A study on the impact of interference on throughput with multiple APs, based on a novel approach that determines the possibility of parallel transmissions, was undertaken. In the study, a useful and practical classification of interference scenarios was given. It was found that topologies with parallel transmissions exhibited significantly higher

throughputs than those that only had single transmission. The number of conflict pairs, a metric that had a good correlation to the expected throughput across all interference classes, was identified. Employing this metric, the client assisted MICPA scheme was proposed. In this scheme, clients' measurements were used to assist the AP in determining the channel with the minimum number of conflict pairs in order to maximize its expected throughput. Extensive simulation results have shown that the MICPA scheme was able to provide a significant reduction of up to 80% in the number of conflict pairs. Furthermore, meaningful gains of more than 10% and 40% in throughput were achieved over the AP-only MINE and the random schemes respectively. Investigation into the effects of client spread and deployment densities had found that the MICPA scheme is best deployed in high client spread and moderate deployment density (normalized density close to unity) scenarios.

Finally, it can be concluded that practical channel assignment strategies for throughput enhancement in high density WLANs were successfully explored, investigated and developed. Their superior performances were demonstrated and verified through extensive simulations.

6.2 Suggestions for Future Work

In this thesis, practical channel assignment schemes in high density WLANs that are able to provide superior throughputs were successfully developed. However, there are still many interesting directions where this research can be extended. Subsequently, suggestions for future work are given in this section.

High density WLAN deployments are owned by multiple entities that have the liberty to purchase WLAN equipment from any vendor. Although there are currently not many

channel assignment schemes that have been implemented in off-the-shelf APs, this may soon change due to the increased deployment density. The fact that channel assignment is not standardized means that WLAN AP vendors can increase the appeal of their products by implementing proprietary schemes. Therefore, it is expected that multiple channel assignment schemes will have to co-exist within the same network. To the best of our knowledge, the interaction between different channel assignment schemes has not been studied before. The only limited work so far was the performance evaluation of the MINE scheme when co-existing with the DSATUR scheme in Section 3.2.6. Nevertheless, more comprehensive studies can be undertaken which address the characteristics that promote mutual benefits, the consciousness and learning of co-existent schemes, the appropriate utilization or exploitation of this information and many other important issues. These studies can ensure a truly harmonious co-existence between various channel assignment schemes for the betterment of all parties.

As was mentioned, high density WLAN deployments belong to multiple owners. Most of these deployments consist of just one or two APs such as home networks. However, there are other deployments that have a considerable number of APs such as wireless internet service providers and enterprises [87-89]. While distributed channel assignment schemes can be deployed in both cases, larger sized deployments have opportunities to capitalize on the communication and cooperation among the APs that they own. Therefore, these deployments can employ hybrid channel assignment schemes that possess characteristics of both centralized and distributed channel assignment schemes. Hybrid schemes can leverage on the control and shared information of a group of APs, which are not available in distributed schemes. The efficient utilization of this control and how shared information can be exploited fully are just some of the research questions that can be explored. Furthermore, hybrid schemes, being partly centralized

can jointly consider channel assignment in combination with AP placement [90-91], load balancing [19, 92] and power control [93-94].

Multiple radio interfaces were proposed that can potentially improve system performance in wireless networks [95-96]. At the same time, WLAN APs that have multiple radio interfaces have recently appeared in the market. The most common of these are the dual-radio APs that can operate simultaneously on two non-overlapping channels in both the 2.4 GHz and 5 GHz unlicensed bands. Dual-radio APs can potentially provide multifold increase in capacity and alleviate the problem of increased contention and interference in high density WLAN deployments. However, these products are currently only targeted to enterprises due to their high prices. Nevertheless, with the advances in semiconductor technologies, it will just be a matter of time before they also become affordable to the home user. Assigning channels in a way that optimizes the simultaneous transmissions on two or more non-overlapping channels for enhanced throughputs is a very promising research direction and can become a major area of study. Note that this is distinctly different from the better known research problem of channel assignment in wireless mesh networks where multi-hop is involved and connectivity between mesh routers is required [97-98].

REFERENCES

- [1] K. J. Negus and A. Petrick, "History of Wireless Local Area Networks (WLANs) in the Unlicensed Bands," *INFO Journal*, vol. 11, pp. 36-56, Aug. 2009.
- [2] A. LaMarca, Y. Chawathe, S. Consolvo, J. Hightower, I. Smith, J. Scott, T. Sohn, J. Howard, J. Hughes, F. Potter, J. Tabert, P. Powledge, G. Borriello, and B. Schilit, "Place Lab: Device Positioning Using Radio Beacons in the Wild," in *Proc. International Conference on Pervasive Computing (PERVASIVE)*, May 2005, pp. 116-133.
- [3] B. Bing, *Emerging Technologies in Wireless LANs: Theory, Design, and Deployment*. New York: Cambridge University Press, 2008.
- [4] L. D. Paulson, "A New Wi-Fi for Peer-to-Peer Communications," *IEEE Computer*, vol. 41, pp. 19-20, June 2008.
- [5] S. C. Yang, "Toward a Wireless World," *IEEE Technology and Society Magazine*, vol. 26, pp. 32-42, June 2007.
- [6] ABI Research, (Feb. 2007). More than a Billion Wi-Fi Chipsets to Ship in 2012. [Online]. Available: <http://www.abiresearch.com/press/809>
- [7] P. Zheng and L. Ni, *Smart Phone and Next Generation Mobile Computing*. San Francisco: Morgan Kaufmann, 2005.
- [8] T. Henderson, D. Kotz, and I. Abyzov, "The Changing Usage of a Mature Campus-Wide Wireless Network," *Computer Networks*, vol. 52, pp. 2690-2712, Oct. 2008.
- [9] J. P. Conti, "Metro Wi-Fi," *IET Engineering & Technology* vol. 3, pp. 72-76, Mar 2008.
- [10] J. L. Yang, "Tracking Your Wi-Fi to Supercharge Local Search," *Fortune Magazine*, vol. 154, July 2006.

- [11] Electronics News, (Mar. 2009). Wi-Fi Access Point Shipments to Exceed 70m by 2010. [Online]. Available: <http://www.electronicnews.com.au/Article/Wi-Fi-access-point-shipments-to-exceed-70m-by-2010/474993.aspx>
- [12] V. Hayes and W. Lemstra, "Licence-Exempt: The Emergence of Wi-Fi," *INFO Journal*, vol. 11, pp. 57-71, 2009.
- [13] A. Akella, G. Judd, S. Seshan, and P. Steenkiste, "Self-Management in Chaotic Wireless Deployments," *Wireless Networks*, vol. 13, pp. 737-755, Dec. 2007.
- [14] B. Alexander, *802.11 Wireless Network Site Surveying and Installation*. Indianapolis: Cisco Press, 2004.
- [15] M. S. Gast, *802.11 Wireless Networks: The Definitive Guide*, 2nd ed. California: O'Reilly & Associates, 2005.
- [16] T. Dasilva, K. Eustice, and P. Reiher, "Johnny Appleseed: Wardriving to Reduce Interference in Chaotic Wireless Deployments," in *Proc. ACM International Conference on Modeling, Analysis and Simulation of Wireless and Mobile Systems (MSWiM)*, Oct. 2008, pp. 122-131.
- [17] A. Hills and B. Friday, "Radio Resource Management in Wireless LANs," *IEEE Communications Magazine*, vol. 42, pp. S9-S14, Dec. 2004.
- [18] K. K. Leung and B. J. Kim, "Frequency Assignment for IEEE 802.11 Wireless Networks," in *Proc. IEEE Vehicular Technology Conference (VTC)*, Oct. 2003, vol. 3, pp. 1422-1426.
- [19] A. Mishra, V. Brik, S. Banerjee, A. Srinivasan, and W. Arbaugh, "A Client-driven Approach for Channel Management in Wireless LANs," in *Proc. IEEE Conference on Computer Communications (INFOCOM)*, Apr. 2006, pp. 1-12.
- [20] I. Katzela and M. Naghshineh, "Channel Assignment Schemes for Cellular Mobile Telecommunication Systems: A Comprehensive Survey," *IEEE Personal Communications*, vol. 3, pp. 10-31, June 1996.

- [21] T. S. Rappaport, *Wireless Communications: Principles and Practice*. New Jersey: Prentice Hall, 2002.
- [22] IEEE 802.11, *IEEE Standard for Wireless LAN Medium Access Control (MAC) and Physical Layer (PHY) Specifications*, 2007.
- [23] G. Hiertz, D. Denteneer, L. Stibor, Y. Zang, X. P. Costa, and B. Walke, "The IEEE 802.11 Universe," *IEEE Communications Magazine*, vol. 48, pp. 62-70, Jan. 2010.
- [24] IEEE 802.11a, *IEEE Standard for Wireless LAN Medium Access Control (MAC) and Physical Layer (PHY) Specifications: High-speed Physical Layer in the 5 GHz Band*, 2003.
- [25] IEEE 802.11b, *IEEE Standard for Wireless LAN Medium Access Control (MAC) and Physical Layer (PHY) Specifications: Higher-Speed Physical Layer Extension in the 2.4 GHz Band*, 1999.
- [26] IEEE 802.11g, *IEEE Standard for Wireless LAN Medium Access Control (MAC) and Physical Layer (PHY) specifications: Further Higher Data Rate Extension in the 2.4 GHz Band*, 2003.
- [27] J. Geier, *Wireless LANs: Implementing High Performance IEEE 802.11 Networks*, 2nd ed. Indianapolis: Sams Publishing, 2001.
- [28] B. O'Hara and A. Petrick, *The IEEE 802.11 Handbook: A Designer's Companion*, 2nd ed. New York: IEEE Press, 2005.
- [29] M. Heusse, F. Rousseau, G. Berger-Sabbatel, and A. Duda, "Performance Anomaly of 802.11b," in *Proc. IEEE Conference on Computer Communications (INFOCOM)*, Mar. 2003, pp. 836-843.
- [30] Y. Bejerano and R. S. Bhatia, "MiFi: A Framework for Fairness and QoS Assurance for Current IEEE 802.11 Networks with Multiple Access Points " *IEEE/ACM Transactions on Networking*, vol. 14, pp. 849-862, Aug. 2006.

- [31] B. Sikdar, "An Analytic Model for the Delay in IEEE 802.11 PCF MAC-Based Wireless Networks," *IEEE Transactions on Wireless Communications*, vol. 6, pp. 1542-1550, Apr. 2007.
- [32] S. Ray, D. Starobinski, and J. B. Carruthers, "Performance of Wireless Networks with Hidden Nodes: A Queuing-Theoretic Analysis," *Computer Communications*, vol. 28, pp. 1179-1192, June 2005.
- [33] A. Tsertou and D. I. Laurenson, "Revisiting the Hidden Terminal Problem in a CSMA/CA Wireless Network," *IEEE Transactions on Mobile Computing*, vol. 7, pp. 817-831 July 2008.
- [34] S. Gollakota and D. Katabi, "ZigZag Decoding: Combating Hidden Terminals in Wireless Networks," in *Proc. ACM Conference of the Special Interest Group on Data Communication (SIGCOMM)*, Aug. 2008, pp. 159-170.
- [35] G. Bianchi, "Performance Analysis of the IEEE802.11 Distributed Coordination Function," *IEEE Journal on Selected Areas in Communications (JSAC)*, vol. 18, pp. 535-547, Mar. 2000.
- [36] H. Wu, Y. Peng, K. Long, S. Cheng, and J. Ma, "Performance of Reliable Transport Protocol over IEEE 802.11 Wireless LAN: Analysis and Enhancement," in *Proc. IEEE Conference on Computer Communications (INFOCOM)*, June 2002, vol. 2, pp. 599-607.
- [37] P. Chatzimisios, A. C. Boucouvalas, and V. Vitsas, "Effectiveness of RTS/CTS handshake in IEEE 802.11a Wireless LANs," *IET Electronics Letters*, vol. 40, pp. 915-916, July 2004.
- [38] I. Tinnirello, S. Choi, and Y. Kim, "Revisit of RTS/CTS Exchange in High-Speed IEEE 802.11 Networks," in *Proc. IEEE International Symposium on a World of Wireless, Mobile and Multimedia Networks (WoWMoM)*, June 2005, pp. 240-248.
- [39] C. Kai, Y. Chen, and N. Yu, "Performance Analysis of DCF under two access mechanisms in IEEE802.11a WLAN," in *Proc. International Conference on Mobile Technology, Applications and Systems (MTAS)*, Nov. 2005, pp. 1-7.

- [40] Wi-Fi Alliance, (Jan. 2010). Enthusiasm for Wi-Fi in Consumer Electronics Continues to Grow. [Online]. Available: http://www.wi-fi.org/news_articles.php?f=media_news&news_id=946
- [41] A. Hills, "Large-Scale Wireless LAN Design," *IEEE Communications Magazine*, vol. 39, pp. 98-107, Nov. 2001.
- [42] A. Hills and J. Schlegel, "Rollabout: A Wireless Design Tool " *IEEE Communications Magazine*, vol. 42, pp. 132-138, Feb. 2004.
- [43] C. Hurley, M. Puchol, R. Rogers, and F. Thornton, *WarDriving: Drive, Detect, Defend. A Guide to Wireless Security*. Rockland: Syngress Publishing, 2004.
- [44] M. Kim, J. J. Fielding, and D. Kotz, "Risks of Using AP Locations Discovered Through War Driving," in *Proc. International Conference on Pervasive Computing (PERVASIVE)*, May 2006, pp. 67-82.
- [45] WiGLE: Wireless Geographic Logging Engine. [Online]. Available: <http://www.wigle.net/>
- [46] K. Jones and L. Liu, "What Where Wi: An Analysis of Millions of Wi-Fi Access Points," in *Proc. IEEE International Conference on Portable Information Devices (PORTABLE)*, May 2007, pp. 1-4.
- [47] G. Valadon, F. L. Goff, and C. Berger, "A Practical Characterization of 802.11 Access Points in Paris," in *Proc. Advanced International Conference on Telecommunications (AICT)*, May 2009, pp. 220-225.
- [48] Y. Zhao and K. K. Leung, "Adaptive Channel Allocation for IEEE802.11 Wireless LAN," in *Proc. European Wireless Conference (EW)*, Apr. 2006.
- [49] D. Kotz and K. Essien, "Analysis of a Campus-Wide Wireless Network," *Wireless Networks*, vol. 11, pp. 115-133, Jan. 2005.

- [50] P. Mahonen, J. Riihijarvi, and M. Petrova, "Automatic Channel Allocation for Small Wireless Local Area Networks using Graph Colouring Algorithm Approach," in *Proc. IEEE International Symposium on Personal, Indoor and Mobile Radio Communications (PIMRC)*, Sept. 2004, pp. 536-539.
- [51] J. Riihijarvi, M. Petrova, and P. Mahonen, "Frequency Allocation for WLANs using Graph Colouring Techniques," in *Proc. Conference on Wireless On-Demand Network Systems and Services (WONS)*, Jan. 2005, pp. 216-222.
- [52] J. Riihijarvi, M. Petrova, P. Mahonen, and J. d. A. Barbosa, "Performance Evaluation of Automatic Channel Assignment Mechanism for IEEE 802.11 Based on Graph Colouring," in *Proc. IEEE International Symposium on Personal, Indoor and Mobile Radio Communications (PIMRC)*, Sept. 2006, pp. 1-5.
- [53] M. Balazinska and P. Castro, "Characterizing Mobility and Network Usage in a Corporate Wireless Local-Area Network," in *Proc. International Conference on Mobile Systems, Applications, and Services (MobiSys)*, May 2003 pp. 303-316.
- [54] E. G. Villegas, R. V. Ferro, and J. P. Aspas, "New Algorithm for Distributed Frequency Assignments in IEEE 802.11 Wireless Networks," in *Proc. European Wireless Conference (EW)*, Apr. 2005, pp. 211-217.
- [55] E. G. Villegas, R. V. Ferro, and J. P. Aspas, "Implementation of a Distributed Dynamic Channel Assignment Mechanism for IEEE 802.11 Networks," in *Proc. IEEE International Symposium on Personal, Indoor and Mobile Radio Communications (PIMRC)*, Sept. 2005, vol. 3, pp. 1458-1462.
- [56] E. G. Villegas, R. V. Ferre, and J. Paradells, "Frequency Assignments in IEEE 802.11 WLANs with Efficient Spectrum Sharing," *Wiley Journal on Wireless Communications and Mobile Computing*, vol. 9, pp. 1125-1140, Aug. 2009.
- [57] A. Mishra, S. Banerjee, and W. Arbaugh, "Weighted Coloring based Channel Assignment for WLANs," *ACM SIGMOBILE Mobile Computing and Communications Review*, vol. 9, pp. 19-31, July 2005.

- [58] D. J. Leith and P. Clifford, "A Self-Managed Distributed Channel Selection Algorithm for WLANs," in *Proc. International Symposium on Modeling and Optimization in Mobile, Ad-Hoc and Wireless Networks (WiOpt)*, Apr. 2006, pp. 1-9.
- [59] D. J. Leith, P. Clifford, D. Malone, and D. Reid, "Optimal WLAN Channel Selection without Communication," Hamilton Institute Report, July 2006.
- [60] D. Malone, P. Clifford, D. Reid, and D. J. Leith, "Experimental Implementation of Optimal WLAN Channel Selection without Communication," in *Proc. IEEE New Frontiers in Dynamic Spectrum Access Networks (DySPAN)*, Apr. 2007, pp. 316-319.
- [61] H. Luo and N. K. Shankaranarayanan, "A Distributed Dynamic Channel Allocation Technique for Throughput Improvement in a Dense WLAN Environment," in *Proc. IEEE International Conference on Acoustics, Speech & Signal Processing (ICASSP)*, May 2004, vol. 5, pp. V-345-V-348.
- [62] M. Driberg, F.-C. Zheng, R. Ahmad, and S. Olafsson, "An Improved Distributed Dynamic Channel Assignment Scheme for Dense WLANs," in *Proc. 6th International Conference on Information, Communications and Signal Processing (ICICS)*, Dec. 2007, pp. 1-5.
- [63] M. Driberg, F.-C. Zheng, R. Ahmad, and S. Olafsson, "An Asynchronous Distributed Dynamic Channel Assignment Scheme for Dense WLANs," in *Proc. IEEE International Conference on Communications (ICC)*, May 2008, pp. 2507-2511.
- [64] M. Driberg, F.-C. Zheng, R. Ahmad, and S. Olafsson, "An Asynchronous Channel Assignment Scheme: Performance Evaluation," in *Proc. IEEE Vehicular Technology Conference (VTC) Spring*, May 2008, pp. 2147-2151.
- [65] M. Driberg, F.-C. Zheng, R. Ahmad, S. Olafsson, and M. Fitch, "Effectiveness of Asynchronous Channel Assignment Scheme in Heterogeneous WLANs," in *Proc. International Symposium on Wireless and Pervasive Computing (ISWPC)*, Feb. 2009, pp. 1-5.

- [66] M. Drieberg, F.-C. Zheng, and R. Ahmad, "Performance of Asynchronous Channel Assignment Scheme in Non-Uniform and Dynamic Topology WLANs," in *Proc. IEEE International Symposium on Personal, Indoor and Mobile Radio Communications (PIMRC)*, Sept. 2009, pp. 2085-2089.
- [67] Cisco Systems, (Dec. 2006). Cisco Aironet 1230AG Series 802.11A/B/G Access Point: Data Sheet. [Online]. Available: http://www.ciscosystems.com/en/US/prod/collateral/wireless/ps5678/ps6108/product_data_sheet0900aecd801b9068.pdf
- [68] D. Schwab and R. Bunt, "Characterising the Use of a Campus Wireless Network," in *Proc. IEEE Conference on Computer Communications (INFOCOM)*, Mar. 2004, pp. 862-870.
- [69] M. Drieberg, F.-C. Zheng, and R. Ahmad, "MINEK: A Practical Distributed Channel Assignment Scheme for Dense WLANs," accepted for publication in *IET Communications*.
- [70] G. Bianchi and I. Tinnirello, "Kalman Filter Estimation of the Number of Competing Terminals in an IEEE 802.11 Network," in *Proc. IEEE Conference on Computer Communications (INFOCOM)*, Mar. 2003, vol. 2, pp. 844-852.
- [71] H. Ma, X. Li, H. Li, P. Zhang, S. Luo, and C. Yuan, "Dynamic Optimization of IEEE 802.11 CSMA/CA Based on the Number of Competing Stations," in *Proc. IEEE International Conference on Communications (ICC)*, June 2004, pp. 191-195.
- [72] L. Zhao, X. Zou, H. Zhang, W. Ding, and J. Zhang, "Game-Theoretic Cross-Layer Design in WLANs," in *Proc. International Wireless Communications and Mobile Computing Conference (IWCMC)* Aug. 2008, pp. 570-575.
- [73] Z.-N. Kong, D. H. K. Tsang, and B. Bensaou, "Adaptive RTS/CTS Mechanism for IEEE 802.11 WLANs to Achieve Optimal Performance," in *Proc. IEEE International Conference on Communications (ICC)*, June 2004, pp. 185-190.

- [74] P. Chatzimisios, A. C. Boucouvalas, and V. Vitsas, "Optimisation of RTS/CTS Handshake in IEEE 802.11 Wireless LANs for Maximum Performance," in *Proc. IEEE Global Communications Conference (GLOBECOM)*, Nov. 2004, pp. 270-275
- [75] Y. Bejerano, S. J. Han, and L. Li, "Fairness and Load Balancing in Wireless LANs Using Association Control," *IEEE/ACM Transactions on Networking*, vol. 15, pp. 560-573, June 2007.
- [76] H. Gong and J. Kim, "Dynamic Load Balancing Through Association Control of Mobile Users in WiFi Networks," *IEEE Transactions on Consumer Electronics*, vol. 54, pp. 342-348 May 2008.
- [77] A. Mishra, M. Shin, and W. Arbaugh, "An Empirical Analysis of the IEEE 802.11 MAC Layer Handoff Process," *ACM SIGCOMM Computer Communication Review*, vol. 33, pp. 93-102, Apr. 2003.
- [78] S. Pack, J. Choi, T. Kwon, and Y. Choi, "Fast-Handoff Support in IEEE 802.11 Wireless Networks," *IEEE Communications Surveys & Tutorials*, vol. 9, pp. 2-12, Mar. 2007.
- [79] D. Simon, *Optimal State Estimation: Kalman, H-Infinity, and Nonlinear Approaches*. New Jersey: John Wiley & Sons, 2006.
- [80] P. Zarchan and H. Musoff, *Fundamentals Of Kalman Filtering: A Practical Approach*. Virginia: American Institute of Aeronautics and Astronautics, 2005.
- [81] C. Na, J. K. Chen, and T. S. Rappaport, "Measured Traffic Statistics and Throughput of IEEE 802.11b Public WLAN Hotspots with Three Different Applications," *IEEE Transactions on Wireless Communications*, vol. 5, pp. 3296-3305, Nov. 2006.
- [82] R. K. Jain, D.-M. W. Chiu, and W. R. Hawe, "A Quantitative Measure Of Fairness And Discrimination For Resource Allocation In Shared Computer Systems," *Digital Equipment Corporation Technical Report 301*, 1984.

- [83] O. Ekici and A. Yongacoglu, "IEEE 802.11a Throughput Performance with Hidden Nodes," *IEEE Communications Letters*, vol. 12, pp. 465-467, June 2008.
- [84] M. Garetto, T. Salonidis, and E. W. Knightly, "Modeling Per-Flow Throughput and Capturing Starvation in CSMA Multi-Hop Wireless Networks," *IEEE/ACM Transactions on Networking*, vol. 16, pp. 864-877, Aug. 2008.
- [85] S. C. Liew, C. Kai, J. Leung, and B. Wong, "Back-of-the-Envelope Computation of Throughput Distributions in CSMA Wireless Networks," in *Proc. IEEE International Conference on Communications (ICC)*, June 2009, pp. 1-6.
- [86] M. Driberg, F.-C. Zheng, and R. Ahmad, "Impact of Interference on Throughput in Dense WLANs with Multiple APs," in *Proc. IEEE International Symposium on Personal, Indoor and Mobile Radio Communications (PIMRC)*, Sept. 2009, pp. 752-756.
- [87] Y. Chou, "A Seamless City: The Case Study of Taipei's WiFi Project," in *Proc. ITS European Regional Conference*, Sept. 2005, pp. 1-18.
- [88] BT OpenZone, (Feb. 2010). BT Hits the One Million Spot. [Online]. Available: http://www.btopenzone.com/news/news_20100209.jsp
- [89] R. Murty, J. Padhye, A. Wolman, and B. Zill, "Designing High Performance Enterprise Wi-Fi Networks," in *Proc. USENIX/ACM Symposium on Networked Design and Implementation (NSDI)*, Apr. 2008, pp. 73-88.
- [90] Y. Lee, K. Kim, and Y. Choi, "Optimization of AP Placement and Channel Assignment in Wireless LANs," in *Proc. IEEE Conference on Local Computer Networks (LCN)*, Nov. 2002, pp. 831-836.
- [91] A. Eisenblatter, H.-F. Geerdes, and I. Siomina, "Integrated Access Point Placement and Channel Assignment for Wireless LANs in an Indoor Office Environment," in *Proc. IEEE International Symposium on a World of Wireless, Mobile and Multimedia Networks (WoWMoM)*, June 2007, pp. 1-10.

- [92] H. Al-Rizzo, M. Haidar, R. Akl, and Y. Chan, "Enhanced Channel Assignment and Load Distribution in IEEE 802.11 WLANs," in *Proc. IEEE International Conference on Signal Processing and Communications (ICSPC)* Nov. 2007, pp. 768-771.
- [93] N. Ahmed and S. Keshav, "A Successive Refinement Approach to Wireless Infrastructure Network Deployment," in *Proc. IEEE Wireless Communications and Networking Conference (WCNC)*, Apr. 2006, pp. 511-519.
- [94] J. Chen, S. Olafsson, Y. Yang, and X. Gu, "Joint Distributed Transmit Power Control and Dynamic Channel Allocation for Scalable WLANs," in *Proc. IEEE Wireless Communications and Networking Conference (WCNC)*, Apr. 2009, pp. 1-6.
- [95] P. Bahl, A. Adya, J. Padhye, and A. Walman, "Reconsidering Wireless Systems with Multiple Radios," *ACM SIGCOMM Computer Communication Review*, vol. 34, pp. 39-46, Oct. 2004.
- [96] J. Zhu and S. Roy, "802.11 Mesh Networks with Two-Radio Access Points," in *Proc. IEEE International Conference on Communications (ICC)*, May 2005, pp. 3609-3615.
- [97] H. Skalli, S. Ghosh, S. K. Das, L. Lenzini, and M. Conti, "Channel Assignment Strategies for Multiradio Wireless Mesh Networks: Issues and Solutions," *IEEE Communications Magazine*, vol. 45, pp. 86-95, Nov. 2007.
- [98] M. K. Marina, S. R. Das, and A. P. Subramanian, "A Topology Control Approach for Utilizing Multiple Channels in Multi-Radio Wireless Mesh Networks," *Computer Networks*, vol. 54, pp. 241-256, Feb. 2010.

APPENDIX A

OPNET SIMULATION DEVELOPMENT

Performance evaluation of the MINEK scheme can be obtained through packet level simulations using OPNET. OPNET is well established as the leading commercial network simulator software. Simulations at packet level provide an accurate modeling of the behaviour and performance of the MINEK scheme in realistic networks. In this appendix, the description of the simulation developments carried out in OPNET is presented.

OPNET stands for optimized network engineering tools. It provides a comprehensive development environment for the modeling of communication networks and distributed systems. OPNET is a discrete event simulator, which allows the analysis of the characteristics and performance of the modeled systems at the packet level. It supports all stages of modeling including model design, simulation, data collection and data analysis.

OPNET comes equipped with a vast library of models that can be used to build networks quickly and easily. If desired, users can also build their own fully customized models. The modeling in OPNET is based on a hierarchical structure consisting of network, node and process models as shown in Fig. A.1. Network models are built using nodes and links. Node models contain modules and packet streams. Process models define the behaviour of modules. They consist of states and transitions that are graphically represented by state transition diagrams. Communication links are defined

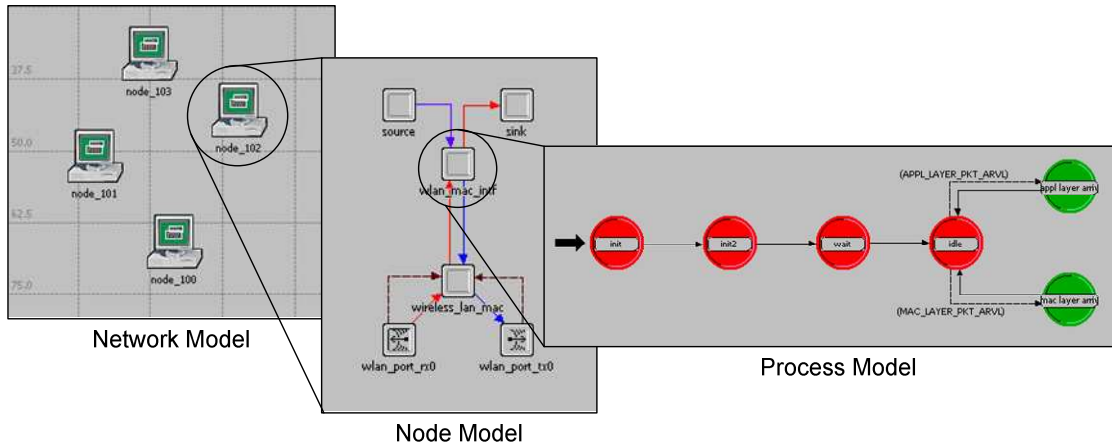


Figure A.1: Network, node and process models in OPNET.

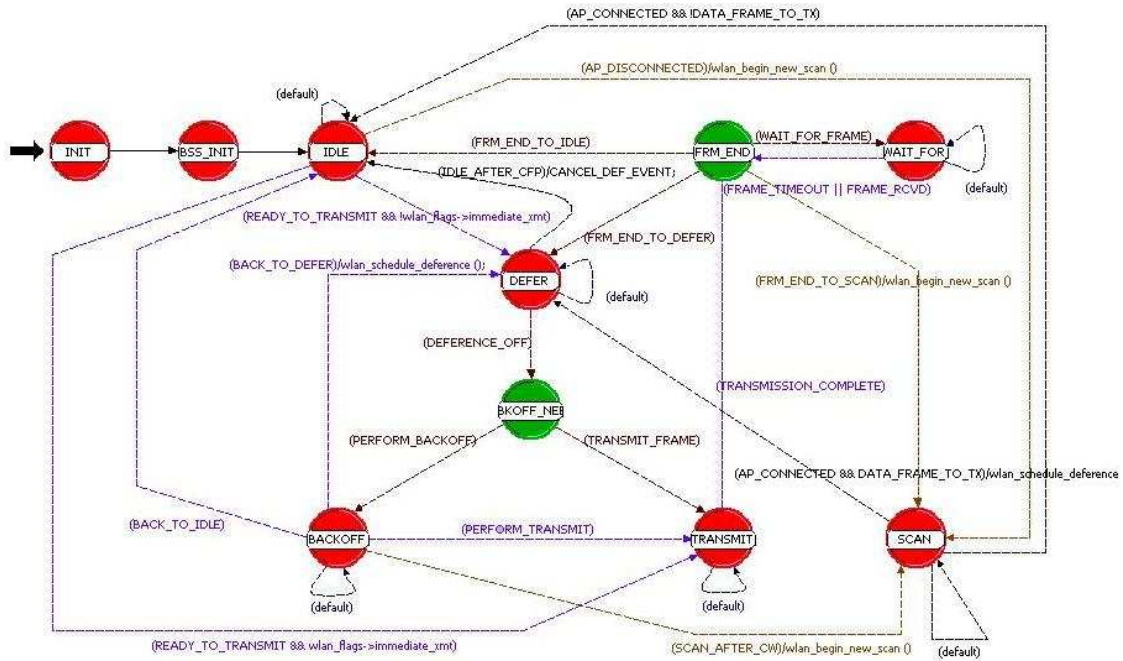


Figure A.2: WLAN MAC process model.

by pipeline stages which include effects of propagation, delays and errors. The basic workflow in OPNET consists of creating a network model, selecting statistics, running simulations and analyzing results.

The base model used is the WLAN station from the Wireless Model library. This model comprises a source, a sink, a transmitter, a receiver, the MAC interface module

and the MAC module shown in Fig. A.1. The central component of this model is the MAC module. The MAC module is defined by the underlying WLAN MAC process model, shown in Fig. A.2. This WLAN station model implements the complete DCF specifications.

However, for the purpose of evaluating the performance of MINEK scheme in particular and channel assignment schemes in general, several features were clearly lacking. For example, the model did not support dynamic channel changes during run time. Before any modification could even be attempted, a clear understanding of the node model and the associated process models was needed. To make matters worse, there was no formal documentation provided with these models. Therefore, an understanding of the node model and processes models' states, transitions and functions was acquired by perusing through tens of thousand lines of codes. Although tedious at times, this provided the necessary groundwork for implementing new features and the MINEK scheme.

The implementation, debugging and verification of the required new features and MINEK scheme in the model took significant effort and time. The simulation developments which were carried out are summarized as follows:

- 1) Automated topology generation and parameter setting: OPNET provides a graphical user interface (GUI) that allows users to drag and drop models and links to build the required topology and to set high-level parameters. However, using the GUI to setup a topology consisting of several hundred APs and nodes and to set their parameters becomes prohibitive.
 - i) A model assistant configuration file that contains the required topology and parameter settings was generated externally in an automated manner.

- ii) This file was then applied manually in OPNET's GUI (Topology > Model Assistant > Apply File).
- 2) Transmission parameters:
- i) Transmission range = 50m. Modified the path loss exponent in the power model pipeline stage of the wireless link.
 - ii) Propagation delay = 1 μ s. Modified the start and end propagation delays in the propdel model pipeline stage of the wireless link.
- 3) Dynamic channel changes during run time:
- i) Removed the reduction of potential receivers during initialization of the WLAN MAC process model which prevents the appropriate nodes from receiving packets after channel changes.
 - ii) Channel change was performed using function *wlan_set_transceiver_channel*.
- 4) MINEK: Measurement collection of p_k , the measurement of the conditional collision probability. It was calculated once the number of c_i was equal to B time slots. There were several possibilities that had to be taken into account.
- i) Backoff interrupted by busy channel. Calculated the number of empty slots based on the elapsed time divided by slot time. Set the corresponding number of $c_i = 0$.
 - ii) Backoff completed. Obtained the number of backoff slots selected. Set the corresponding number of $c_i = 0$.
 - iii) Self successful transmission. Set $c_i = 0$.
 - iv) Self collision. Set $c_i = 1$.
 - v) Others' successful transmission. Set $c_i = 1$.
 - vi) Others' collision. Set $c_i = 1$.

- 5) MINEK: Measurement collection of s_i , the number of successful transmission by AP. Two possibilities exist here.
- i) Self successful transmission. Obtained self BSSID. Set $s_i = s_i + 1$.
 - ii) Others' successful transmission. Obtained BSSID from packet header. Set $s_i = s_i + 1$.
- 6) MINEK: Algorithm.
- i) Ran EKF estimator when a new p_k measurement was available.
 - ii) Checked if there had been a channel change and determined \hat{u}_k , the estimated net difference in the number of nodes.
 - iii) Checked if there had been an alarm and set variance Q_k accordingly.
 - iv) Implemented all EKF equations that provide an updated \hat{n}_k estimate.
 - v) Implemented all change detection filter equations that set an alarm if necessary.
 - v) Summed the number of successful transmissions by all APs and determined if they exceeded the specified threshold.
 - vi) Implemented the equations that provide an updated $\hat{n}_{k,i}$ estimate.
 - vii) Determined the number of neighbour nodes for all available channels and the channel with the minimum number of neighbour nodes.
 - viii) Checked if all conditions were satisfied for a channel change.
 - ix) Changed channel and reset the appropriate parameters.
- 7) Automated results collection and post processing: Statistics of interests are selected and results are shown in graphs using OPNET's GUI. Raw results can be obtained by exporting data in the graphs manually to Microsoft Excel, which is subsequently used for post processing. However, this process, being largely manual is time consuming.

- i) A dummy node model that initializes the parameters for file input/output was developed and added to the network model.
- ii) The sink module in the WLAN station model processes packets that have been received successfully. The corresponding sink process was modified to enable the required information to be written to an external data file each time a packet is received successfully.
- iii) The external data file could then be post processed using an external program.

Once OPNET simulation development was completed, performance evaluation of the MINEK scheme could be carried out.